UNIVERSITY OF CALIFORNIA
SANTA CRUZ

MECHANISMS CONTROLLING WOLBACHIA TITER AND TRANSMISSION

A dissertation submitted in partial satisfaction
of the requirement for the degree of

DOCTOR OF PHILOSOPHY

in

MOLECULAR, CELL AND DEVELOPMENTAL BIOLOGY

by

Pamela M. White

September 2017

The Dissertation of Pamela M. White
is approved:

_____
Professor William Sullivan, Chair

_____
Professor Susan Strome

_____
Professor Jordan Ward

_____
Tyrus Miller
Vice Provost and Dean of Graduate Studies

Table of Contents

List of figures

List of tables

Abstract

Mechanisms Controlling *Wolbachia* Titer and Transmission

Pamela White

Wolbachia are gram-negative, obligate, intracellular bacteria infecting a majority of insect species and filarial nematodes. In both insects and nematodes *Wolbachia* are primarily transmitted through the female germ line. *Wolbachia* carried by filarial nematodes are the cause of the neglected diseases African river blindness and lymphatic filariasis afflicting millions worldwide. In order to combat these diseases, we created a *Wolbachia*-infected Drosophila cell line that enabled high throughput screening for novel potent anti-*Wolbachia* compounds. Of the 36,231 compounds screened in house, 8 compounds dramatically reduced *Wolbachia* titer both in the cell and nematode based screen. Significantly, we discovered that the albendazole metabolite, albendazole sulfone, reduces *Wolbachia* titer in Drosophila melanogaster and the filarial nematode *Brugia malayi* perhaps by directly targeting *Wolbachia* FtsZ. Using the *Wolbachia*-infected cell line, we discovered that in addition to vertical germ line transmission, *Wolbachia* are efficiently transmitted horizontally via cell-to-cell transmission. We show that horizontal transfer is independent of cell-to-cell contact, can efficiently take place within hours, and uses both host cell phagocytic and clathrin/dynamin-dependent endocytic machinery. Modifications to our high-throughput screen in combination with genome-wide RNA interference (RNAi) identified host factors that influence *Wolbachia* titer. When these host factors were tested in *Drosophila melanogaster in vivo* we found that maintenance of *Wolbachia* titer relies on an intact host Endoplasmic Reticulum (ER) associated degradation (ERAD) system. These data, in combination with electron microscopy studies, demonstrated that *Wolbachia* is intimately associated with the host ER and suggested a previously unsuspected mechanism for the potent ability of *Wolbachia* to prevent RNA virus replication. To examine the impact of nutritional on *Wolbachia* titer, Drosophila were fed sucrose- and yeast-enriched diets. These conditions resulted in increased and decreased *Wolbachia* titer in Drosophila oogenesis, respectively,

and that somatic TOR and insulin signaling mediate the response of the yeast-enriched diet on *Wolbachia*. Taken together, these studies provide initial insights into the molecular and cellular interactions between *Wolbachia* and its insect and nematode hosts.

Dedication

I dedicate my dissertation to

my husband William C. Rice.

Acknowledgements

I would like to thank Bill Sullivan for his mentorship, guidance, and advice. His continued belief and support of my abilities has made this achievement possible. I would like to thank my thesis committee members Susan Strome and Jordan Ward as well as Bill Saxton, Scott Lokey, and Fitnat Yildiz for their time, suggestions, and advice. I would like to thank Martha Zuniga, Manny Ares, Melissa Jurica, and Carrie Partch for their discussions and writing advice. I would like to thank the Sullivan lab and my fellow graduate students for friendly discussions, exchange of ideas, and reagents, especially: Travis Karg, Brandt Warecki, Lotti Brose, Donna Fullerton, and Joey Dahl. I would like to thank Nan Ho and Jill Carbone for nourishing my interest in biology early in my education. Finally, I would like to thank my unofficial mentor and friend Laura Serbus who I could always turn to for experimental, career, and writing advice. Having someone who is always there for me has been invaluable during this journey.

The text of this dissertation includes reprints of the following previously published material:

[Chapter 2] Serbus, L.R., Landmann, F., Bray, W.M., White, P.M., Ruybal, J., Lokey, R.S., Debec, A. and Sullivan, W., 2012. A cell-based screen reveals that the albendazole metabolite, albendazole sulfone, targets Wolbachia. PLoS pathogens, 8(9), p.e1002922. [1]

[Chapter 3] White, P.M., Pietri, J.E., Debec, A., Russell, S., Patel, B. and Sullivan, W., 2017. Mechanisms of horizontal cell-to-cell transfer of Wolbachia spp. in Drosophila melanogaster. Applied and environmental microbiology, 83(7), pp.e03425-16. [2]

[Chapter 4] White, P.M., Serbus, L.R., Debec, A., Codina, A., Bray, W., Guichet, A., Lokey, R.S. and Sullivan, W., 2017. Reliance of Wolbachia on high rates of host proteolysis revealed by a genome-wide RNAi screen of Drosophila cells. Genetics, 205(4), pp.1473-1488. [3]

[Chapter 5] Serbus, L.R., White, P.M., Silva, J.P., Rabe, A., Teixeira, L., Albertson, R. and Sullivan, W., 2015. The impact of host diet on Wolbachia titer in Drosophila. PLoS pathogens, 11(3), p.e1004777. [4]

William Sullivan listed in these publications directed and supervised the research which forms the basis for the dissertation.

Chapter 1

Introduction

Wolbachia are intracellular maternally transmitted bacteria present in the majority of insect species as well as some mites, crustaceans and filarial nematodes [5, 6]. *Wolbachia* were initially studied in insects because they induce unconventional reproductive phenotypes including sperm-egg cytoplasmic incompatibility, feminization of males, male-killing, and parthenogenesis [7, 8]. *Wolbachia* are essential endosymbionts of some filarial nematodes and recent studies demonstrated that the host immune response to these bacteria cause African river blindness and also contribute to lymphatic filariasis [9, 10]. One sixth of the world population is at risk of infection by *Wuchereria bancrofti*, *Brugia timori*, and *Brugia malayi*, the filarial nematode species that cause lymphatic filariasis [11]. *Wolbachia* released from filarial nematodes into the human body trigger an inflammatory reaction that underlies the lymphedema and corneal occlusion associated with these neglected diseases [12-22].

Although *Wolbachia* are widespread in nature and of great interest to both the basic and translational biomedical communities, the fundamental cell and molecular biology of *Wolbachia*-host interactions remain under explored. Consequently, there are a number of outstanding questions. Of particular significance is identifying the mechanisms that regulate *Wolbachia* abundance throughout various cell types in both its nematode and insect hosts. Additionally, do external factors such as diet influence *Wolbachia* abundance? While efficient germ line transmission of *Wolbachia* is well established, it remains unclear whether horizontal transmission plays a major role in the *Wolbahcia* life cycle. And if so, what are the mechanisms mediating cell-to-cell transfer of *Wolbachia*? My thesis directly addresses each of these issues. In addition, because *Wolbachia* is the cause of filarial nematode-based neglected diseases, these studies have enabled me to develop a strategy for high-throughput screening for novel anti-*Wolbachia* compounds that can be used to combat these diseases.

Wolbachia are obligate symbionts of filarial nematodes required for normal embryogenesis, larval development and most significantly adult survival [23-31]. A recent study demonstrated that loss of *Wolbachia* in the adult results in high levels of apoptosis throughout the nematode [27]. Studies have also found that much of the pathology associated with filarial nematode diseases is due to induction of innate and adaptive host immune responses upon release of *Wolbachia* from their nematode hosts [12-22]. These discoveries suggest that compounds directly targeting *Wolbachia* may be a powerful and complementary alternative to the conventional approaches for treating these diseases. The major advantage of this approach is that it targets adults as well as microfilaria and the *Wolbachia* will be eliminated prior to death of the nematode, reducing the destructive effects of the human immune response. Microfilaria is the first larval stage that is released from the adult nematodes. In addition, loss of *Wolbachia* leads to a slow death of the adults, providing time for the infected individual to clear the dead nematodes without deleterious side effects [24, 32-37].

Prior to my arriving in the lab, a cell line was created by Dr. Alain Debec from primary embryonic cultures of *Drosophila melanogaster* infected with *w*Mel *Wolbachia* strain [38]. *Wolbachia* is stably maintained in these cultures and exhibits a close association with microtubules as found in Drosophila somatic and germ line tissues [39, 40]. The cell line is called JW18 and expresses GFP-tagged Jupiter transgene. Jupiter is a microtubule-associated protein that labels microtubules and facilitates high-throughput, cell-based screening approaches [41]. Using these cells, we developed the first high-throughput screen to identify compounds that decrease *Wolbachia* titer. Chapter 2 discusses results of the first two libraries that we screened, from the Spectrum Collection and the National Cancer Institute, totaling 4,926 compounds. From the compounds screened, we found 40 that reduced *Wolbachia* titer. This chapter will discuss the structural similarities that we found as well as one drug metabolite, albendazole sulfone, which potentially targets *Wolbachia* FtsZ.

Working with the JW18 cells for the high-throughput screen, I discovered *Wolbachia* is capable of efficient cell-to-cell transfer. This discovery provided a unique opportunity to

explore the mechanisms of *Wolbachia* cell-to-cell transmission. In addition, these findings are in accord with previous reports of horizontal transmission between arthropods has also been documented in nature [42-44]. In these cases, the simplest routes of transmission appear to be the hemolymph or the gut, as *Wolbachia* present in these tissues can easily exit the host through excretion or injury and come into contact with an uninfected host [45]. Support for this route comes from previous studies demonstrating purified *Wolbachia* can remain viable in an extracellular environment and infect mosquito cell lines, ovaries, and testes when co-cultured [46, 47]. Indeed, *Wolbachia* cells injected into the hemolymph of an uninfected fly can navigate to the germ line after crossing multiple somatic tissues not only in Drosophila [48, 49] but also in parasitoid wasps [50]. It remains unclear how *Wolbachia* achieves this, as it must traverse a number of membrane and extracellular matrix barriers.

Insight into the mechanisms driving horizontal *Wolbachia* transmission will likely come from work on the well-studied mechanisms by which other pathogenic bacteria invade host cells, which can be categorized as mechanisms that utilize or alter internalization processes, such as pinocytosis, phagocytosis, and endocytosis [51]. Pinocytosis involves the invagination of specialized plasma membrane regions to form pockets that allow for the nonspecific entry of extracellular particles [52]. Phagocytosis involves the formation of membrane protrusions, driven by actin rearrangements, to engulf large receptor-bound particles [53]. However, the use of host cellular pathways for invasion often requires active manipulation by the microbe. Bacterial entry via modification of host cellular machinery is known to be accomplished via two general mechanisms, the clathrin-dependent “zipper method” and the bacterial effector-dependent “trigger method” [54]. In the zipper method, bacteria bind to receptors on the cell surface that induce actin extensions of the membrane through a clathrin-dependent pathway and serve to engulf the cell. Bacteria that utilize the trigger method synthesize type III secretion systems through which they secrete effector proteins to restructure the host cytoskeleton in order to facilitate attachment and invasion [54-56]. In addition, invasive microbes may also up- or downregulate host cellular signaling pathways to disable host

defenses and increase their own survival [57, 58]. While viruses primarily utilize the same pathways to enter host cells, some enveloped viruses can enter through passive membrane fusion by simply blending their host-derived envelope with the plasma membrane of a new host cell [59].

As mentioned, I realized that our *Wolbachia* infected cell lines, created for our high-throughput screen, are also the perfect system to research horizontal transmission. In Chapter 3, experiments relying on combinations of *Wolbachia* infected and uninfected cells in combination with fluorescence *in situ* hybridization (FISH) enabled us to show that horizontal transfer is independent of cell-to-cell contact, can efficiently take place within hours, and uses both host cell phagocytic and clathrin/dynamin-dependent endocytic machinery.

A major effort of my thesis project was to identify host factor that control the intracellular abundance of *Wolbachia*. To address this comprehensively, we employed a genome-wide RNA interference (RNAi) screen using the JW18 cells. We did this by modifying our existing high-throughput screen to identify genes instead of drugs that influence *Wolbachia* titer. Our approach was motivated by the success of a number of previous cell-based screens using Drosophila cell lines [60]. Using Drosophila cells, genome-wide RNAi screens were performed to identify host genes that alter *Listeria monocytogenes*, *Mycobacterium fortuitum*, *Chlamydia caviae*, and *Francisella tularensis* infection and proliferation [61-64]. We specifically assayed for RNAi-mediated gene knockdowns that either up- or down-regulate *Wolbachia* titer.

This screen revealed that host ubiquitin and proteolysis pathways play an especially critical role in maintaining *Wolbachia* titer. When this was further tested in *Drosophila melanogaster in vivo* we found that maintenance of *Wolbachia* titer relies on an intact host Endoplasmic Reticulum (ER) associated degradation (ERAD) system. This in combination with electron microscopy studies demonstrated that *Wolbachia* is intimately associated with the host ER and suggested a previously unsuspected mechanism for the potent ability of *Wolbachia* to prevent RNA virus replication.

In addition to host factors that regulate *Wolbachia* titer, we also examined the role of environmental factors in regulating *Wolbachia* abundance. Specifically we examined the effect of diet on *Wolbachia* titer in oocytes of *D. melanogaster*. The data demonstrate that yeast-enriched diets suppress *Wolbachia* titer while sucrose-enriched diets increase titer in the oocyte. Using genetic and chemical disruptions, we discovered that the somatic insulin and TORC1 pathways (Figure 5.1) are required for yeast-based suppression of oocyte *Wolbachia* titer. Using qPCR to determine *Wolbachia* titer body wide, we found that a yeast-enriched diet substantially increases somatic *Wolbachia* titer while sucrose-enriched diets show no change.

Chapter 2

A Cell-Based Screen Reveals that the Albendazole Metabolite, Albendazole Sulfone, Targets *Wolbachia*

2.1 Abstract

Wolbachia endosymbionts carried by filarial nematodes give rise to the neglected diseases African river blindness and lymphatic filariasis afflicting millions worldwide. Here we identify new *Wolbachia*-disrupting compounds by conducting high-throughput cell-based chemical screens using a *Wolbachia*-infected, fluorescently labeled Drosophila cell line. This screen identified several *Wolbachia*-disrupting compounds including three that resembled albendazole, a widely used anthelmintic drug that targets nematode microtubules. Follow-up studies demonstrate that a common albendazole metabolite, albendazole sulfone, reduces intracellular *Wolbachia* titer both in *Drosophila melanogaster* and *Brugia malayi*, the nematode responsible for lymphatic filariasis. Significantly, albendazole sulfone does not disrupt Drosophila microtubule organization, suggesting that this compound reduces titer through direct targeting of *Wolbachia*. Accordingly, both DNA staining and FtsZ immunofluorescence demonstrates that albendazole sulfone treatment induces *Wolbachia* elongation, a phenotype indicative of binary fission defects. This suggests that the efficacy of albendazole in treating filarial nematode-based diseases is attributable to dual targeting of nematode microtubules and their *Wolbachia* endosymbionts.

2.2 Introduction

Wolbachia are intracellular maternally transmitted bacteria present in the majority of all insect species as well as some mites, crustaceans and filarial nematodes [5, 6]. *Wolbachia* were initially studied in insects because they induce unconventional reproductive phenotypes including sperm-egg cytoplasmic incompatibility, feminization of males, male-killing, and

parthenogenesis [7, 8]. *Wolbachia* are essential endosymbionts of some filarial nematodes and recent studies demonstrated that they are the causative agent of African river blindness and also contribute to lymphatic filariasis [9, 10]. One sixth of the world population is at risk of infection by *Wuchereria bancrofti*, *Brugia timori*, and *Brugia malayi*, the filarial nematode species that cause lymphatic filariasis [11]. *Wolbachia* released from filarial nematodes into the human body trigger an inflammatory reaction that underlies the lymphedema and corneal occlusion associated with these neglected diseases [12-22].

Lymphatic filariasis and African river blindness have traditionally been treated through the administration of three drugs, singly or in combination: diethylcarbamazine (DEC), ivermectin (IVM) and albendazole (ALB). These drugs target the filarial nematodes associated with these diseases, namely *Onchocerca volvulus*, *B. timori*, *B. malayi*, and *W. bancrofti* [9, 10, 65]. DEC disrupts the nematodes by targeting the arachidonic acid metabolic pathway in the host [66]. IVM disrupts glutamate-gated chloride channels in the nematode that control release of excretory/secretory vesicles that would normally suppress the immune response [67, 68]. ALB is a benzimidazole used to disrupt the nematode microtubule cytoskeleton [69]. Orally administered ALB is rapidly metabolized in the intestinal mucosa and liver into albendazole sulfoxide (ALB-SO) and albendazole sulfone (ALB-SO2) [70, 71]. ALB-SO is normally considered to be the “active,” form of albendazole against systemic parasites, while ALB-SO2 is considered to be an inactive form of the drug [72]. All three drugs exhibit microfilaricidal effects [65]. The macrofilaricidal effects of ALB are not clear, though specific formulations induce worm sterility in animal models [73]. In addition, a number of clinical trials demonstrate that ALB when used in combination with DEC or IVM is macrofilaricidal [74-78].

Wolbachia are obligate symbionts of filarial nematodes required for normal embryogenesis, larval development and perhaps most significantly adult survival [23-31]. A recent study demonstrated that loss of *Wolbachia* in the adult results in high levels of apoptosis throughout the nematode [27]. Studies have also found that much of the pathology associated with

filarial nematode diseases is due to induction of innate and adaptive host immune responses upon release of *Wolbachia* from their nematode hosts [12-22]. These discoveries suggest that compounds directly targeting *Wolbachia* may be a powerful alternative to the more traditional approaches for treating these diseases. The major advantage of this approach is that it targets adults as well as microfilaria and the *Wolbachia* will be eliminated prior to death of the nematode, reducing the destructive effects of the human immune response. In addition, loss of *Wolbachia* leads to a slow death of the adults, providing time for the infected individual to clear the dead nematodes without deleterious side effects [24, 32-37]. Finally, antihelminthic drugs such as ivermectin, administered to patients co-infected with *Loa loa* nematodes, can potentially trigger lethal encephalitis [79]. *Loa loa* does not require or maintain *Wolbachia* and thus will not be affected by anti-*Wolbachia* therapies, thereby avoiding these deleterious side effects [80]. The promise of anti-*Wolbachia* based therapies in combating lymphatic filariasis has been demonstrated in clinical trials in which daily doses of doxycycline (DOX) for 4 weeks resulted in nematode sterility and death [10]. In addition, the pathologies associated with the infection, lymphedema and hydrocele, were dramatically reduced [12, 13].

These studies also revealed that a three-week course of DOX was insufficient to produce significant mortality of the adult nematodes, highlighting the need to identify more potent anti-*Wolbachia* compounds [81]. To this end, we generated a *Wolbachia*-infected Drosophila cell line and conducted an automated, cell-based screen to identify lead compounds that reduced intracellular *Wolbachia* infection. This screen of two libraries totaling 4,926 compounds identified 40 anti-*Wolbachia* compounds, including several that structurally resemble ALB. Our follow-up testing indicated that ALB-SO2 directly targets *Brugia* by depolymerizing its microtubules. Here we demonstrate that ALB-SO2 also disrupts *Brugia Wolbachia* independently of its effects on the *Brugia* cytoskeleton. Furthermore, ALB-SO2 treatment of *Brugia* led to visibly elongated *Wolbachia* morphology indicative of a binary fission failure, consistent with a direct impact of ALB-SO2 upon *Wolbachia*.

2.3 Results

Development of a Drosophila cell line constitutively infected with *Wolbachia*

To identify compounds that affect intracellular *Wolbachia* titer, we generated new Drosophila tissue culture cells constitutively infected with *Wolbachia* [82] (see Methods). There is currently no stable nematode tissue culture line, nor any type of cell line constitutively infected with *Wolbachia* derived from filarial nematodes. *Wolbachia*-infected insect cells provide an opportunity to identify drugs that disrupt *Wolbachia* through conserved molecular pathways. The cell line used for this study, JW18, is particularly amenable to high throughput screening as *Wolbachia* are maintained in approximately 90% or more of the host cell population (n = 1,053 cells scored). The *Wolbachia* load in 6.7% of infected cells ranges from 1–46 bacteria, while *Wolbachia* load in the other 93% of infected cells is obscured by crowding of the bacteria (n = 205 cells scored). The mitotic index of JW18 and tetracycline-cured JW18 cells, henceforth referred to as JW18TET, was 0.27% and 0.68% respectively, which are not significantly different according to Chi square tests (n = 1,876 and 2,339). Furthermore, no significant difference was observed in the frequency of binucleate cells between JW18 (9.1%, n = 873) and JW18TET cells (11%, n = 1,081). Thus, *Wolbachia* do not exert an obvious influence on the regulatory or structural mechanisms governing progression of the cell cycle in the JW18 cell line. However, this analysis does not preclude more subtle cycle cell effects.

To test whether *Wolbachia* exhibit normal interactions with the host cytoskeleton, we used a cell line that constitutively expresses a GFP-Jupiter fusion protein that binds to and labels microtubules [41] (Figure 2.1). During interphase, *Wolbachia* are closely associated with Jupiter-GFP-labeled microtubules (Figure 2.1A–B, Video S1). Live imaging demonstrates that *Wolbachia* move processively along those interphase microtubules (Video S2), consistent with earlier reports of *Wolbachia*-microtubule interactions [39, 40, 83, 84]. During

mitosis, *Wolbachia* were asymmetrically distributed throughout the cytoplasm in 82% of cells (n = 56, Figure 2.1C–F, Table S1), reminiscent of *Wolbachia* localization patterns observed in embryonic and larval neuroblasts [40]. These data indicate that *Wolbachia* distribution in the JW18 cell line is consistent with that of intact Drosophila tissues.

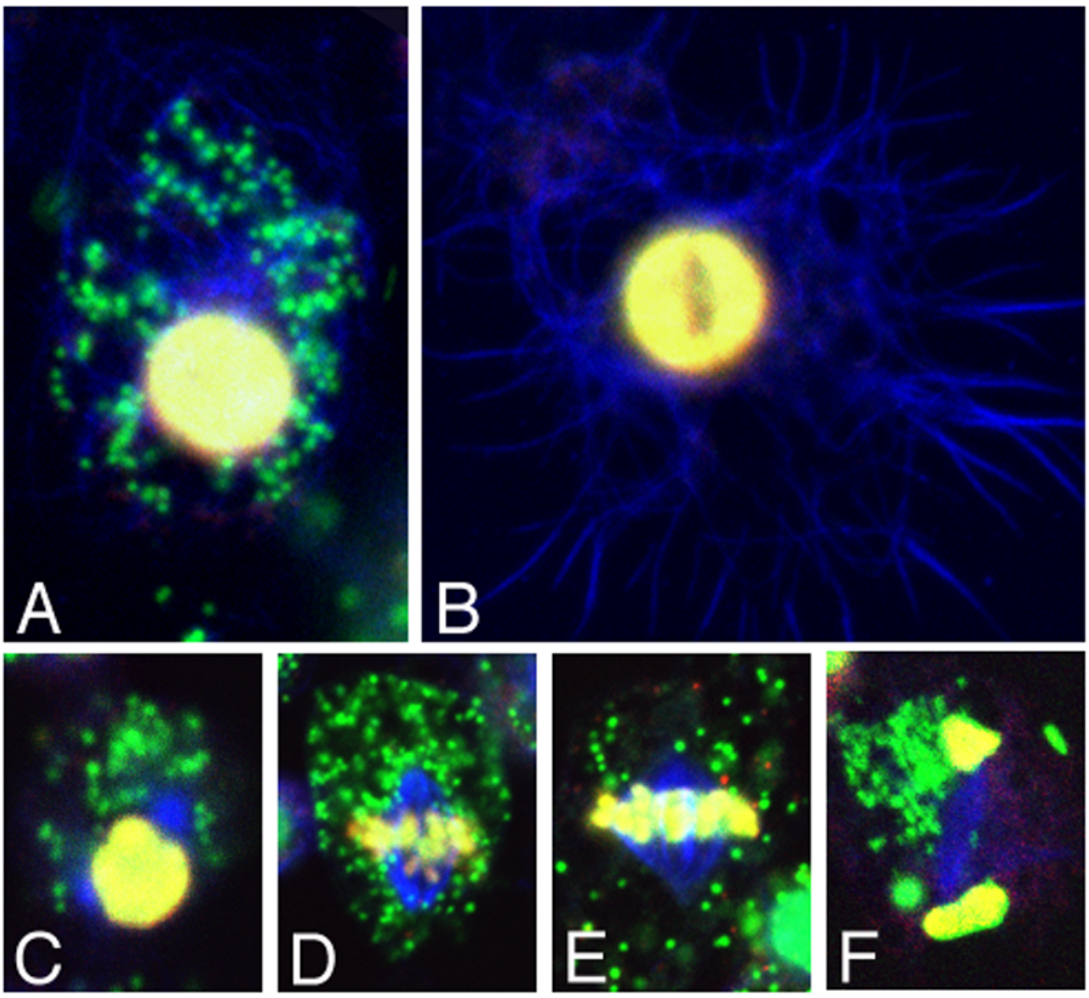

Figure 2.1: ***Wolbachia* distribution in JW18 cells.** Interphase of A) JW18 and B) JW18TET cells. Mitotic cells in C) prophase, D) prometaphase, E) metaphase, and F) late anaphase. Blue: Jupiter-GFP. Green: DAPI-labeled *Wolbachia*. Yellow: Histone H1 (A–B) and phospho-histone (C–F).

Automated cell based screening for anti-*Wolbachia* compounds

High-throughput cell-based screens using automated microscopy have proven effective in identifying new compounds targeting specific biological processes [85, 86]. Here we used the JW18 cell line in a 384 well format to screen 2,000 compounds from the Spectrum Collection and 2,926 compounds from the National Cancer Institute for reduction of *Wolbachia* titer. These libraries include structurally and functionally diverse synthetic compounds, FDA-approved drugs, compounds with biological activity and a set of natural products. After a 5-day incubation period, the cells were fixed, stained, and imaged using automated robotics (Figure S1, Methods). Customized software was used to analyze the images and score the percentage of *Wolbachia*-infected cells in each well. Treatment wells showing significant reduction of *Wolbachia*-infected cells in at least 2 of 3 replicates as compared to the JW18 control and the entire cell population in general were scored as preliminary hits. Compounds known to be generally hazardous were excluded, resulting in a finalized hit list.

18 compounds from the Spectrum library, and 22 compounds from the NCI library exhibited consistent, potent anti-*Wolbachia* activity in the screen (Figure 2.2, Table S2). A number of these compounds are already known to exert antimicrobial activity, consistent with expectations from the assay. For example, one of the hits CID484401 (totarol acetate) is a known inhibitor of the essential bacterial division protein, FtsZ [87]. CID42640 is a DNA damaging agent that has been shown to inhibit *Mycobacterium tuberculosis* [88]. Significantly, the hit CID313612 is structurally similar to CID42640. CID16524 (pyronin B) is a quaternary ammonium compound; many such compounds serve as the antimicrobial agents in commercial disinfectants [89]. An additional hit compound, CID6364517 has also been shown in a prior screen to exert antibacterial activity against *Streptococcus pyrogenes* (Pub-chem BioAssay AID1900 and AID1915, conducted by the Broad Institute). Furthermore, a number of chemotherapy drugs were identified by the screen: CID30323 (daunorubicin), CID31703 (doxorubicin), CID65348 (epirubicin) and CID4212 (mitoxantrone) were identified as hits, along with the derivatives CID5351490 (cinerubin B) and CID27590

(mitomycin B). Many of these drugs were originally isolated from bacteria in nature. It is presumed that these compounds are used to gain a competitive advantage over neighboring bacteria. As such, this class of drugs is referred to as to ‘‘anticancer antibiotics’’ [90-93].

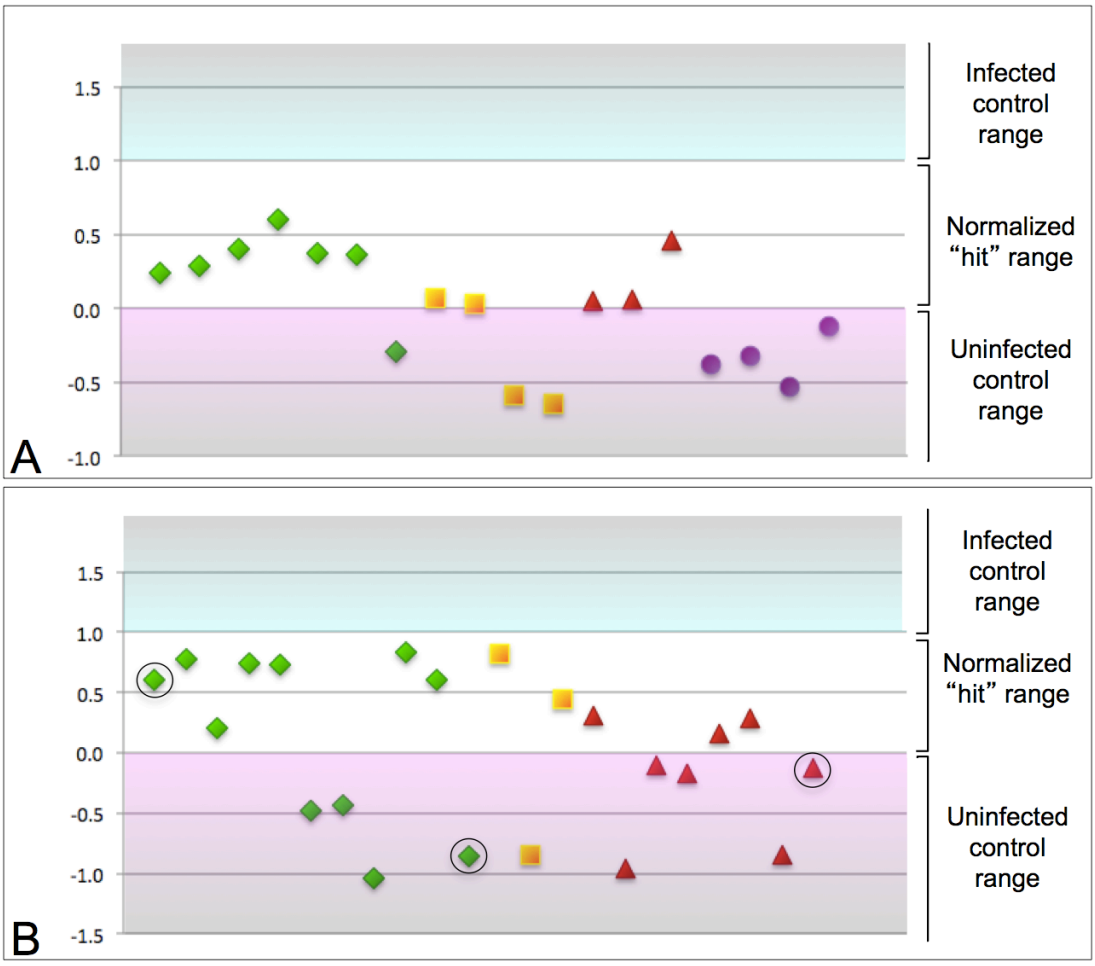

Figure 2.2: **Summary of screening hits.** The *Wolbachia* depletion activity of each finalized ‘‘hit’’ compound is displayed as a graphical plot. As the hit range for each plate varied slightly, the range for all plates was normalized to a span from 0–1 to enable a comparative display of all hits. A) Spectrum library hits. B) NCI library hits. Green triangles: hit compounds exhibiting low toxicity. Yellow squares: moderately toxic compounds. Red triangles: toxic compounds. Purple circles: toxicity of the compound unclear. Circled, from left to right: Albendazole-like hits CID5382764, CID5458770, and CID5351210.

Doxycycline (DOX) did not come up as a hit in this screen. This was unexpected as DOX has proven to be an effective anti-*Wolbachia* reagent in lab and clinical settings [10]. However, treating the same *Wolbachia* strain with DOX in the context of Drosophila

oogenesis revealed marked *Wolbachia* susceptibility to DOX (Figure 2.3A–C). This suggests that the mechanism accounting for this difference in DOX efficacy is dependent upon properties of the host cell rather than the *Wolbachia* strain. It may be that efflux pumps in the JW18 cell line are particularly effective at expelling DOX. Alternatively, the bacteriostatic effects of DOX may not readily be detected in our assay because of the relative growth rates of *Wolbachia* and the JW18 host cells. Regardless of the mechanism, it is not general, as this screen yielded a number of new potent anti-*Wolbachia* compounds.

To further investigate the hit compounds identified by the screen, we first examined their structures. This revealed that the benzimidazole CID5382764 and the benzthiazoles CID5458770 and CID5351210 share structural similarity to ALB, the widely used, FDA-approved anti-helmintic drug known for disrupting helminthic microtubules (Figure 2.4). The hit compounds were also assessed for cytotoxicity by consulting prior screens run by the NCI against human cancer cell lines and measuring the impact of the compounds on cell proliferation in our own assay. This indicated that 11 of 22 hits from the NCI library and 7 of 18 hits from the Spectrum library exhibit unacceptable toxicity levels, while the remaining 22 hit compounds exhibited low or unknown cytotoxicity (Figure 2.2, Table S2). By this measure, two of the ALB-like compounds, CID5458770 and CID5382764, were indicated to be non-toxic (Figure 2.2).

Albendazole-like compounds reduce *Wolbachia* titer in Drosophila oogenesis

Drosophila has proven a particularly effective model system for *in vivo* compound testing of a wide array of biological processes [94]. Here we used the Drosophila oocyte as a secondary screen for retesting the ALB-like hits identified in the cell-based screen.

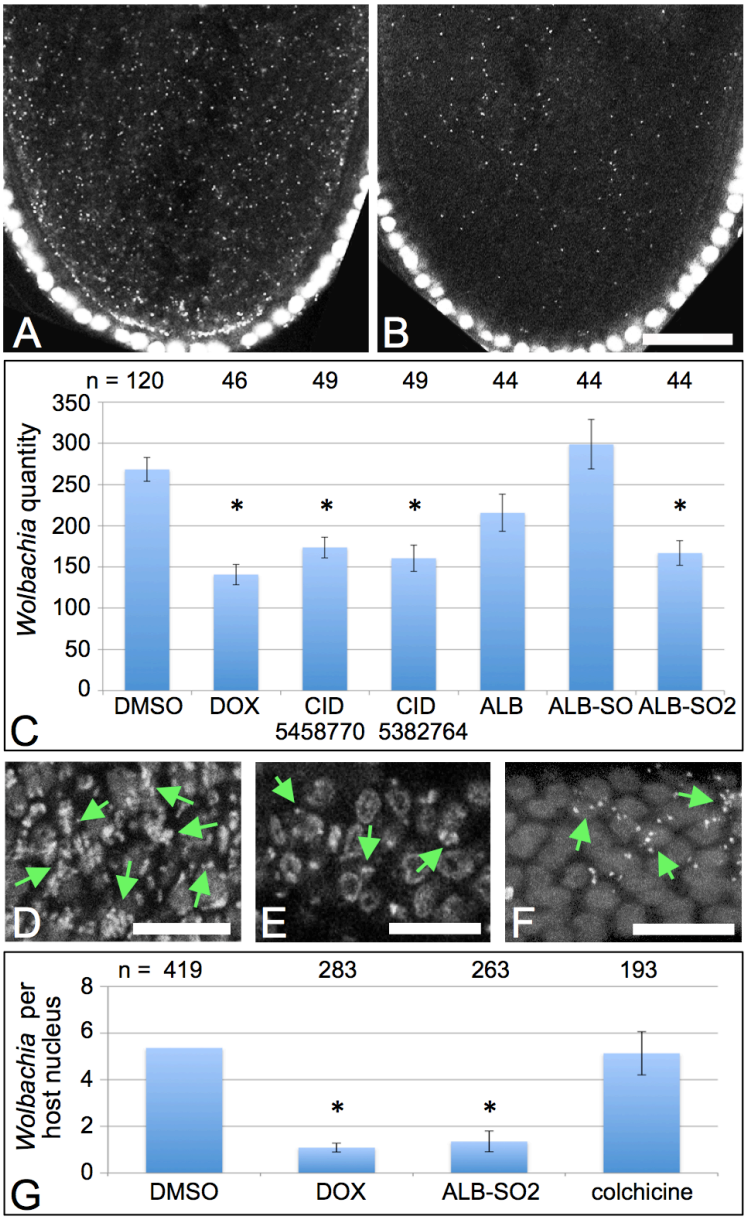

Figure 2.3: **Albendazole-like compounds suppress *Wolbachia* titer in both *D. melanogaster* and *B. malayi*.** Propidium iodide staining indicates host DNA as large circles and *Wolbachia* as small puncta. A–C) Assessment of *Wolbachia* titer in stage 10A *D. melanogaster* oocytes. Posterior pole is down. A) DMSO control. B) Doxycycline-treated. C) Average quantity of *Wolbachia* detected in single oocyte focal planes. D–F) *Wolbachia* staining in the *B. malayi* mitotic proliferation zone. Green arrows indicate *Wolbachia* puncta. D) DMSO control. E) Doxycycline-treated. F) Albendazole sulfone-treated. G) Average quantity of *Wolbachia* per host nucleus in the distal ovary of treated *Brugia malayi*. Conditions that significantly deplete *Wolbachia* are indicated by asterisks. Scale bars: A–B) 30 mm. D–F) 10 mm.

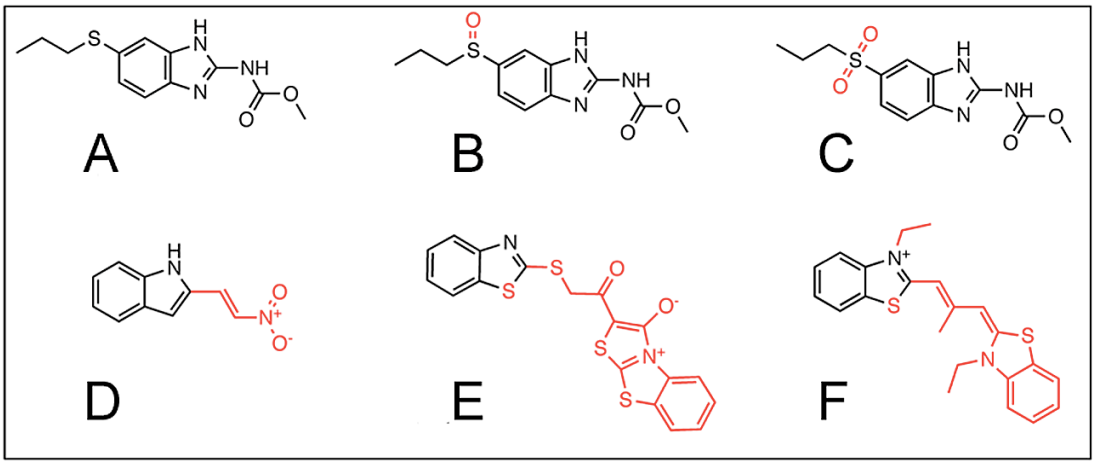

Figure 2.4: **Chemical Structures of Albendazole, Albendazole metabolites and the Albendazole-like NCI hit compounds.** Structural differences from the parent compound are indicated in red. A) ALB. B) ALB-SO. C) ALB-SO2. D) CID5382764. E) CID5458770. F) CID5351210.

This system provides the advantages that the *Wolbachia* strain is the same as in the JW18 cell line, and *Wolbachia* titer in the oocyte is known to greatly increase between stage 3 and 10A, approximately a 40-hour period [83, 95, 96]. Starved adult Drosophila were fed yeast paste containing compounds at a concentration of 100 uM for 24 hours. Stage 10A oocytes were fixed and labeled, followed by imaging and quantification of their *Wolbachia* as described in the Methods. Average titer measurements from single focal planes have been shown to be representative for comparing *Wolbachia* titer between different conditions [95]. DMSO control oocytes exhibited 268+/-214.3 *Wolbachia* within a single oocyte focal plane (Figure 2.3A–C). Oocytes treated with DOX exhibited 141+/-212.4 *Wolbachia* ($p < 0.001$). Treatments with CID5458770 yielded oocytes displaying 174+/-212.7 *Wolbachia* ($p<0.001$). Furthermore, CID5382764-treated oocytes exhibited 161+/-215.9 *Wolbachia* ($p<0.001$, Figure 2.3). Thus, both of the non-toxic, ALB-like hits identified by the cell screen deplete *Wolbachia* titer in Drosophila oogenesis similarly to DOX.

These results motivated us to determine whether ALB and its common metabolites, ALB-SO and ALB-SO2 (Figure 2.4), also affect *Wolbachia* titer *in vivo*. *Wolbachia* counts from single

oocyte focal planes indicated that ALB and ALB-SO treatments did not significantly affect *Wolbachia* titer, with 216+/-222.5 and 299+/-230.0 *Wolbachia* detected per oocyte, respectively (Figure 2.3C). However, ALB-SO2-treated oocytes exhibited markedly fewer *Wolbachia* than the control, with 167+/-214.8 *Wolbachia* evident per oocyte ($p<0.001$, Figure 2.3). This indicates that the ALB-SO2 metabolite exerts anti-*Wolbachia* effects in Drosophila.

Albendazole sulfone disrupts *Wolbachia* titer in *B. malayi*

To investigate whether the anti-*Wolbachia* effect of ALB-SO2 applies to a disease model, we treated adult *B. malayi* nematodes *in vitro*. After a 3-day incubation period, *Wolbachia* were imaged in the distal tip region of the *Brugia* ovary referred to as the ‘‘mitotic proliferation zone’’ due to enriched replication of host nuclei in this tissue [97]. *Wolbachia* densely populate this region of the distal ovary in DMSO controls (Figure 2.3D). By contrast, *Wolbachia* titer is visibly depleted in worms treated with either ALB-SO2 or DOX (Figure 2.3E–F). Quantitation of *Wolbachia* further supports this observation, with DMSO-treated *Brugia* exhibiting 5.4 *Wolbachia* on average per host nucleus (n = 419 bacteria scored). By contrast, ALB-SO2-treated worms carried significantly fewer bacteria, exhibiting 1.3+/-20.45 *Wolbachia* per host nucleus (n = 263) ($p<0.001$). This depletion was similar to DOX-treated worms, which exhibited 1.1+/-20.19 *Wolbachia* per host nucleus (n = 283) ($p<0.001$). This indicates that the *Wolbachia*-depleting impact of ALB-SO2 extends to *B. malayi*.

Albendazole sulfone has no impact on microtubule organization in Drosophila

A consistent *Wolbachia*-disrupting effect for ALB-SO2 raises the question of the mechanism of action of this metabolite. ALB and other benzimidazoles are known to bind to beta-tubulin and disrupt microtubule polymerization [98-101]. Previous studies from Drosophila have demonstrated that *Wolbachia* titer is affected by host microtubules [83, 95]. This raised the possibility that the reduction of *Wolbachia* titer upon exposure to ALB-SO2 is due to an impact of this compound on microtubule organization. Prior mutant studies identified key

amino acids within beta tubulin that are important for the microtubule-disrupting impact of benzimidazoles. Residues N165 and Y200 are thought to form a hydrogen bond that restricts accessibility to a benzimidazole binding site [102]. Interestingly, most of the beta tubulin homologs in Drosophila encode the residues that correspond to benzimidazole resistance (Figure S2). This suggested that the Drosophila microtubule cytoskeleton should be unaffected by ALB-SO2 treatment.

To test whether ALB-SO2 affects microtubule organization in Drosophila oogenesis, a combination of approaches was used. Intracellular *Wolbachia* localization was examined, taking advantage of the prior finding that *Wolbachia* concentrate at the oocyte posterior cortex in a microtubule-dependent manner [84, 103]. In this study, posterior *Wolbachia* localization was detected in 95% of DMSO controls and 93% of ALB-SO2-treated oocytes ($n = 56$ and 46, respectively, Figure 2.5G–H). This differed significantly from oocytes treated with the microtubule-disrupting drug, colchicine, where only 21% exhibited posterior *Wolbachia* localization ($p < 0.001$, $n = 13$, Figure 2.5I) [84]. The Drosophila oocyte cytoskeleton was also directly examined by immunolabeling microtubules [104]. Stage 10B oocytes are known to undergo large-scale, microtubule-dependent cytoplasmic streaming, coincident with formation of microtubule bundles. As cytoplasmic streaming is a highly dynamic process, this bundling varies somewhat between oocytes, and changes within individual oocytes over time [104, 105]. DMSO controls and oocytes treated with ALB-SO2 exhibited microtubule bundling at stage 10B, while the cytoplasm of colchicine-treated stage 10B oocytes was devoid of filamentous structures (Figure 2.5J–L) [105]. Thus, ALB-SO2 did not affect the overall orientation or structure of the oocyte microtubule cytoskeleton in Drosophila oocytes, though this compound dramatically decreases *Wolbachia* titer (Figure 2.3). This indicates that ALB-SO2 reduces *Wolbachia* titer through a microtubule-independent mechanism in Drosophila.

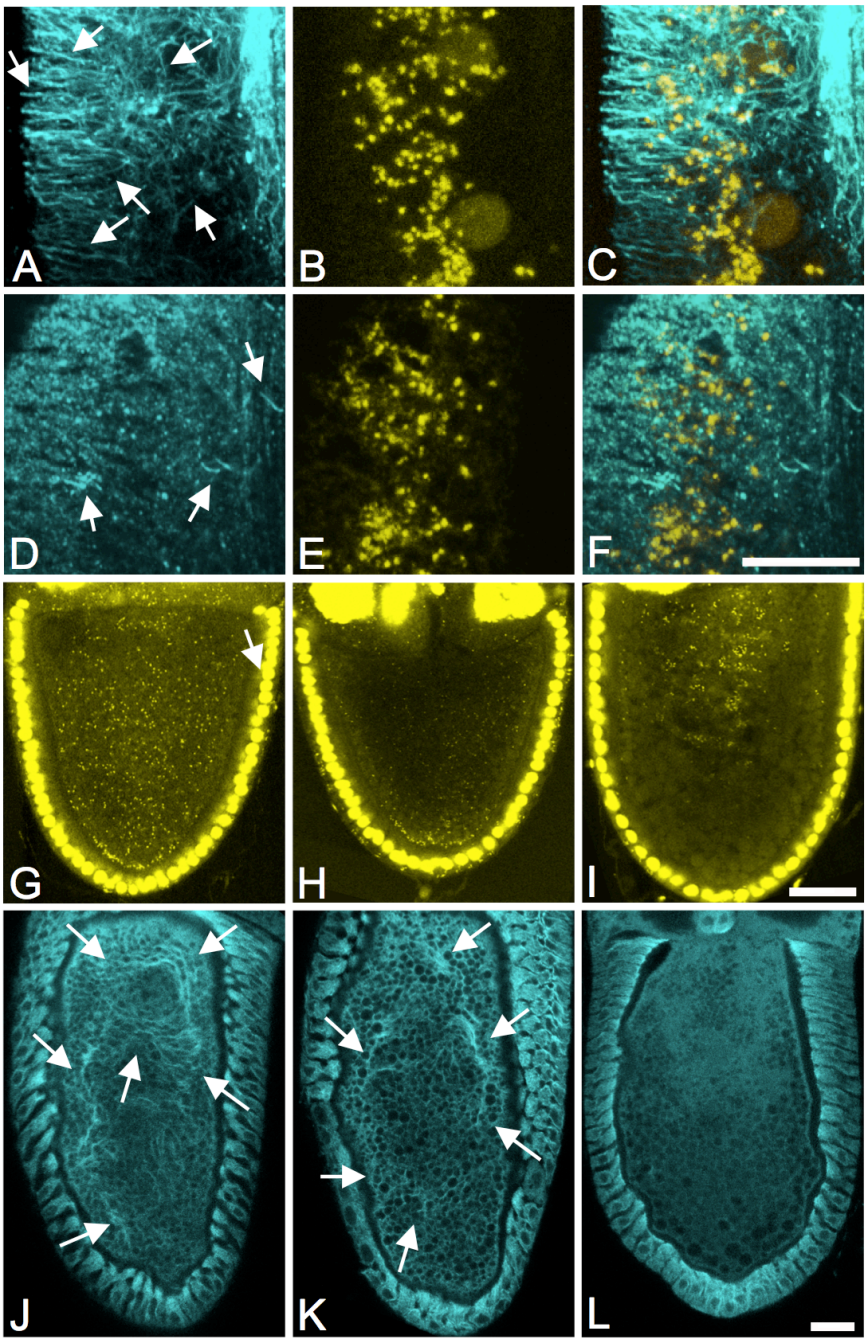

Figure 2.5: **ALB-SO2 visibly disrupts microtubules in *Brugia*, but not in *D. melanogaster*.** A–F) Images from the *Brugia* lateral chord. A–C) DMSO control. D–F) ALB-SO2-treated. G–I) Propidium iodide labeling in stage 10A *Drosophila* oocytes. G) DMSO control. H) ALB-SO2-treated. I) Colchicine-treated. J–L) Anti-alpha tubulin staining in stage 10B oocytes. J) DMSO control. K) ALB-SO2-treated. L) Colchicine-treated. Arrows indicate microtubule bundles. Scale bars: A–F) 12 mm. G–L) 30 mm.

Albendazole sulfone disrupts *Wolbachia* titer in *Brugia* via a microtubule-independent mechanism

The findings above raised the question of whether ALB-SO2 disrupts *Wolbachia* titer independently of microtubules in *B. malayi*, analogous to *Drosophila*. The beta-tubulin genes of *B. malayi* carry the amino acid changes of N165S and Y200F that are associated with susceptibility to benzimidazoles like ALB-SO2 (Figure S2). To assess the impact of ALB-SO2 on *B. malayi* microtubules *in vivo*, whole-mount immunostaining was performed. Examination of *Brugia* hypodermal chords revealed a dense meshwork of microtubules in DMSO-treated controls (Figure 2.5A–C). In contrast, treatment with ALB-SO2 disrupted the *Brugia* microtubule cytoskeleton, although linear remnants remained visible throughout the hypodermal chord (Figure 2.5D–F). This demonstrates that ALB-SO2 disrupts much of the host microtubule cytoskeleton in *B. malayi*.

To determine whether the titer of *Brugia Wolbachia* relies upon host microtubules, we treated *B. malayi* with colchicine. To verify that colchicine disrupts microtubules in *B. malayi*, immunostaining was performed in the hypodermal chords of colchicine-treated worms as above. This analysis revealed that microtubule structure and organization was largely eliminated by colchicine treatment. To then assess the impact of colchicine on *Wolbachia* titer, *Wolbachia* were imaged in the distal ovary. Interestingly, colchicine-treated worms exhibited an average of 5.1+/-20.93 *Wolbachia* per host nucleus (n = 193 bacteria scored), a value that is not significantly different from its DMSO controls by Chi square test (Figure 2.3G). This indicates that microtubule disruption has little impact on *Wolbachia* titer in *B. malayi*. This suggests that ALB-SO2 is also unlikely to suppress *Wolbachia* titer through its microtubule-disrupting effects, and implicates a microtubule-independent mechanism for ALB-SO2 suppression of *Wolbachia* titer in *B. malayi*.

Albendazole sulfone induces *Wolbachia* elongation in *B. malayi* ovary

To further pursue the mechanism by which ALB-SO2 disrupts *Wolbachia*, we examined its impact on *Wolbachia* morphology in *Brugia* tissue. In the mitotic proliferation zone of the distal ovary, ALB-SO2 treatment corresponded to elongation of *Wolbachia* nucleoids as compared to DMSO controls (Figure 2.6C–F). *Wolbachia* were also immunostained with an antibody raised against *Wolbachia* FtsZ, which crisply defines the boundaries of the *Wolbachia* cytoplasm [106]. The FtsZ staining also revealed an elongated *Wolbachia* morphology in ALB-SO2-treated *Brugia* relative to the DMSO control (Figure 2.6G–H). Furthermore, quantification of *Wolbachia* length indicated that only 2.5% of *Wolbachia* in the DMSO controls exceeded 2.5 mm in length, whereas 17% of *Wolbachia* in ALB-SO2 treated worms exceeded this length (n = 201 and 126, respectively) ($p<0.001$) (Figure 2.6I). This demonstrates that ALB-SO2 induces *Wolbachia* elongation in the *Brugia* ovary.

Wolbachia were also examined in the hypodermal chords, which are syncytial somatic tissues that run along the entire length of the *Brugia* body wall. Comparing *Wolbachia* in DMSO and ALB-SO2-treated hypodermal chords revealed little difference in bacterial morphology (Figure 2.6A–B). This indicates that *Wolbachia* in the hypodermal chord do not respond to ALB-SO2, in contrast to *Wolbachia* in the distal ovary of *B. malayi*.

***Wolbachia* elongation occurs independently of host microtubules**

A role for ALB-SO2 in inducing *Wolbachia* elongation could be due to an indirect effect from disrupting host microtubules, or through an alternative mechanism. To distinguish between these possibilities, *B. malayi* ovaries were treated with colchicine and assessed for *Wolbachia* length. Examination of DMSO vs. colchicine-treated *Brugia* revealed no obvious differences in *Wolbachia* morphology between conditions (Figure 2.6J–K). *Wolbachia* length was also quantified, and neither DMSO nor colchicine-treated tissues harbored *Wolbachia* exceeding 2.5 mm in length (Figure 2.6I). This differs significantly from ALB-SO2-treated *Wolbachia*, which frequently exceeded 2.5 mm in length ($p < 0.001$) (Figure 2.6I). Thus,

overall microtubule disruption in *Brugia* did not change *Wolbachia* morphology as was seen for ALB-SO2 treatment. This indicates that ALB-SO2 induces *Wolbachia* elongation independently of host microtubules in *Brugia malayi*.

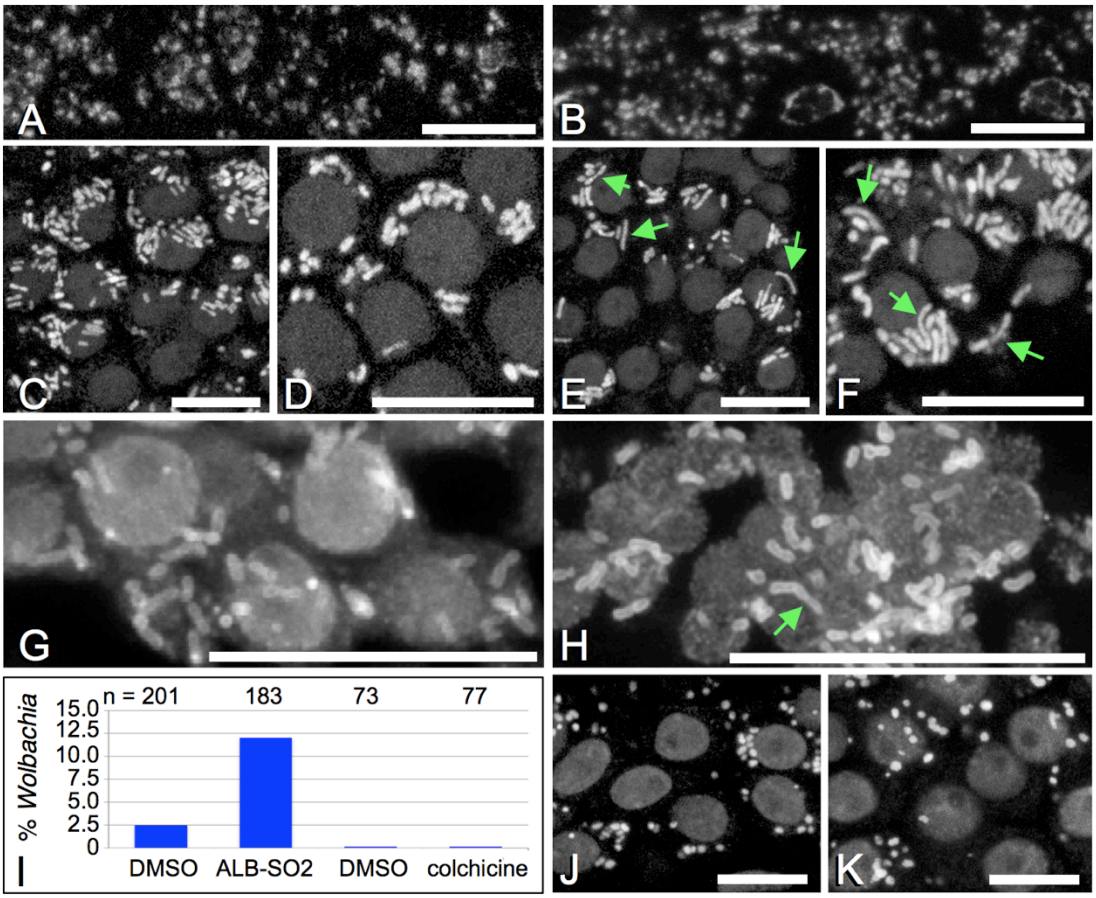

Figure 2.6: **ALB-SO2 treatment induces *Wolbachia* elongation in the Brugia ovary, but not in the lateral chords.** Green arrows indicate highly elongated *Wolbachia*. A–B) DNA staining is shown in the lateral chords. A) DMSO control. B) ALB-SO2-treated. C–F) DNA staining in the mitotic proliferation zone of the distal ovary. C–D) DMSO control. E–F) ALB-SO2-treated. G–H) FtsZ stain indicates *Wolbachia* (rod shapes) as well as host nuclear background. These panels represent maximum projections of 25 individually captured focal planes. I) Percentage of *Wolbachia* population exceeding 2.5 mm in treated *Brugia* ovaries. J–K) DNA stain in DMSO control (J) vs. a colchicine-treated ovary (K). Scale bars: 10 mm.

2.4 Discussion

Here we report the first high-throughput cell-based screen using automated microscopy to identify anti-*Wolbachia* compounds. The cell line used in this screen was established from primary culture preparations from *Wolbachia*-infected *Drosophila* embryos bearing the GFP-tagged microtubule binding protein Jupiter (Figure 2.1). *Wolbachia* have been stably maintained and transmitted in this line for years. Live analysis of interphase JW18 cells reveals that *Wolbachia* closely associate with and move along microtubules (Video S1), consistent with previous studies showing that *Wolbachia* transport and positioning are microtubule-dependent [40, 83, 84]. Although there is variability from generation to generation, approximately 90% of JW18 cells are infected with variable amounts of bacteria. This is consistent with previous studies of *Wolbachia*-infected *Drosophila*, *Spodoptera frugiperda* and *Aedes albopictus* cell lines showing widely variable bacteria loads per cell [107-112]. Perhaps this variation in *Wolbachia* load is due in part to asymmetric partitioning of *Wolbachia* in mitotic JW18 cells (Figure 2.1, Table S1). This same *Wolbachia* strain has previously been reported to segregate asymmetrically in mitotic embryonic *Drosophila* neuroblasts and Aa23 tissue culture cells [40, 110]. In addition, variants have been identified in *D. simulans* in which asymmetric segregation of Wolbachia may occur in the germ line stem cells of the oocyte [113]. This contrasts with other evidence that *Wolbachia* partition evenly during mitosis in early *Drosophila* embryogenesis and in *A. albopictus* C7-10R tissue culture cells [40, 111]. Future work is needed to address the underlying mechanisms that govern segregation of *Wolbachia* in mitotic cells.

Our automated, image-based screens of 4,926 compounds from the NCI and Spectrum libraries revealed 40 compounds that depleted *Wolbachia* titer. Of these, 22 were classified as either non-toxic or of unknown toxicity (Figure 2.2, Table S2). Among the more characterized hit compounds, we identified totarol acetate, an inhibitor of the key bacterial division protein, FtsZ. This finding is consistent with a previous report describing FtsZ as a potential target for anti-*Wolbachia* therapy [114]. We also identified pararosaniline pamoate

and pyrvinium pamoate as *Wolbachia*-depleting hits. These drugs have been employed as antihelmintics to treat patients infected with roundworms like *Enterobius vermicularis* and the trematode *Schistosoma japonicum* [115, 116]. Our result raises an additional possibility that these hosts rely upon endosymbiotic bacteria to support their viability, and an anti-bacterial effect of these drugs thus indirectly compromises the host. No other *Secernentea* outside of the *Filariodea* have been reported to carry *Wolbachia* to date, though the *Rhabditida* order is the only one to have been systematically tested [117]. However, the Trematodes *Acanthatrium oregonense* and *Nanophyetus salmincola* have been reported to harbor the mutualistic bacteria *Neorickettsia risticii* and *N. helminthoseca*, respectively [118]. Furthermore, estradiol was also identified by our screen as a *Wolbachia*-depleting compound. This finding may help to explain why women exhibit symptoms of lymphatic filariasis less often than men in endemic areas, where 10% or fewer of females exhibit symptoms as compared to 10–50% of men [119]. Since *Wolbachia* can induce a TLR-2 and TLR-6-mediated inflammatory response analogous to that observed in lymphatic filariasis patients, the literature invokes a contribution of *Wolbachia* to the pathology of lymphatic filariasis [12-14, 19-21]. Perhaps higher estradiol levels in female patients help to suppress *Wolbachia* load, thereby preventing TLR-2/6 induction and development of lymphatic filariasis symptoms.

An examination of the largely uncharacterized hits from the JW18 screen revealed that CID5458770, CID5382764 and CID5351210 structurally resemble ALB (Figure 2.4). Follow-up studies revealed that the non-toxic ALB-like compounds CID5458770 and CID5382764 exhibited *Wolbachia*-depleting activity in *Drosophila* oogenesis as well. This raised the possibility that ALB or its metabolites may have a similar activity *in vivo*. These studies surprisingly revealed that the ALB-SO2 metabolite depleted intracellular *Wolbachia* titer in *Drosophila* oogenesis, while ALB and ALB-SO did not (Figure 2.3). Furthermore, ALB-SO2 disrupts *Wolbachia* titer and morphology and alters host microtubules in *B. malayi* (Figure 2.3, 2.5, 2.6). These findings contrast with routine descriptions in the literature of ALB-SO2

as an inactive metabolite. It appears that ALB-SO2 inactivity has been interpreted from the lower abundance of the ALB-SO2 metabolite in human serum and urine relative to ALB-SO [70-72] as well as the relatively weaker ability of ALB-SO2 to compete against unlabeled benzimidazoles for binding to *Haemonchus contortus* tubulin *in vitro* [100]. However, the sequence of *Brugia* beta tubulin predicts susceptibility to benzimidazoles like ALB-SO2 (Figure 2.4, Figure S2), and evidence from other non-nematode systems supports a role for ALB-SO2 as an active metabolite. An *in vitro* competitive binding assay using colchicine showed that ALB-SO2 is slightly better at disrupting polymerization of A*scaris suum* tubulin than either ALB or ALB-SO [120]. Studies from the tapeworm *Echinococcus multilocularis* showed ALB-SO2 to be similarly effective to ALB-SO in inducing structural defects and worm lethality. Other studies of the microsporidian parasites *Encephalitozoon cuniculi*, *E. hellem*, and *E. intestinalis* indicated that ALB-SO2 is at least 5 times more effective at inhibiting growth than either ALB or ALB-SO [121]. Building upon those prior findings, this study is the first we are aware of to definitively show an active role for the ALB-SO2 metabolite in filarial nematodes.

A surprising outcome from this study was that ALB-SO2 disrupts *Wolbachia* independently of its effects on host microtubules. Previous studies have shown that host microtubules and microtubule-based motor proteins facilitate replication of Salmonella and Chlamydia [122-129]. Prior work in *Drosophila* indicates that normal levels of *Wolbachia* rely in part upon intact host microtubules as well [83, 95]. This study confirms that *Brugia* microtubules are vulnerable to ALB-SO2 *in vivo*, raising the possibility that ALB-SO2 acts indirectly upon *Wolbachia* through the host cytoskeleton. However, colchicine treatments that eliminate *Brugia* microtubules had no significant impact on *Wolbachia* titer or elongation. Furthermore, ALB-SO2 suppressed *Wolbachia* titer in *Drosophila* even though there was no detectable impact on host microtubules in this system. Thus, ALB-SO2 does not disrupt *Wolbachia* through an influence on the host microtubule cytoskeleton.

The elongation of *Wolbachia* induced by ALB-SO2 suggests a possible mechanism of action for this compound. It has been widely documented that extensive bacterial elongation, referred to as filamentation, ensues when binary fission is disrupted, due to continued growth of the bacteria despite the failure of abscission [101, 130]. Thus, *Wolbachia* elongation in ALB-SO2-treated ovaries suggests that ALB-SO2 is preventing abscission of growing and replicating *Wolbachia*. By contrast, ALB-SO2 treatment had no visible impact on *Wolbachia* length in *Brugia* hypodermal chords. This suggests that the *Wolbachia* bacteria residing within the hypodermal chord are in a non-growing steady state as compared to the proliferating *Wolbachia* population in the distal region of the *B. malayi* ovary. If confirmed, this implies that bacteriostatic drugs may not be effective at clearing *Wolbachia* from the hypodermal chords.

ALB-SO2 could disrupt *Wolbachia* binary fission by targeting a number of different factors. Proper binary fission relies upon assembly of FtsZ filaments at the future fission site, which then leads to recruitment of numerous other factors that help stabilize and constrict the division septum [131]. ALB has been shown to suppress titer and induce filamentation of *Mycobacterium tuberculosis* [132], and numerous studies demonstrate that ALB-like compounds target and disrupt FtsZ in *Staphylococci*, *Escherichia coli* and *M. tuberculosis* [101, 132-143]. A role for ALB-SO2 in disrupting *Wolbachia* FtsZ function would be consistent with this body of work. However, given staining variability and resolution limits of the *Brugia* system, it is not currently possible to distinguish whether FtsZ concentration or distribution *in vivo* is significantly different between DMSO and ALB-SO2-treated conditions. An alternative possibility is that ALB-SO2 disrupts binary fission without directly targeting FtsZ. For example, some ALB-like compounds can intercalate into DNA and thus serve as potential DNA damaging agents [101]. DNA damage is known to induce the FtsZ-inhibitor SulA, leading to bacterial filamentation [144, 145]. It is further possible that ALB-SO2 targets other as-yet unrecognized factors that are key to initiation and execution of *Wolbachia* binary fission.

This study has redefined the mechanism by which ALB acts against filarial nematodes. Building upon work by others, the data of this study suggest that ALB administered to humans disrupts *B. malayi* by a two-fold impact. First, ALB and its metabolites disrupt the filarial microtubule cytoskeleton, leading to rapid death of microfilariae. Second, our study indicates that the ALB-SO2 metabolite is directly targeting *Wolbachia*. Certain formulations of ALB were previously shown to lead to *Brugia* sterility in animal models, but the mechanism underlying this effect was unclear [73]. It is possible that microtubule disruption by ALB and its metabolites directly compromises the structure of the adult germ line in *Brugia*. However, DOX-based elimination of *Wolbachia* from the female germ line has also been shown to induce apoptosis in germ line cells [27]. Perhaps ALB-SO2-mediated disruption of *Wolbachia* contributes further to destruction of the *Brugia* germ line. ALB-SO2 may serve as a valuable asset in the campaign against *Wolbachia*-based disease. Used in tandem with conventional antibiotics, ALB-SO2 may shorten the effective treatment time of anti-*Wolbachia* treatments from the current 4 to 6 weeks [9, 10]. It is likely that more potent derivatives of ALB-SO2 may be discovered with enhanced the specificity for *Wolbachia*. Identification of the ALB-SO2 target will enable optimization of the compound to provide a possible alternative route for future treatment of African river blindness and lymphatic filariasis.

Chapter 3

Mechanisms of Horizontal Cell-to-Cell Transfer of *Wolbachia* in *Drosophila melanogaster*

3.1 Abstract

Wolbachia is an intracellular endosymbiont present in most arthropod and filarial nematode species. Transmission between hosts is primarily vertical, taking place exclusively through the female germ line, although horizontal transmission has also been documented. The results of several studies indicate that *Wolbachia* can undergo transfer between somatic and germ line cells during nematode development and in adult flies. However, the mechanisms underlying horizontal cell-to-cell transfer remain largely unexplored. Here, we establish a tractable system for probing horizontal transfer of *Wolbachia* between *Drosophila melanogaster* cells in culture using fluorescence *in situ* hybridization (FISH). First, we show that horizontal transfer is independent of cell-to-cell contact and can efficiently take place through the culture medium within hours. We further demonstrate that efficient transfer utilizes host cell phagocytic and clathrin/dynamin-dependent endocytic machinery. Lastly, we provide evidence that this process is conserved between species, showing that horizontal transfer from mosquito to *Drosophila* cells takes place in a similar fashion. Altogether, our results indicate that *Wolbachia* utilizes host internalization machinery during infection, and this mechanism is conserved across insect species

3.2 Introduction

Wolbachia are intracellular bacteria that are transmitted through the female germ lines of arthropods and filarial nematodes [7, 84]. In arthropods, *Wolbachia* function as either a mutualist or a parasite, while in filarial nematodes, *Wolbachia* are essential for host survival. Efficient maternal transmission of *Wolbachia* cells in *Drosophila melanogaster* requires their localization to the posterior cortex of the developing embryo, as this is the future site of the

germ line [6]. In filarial nematodes, *Wolbachia* cells undergo a precise pattern of migration during host development that involves not only asymmetric mitotic segregation but also the invasion of germ line precursors from somatic cells [106]. Thus, the ability of *Wolbachia* to undergo cell-to-cell transfer plays an important role in maintaining vertical transmission [146].

While *Wolbachia* are primarily vertically transmitted, horizontal transmission between arthropods has also been documented in nature [42-44]. In these cases, the simplest routes of transmission appear to be the hemolymph or the gut, as *Wolbachia* present in these tissues can easily exit the host through excretion or injury and come into contact with an uninfected host [45]. Support for this route comes from previous studies that found that purified *Wolbachia* can remain viable in an extracellular environment and infect mosquito cell lines, ovaries, and testes when co-cultured [46, 47]. Indeed, *Wolbachia* cells injected into the hemolymph of an uninfected fly can navigate to the germ line after crossing multiple somatic tissues not only in *Drosophila* [48, 49] but also in parasitoid wasps [50]. It remains unclear how *Wolbachia* achieves this, as it must traverse a number of membrane and extracellular matrix barriers.

Insight into the mechanisms driving horizontal *Wolbachia* transmission will likely come from work on the well-studied mechanisms by which other pathogenic bacteria invade host cells, which can be categorized as mechanisms that utilize or alter internalization processes, such as pinocytosis, phagocytosis, and endocytosis [51]. Pinocytosis involves the invagination of specialized plasma membrane regions to form pockets that allow for the nonspecific entry of extracellular particles [52]. Phagocytosis involves the formation of membrane protrusions, driven by actin rearrangements, to engulf large receptor-bound particles [53]. However, the use of host cellular pathways for invasion often requires active manipulation by the microbe. Bacterial entry via modification of host cellular machinery is known to be accomplished via two general mechanisms, the clathrin-dependent “zipper method” and the bacterial effector-dependent “trigger method” [54]. In the zipper method, bacteria bind to receptors on the cell surface that induce actin extensions of the membrane through a clathrin-dependent pathway

and serve to engulf the cell. Bacteria that utilize the trigger method synthesize type III secretion systems through which they secrete effector proteins to restructure the host cytoskeleton in order to facilitate attachment and invasion [54-56]. In addition, invasive microbes may also up- or downregulate host cellular signaling pathways to disable host defenses and increase their own survival [57, 58]. While viruses primarily utilize the same pathways to enter host cells, some enveloped viruses can enter through passive membrane fusion by simply blending their host-derived envelope with the plasma membrane of a new host cell [59]. Within the host cell, *Wolbachia* are encompassed by a self-derived membrane and an outer host-derived membrane [147, 148], which potentially play a role in horizontal transfer by membrane fusion.

Given these possibilities, we sought to identify the mechanisms by which *Wolbachia* are horizontally transferred and to establish a useful system for the further study of this interesting phenomenon.

3.3 Results

Horizontal transfer of *Wolbachia* is independent of cell-to-cell contact

Previous studies established that *Wolbachia* extracted from infected mosquito cell lines can enter uninfected cells and tissues when co-cultured [46, 47]. By extracting *Wolbachia* from *Drosophila* JW18 and LDW1 cells infected with the *w*Mel strain and coculturing this extract with doxycycline-cured JW18 (JW18-DOX) or LDW1 (LDW1-DOX) cells for 1 to 24 h, we confirmed this phenomenon in *Drosophila* (Figure 3.1A and B). That is, free *Wolbachia* cells after entering uninfected JW18-DOX cells were observed through fixed fluorescence imaging (Figure 3.1A). In addition, the early and late stages of free *Wolbachia* cell entry into LDW1-DOX cells were observed using electron microscopy (Figure 3.1B). These observations included contact between free *Wolbachia* cells and the host cell membrane and integration of *Wolbachia* into the host cytoplasm following entry in a vacuole.

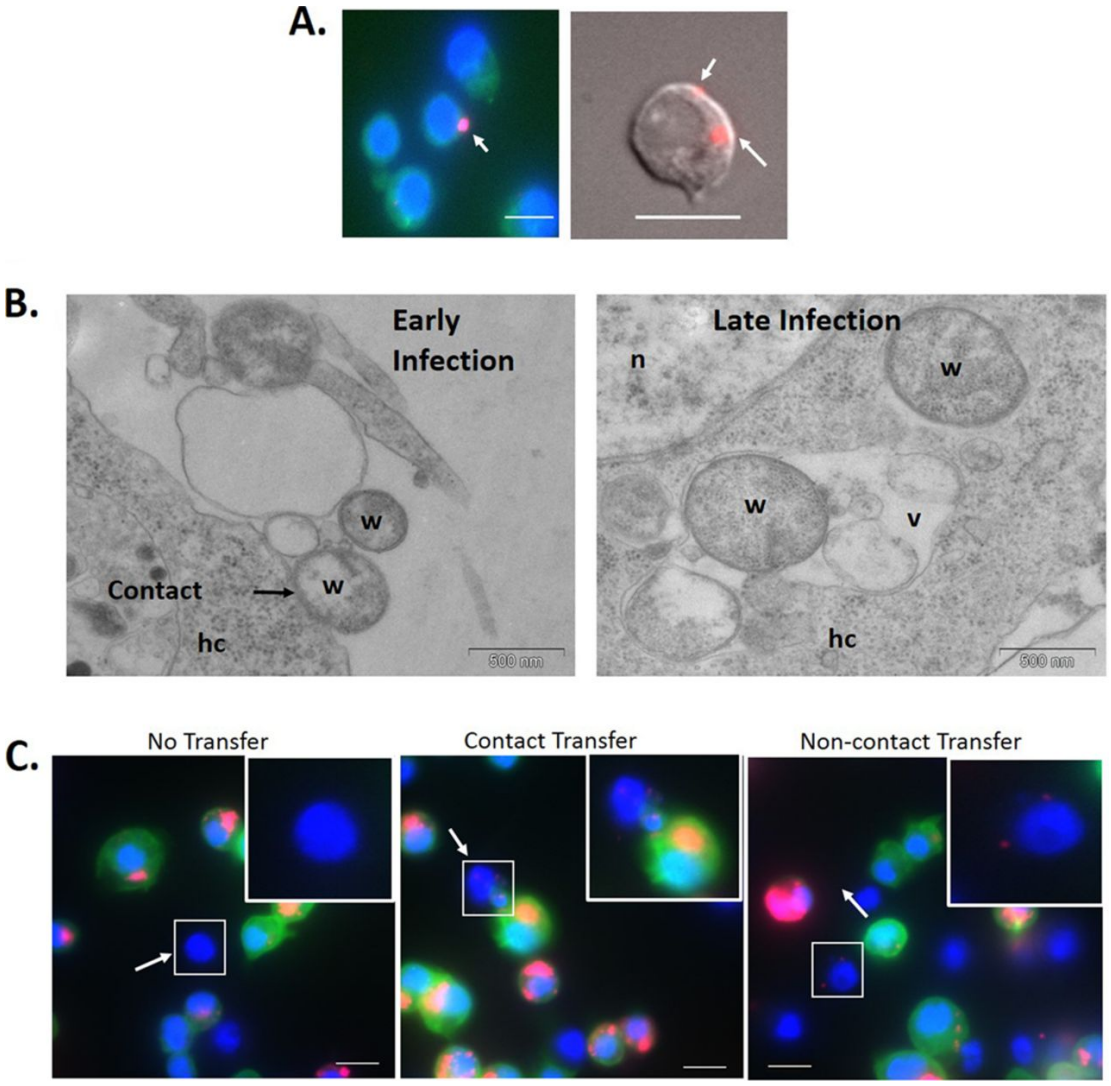

Figure 3.1: **Horizontal transfer of *Wolbachia* between Drosophila cells.** (A) *Wolbachia* extracted from infected JW18 cells were added to JW18-DOX cells and incubated for 24 h. (B) *Wolbachia* extracted from infected LDW1 cells were added to LDW1-DOX cells and incubated for 1 h. (C) Uninfected Drosophila S2 cells and *Wolbachia*-infected JW18 cells were co-cultured on a glass coverslip for 24 h. *Wolbachia* infections in previously uninfected cells can be seen with FISH (A) and DIC (C) imaging or electron microscopy (B) to determine if horizontal transfer of infection took place. Results are typical of the multiple fields of view examined. Red, *Wolbachia*; blue, nuclei stained with DAPI; green, GFP-Jupiter (JW18 only). hc, host cell; n, nucleus; v, vesicle; w, *Wolbachia*. Bar, 10 1-m.

While significant, these experiments did not reflect the in vivo environment of *Wolbachia*, where they must transfer between living cells. Thus, to determine if *Wolbachia* can

horizontally transfer between intact *Drosophila* cells, we co-cultured uninfected S2 cells and *Wolbachia*-infected JW18 cells on the same surface (Figure 3.1C). JW18 cells carry GFP-Jupiter, a tubulin binding protein, which enabled us to distinguish originally infected and uninfected cells by visualization of green fluorescent protein-tagged microtubules [1]. Within 24 h of coculturing, transfer of *Wolbachia* from JW18 to previously uninfected S2 cells was readily apparent (Figure 3.1C). While some S2 cells remained uninfected, many in close proximity to infected JW18 cells became infected, perhaps through cell-to-cell contact. We also observed that S2 cells that were not adjacent to JW18 cells became infected. These results suggest that *Wolbachia* can transfer horizontally from cell to cell in culture. Thus, our next goal was to determine if this phenomenon required contact between infected and uninfected cells.

To address this issue, we utilized a transwell system in which infected JW18 cells and uninfected S2 cells were seeded in chambers separated by a polyester membrane that allowed for the sharing of culture medium and passage of bacteria but prevented contact between larger eukaryotic cells (Figure 3.2A) (see Methods). In these assays, transfer of *Wolbachia* was also observed, similar to when cells were cultured on the same surface (Figure 3.2B and C). The proportion of newly infected cells after 6 h of coculturing was 43% (n = 56). After the cells were co-cultured for 1 day, this number decreased slightly to 26% (n = 90). A similar number, 22% (n = 93), was observed after 2 days of coculturing. The infection rate then rose to 54% by 3 days of coculturing. As a control, JW18-DOX cells were used in place of infected cells in the transwell assay; no *Wolbachia* infections were detected in the S2 cells. Significantly, *Wolbachia* infections acquired through coculture in a transwell localized within the host cell (see Figure 3.S1 in the supplemental material) and were present and abundant 21 days after infection. Thus, the horizontally transferred *Wolbachia* were stably maintained through multiple division cycles (Figure 3.3). These results strongly suggest that *Wolbachia* can horizontally transfer between infected and uninfected cells in culture, and this ability does not require cell-to-cell contact.

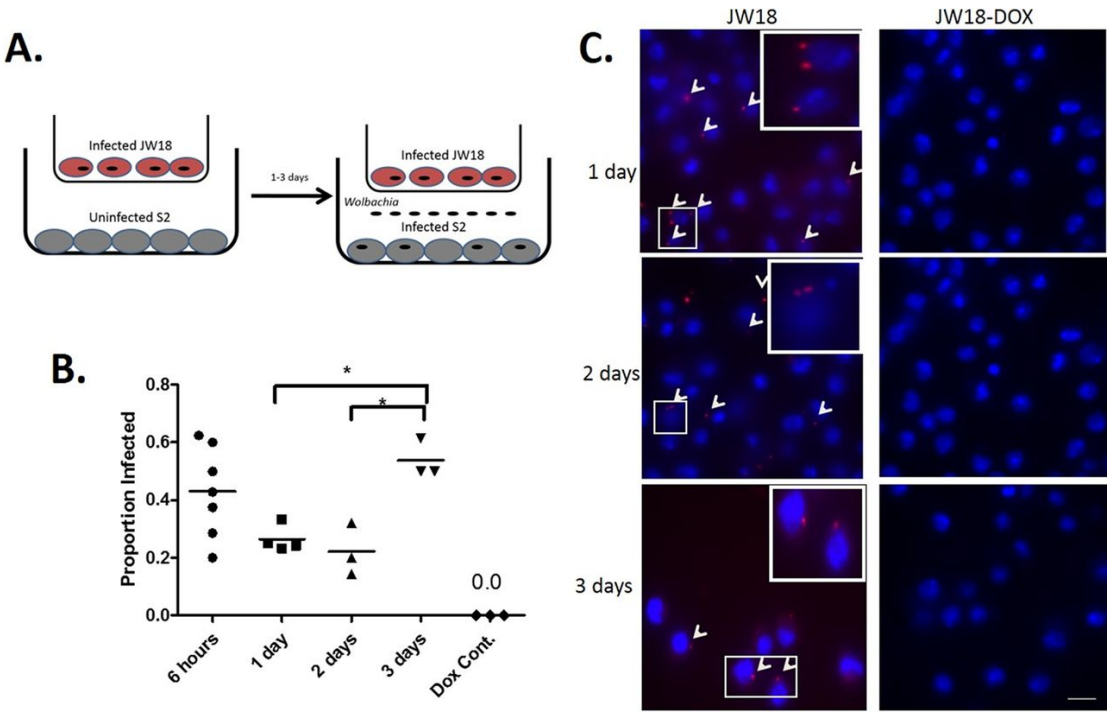

Figure 3.2: **Horizontal transfer of *Wolbachia* between Drosophila cells separated in a transwell.** (A) Uninfected Drosophila S2 cells were seeded beneath *Wolbachia*-infected JW18 cells in a transwell insert. (B) After coculture for 6 h or 1, 2, or 3 days, new *Wolbachia* infections in previously uninfected S2 cells were visualized by FISH in 3 to 7 fields of view for each group. S2 cells plated underneath doxycycline-cured JW18 cells (JW18-DOX) served as a negative control for FISH staining. Data are presented as proportion of infected cells ± SEM and were analyzed by one-way analysis of variance (ANOVA), followed by Newman-Keul's multiple-comparison test ($F = 5.31$; $R^2 = 0.551$; $df = 16$). Differences were deemed significant when the P value was <0.05 (indicated by an asterisk above the bracket). (C) Representative images for 1- to 3-day time points. Red, *Wolbachia* (arrowheads); blue, nuclei stained with DAPI. Bars, 10 μm.

Horizontal transfer of *Wolbachia* uses host clathrin and dynamin

We next sought to investigate the mechanisms involved in the horizontal transfer of *Wolbachia*. Given that many intracellular bacteria enter host cells by engaging components of the endocytic pathway, we hypothesized that this might also hold true for *Wolbachia*. We tested this hypothesis by inhibiting host cell dynamin, a GTPase necessary for the pinching and intracellular release of a variety of endocytic vesicles, using the small-molecule inhibitor dynasore [149]. We then analyzed cell-to-cell transfer rates between infected JW18 and

uninfected S2 cells in our transwell assay. As predicted, treatment with dynasore significantly reduced the efficiency of cell-to-cell transfer relative to dimethyl sulfoxide (DMSO)-treated controls (Figure 3.4A). After 1 day, the infection rate in untreated control cells was 21% (n = 105), compared to 9% (n = 47) in dynasore-treated cells. We observed a similar pattern after 2 days of dynasore treatment, with infection decreasing from 20% in controls (n = 66) to 7% in dynasore-treated groups (n = 42). Dynasore produced the strongest effect after 3 days of treatment, reducing infection from 26% in controls (n = 45) to 8% in treated cells (n = 46). The incomplete inhibition of horizontal transmission by dynasore suggests that *Wolbachia* employ additional mechanisms of internalization.

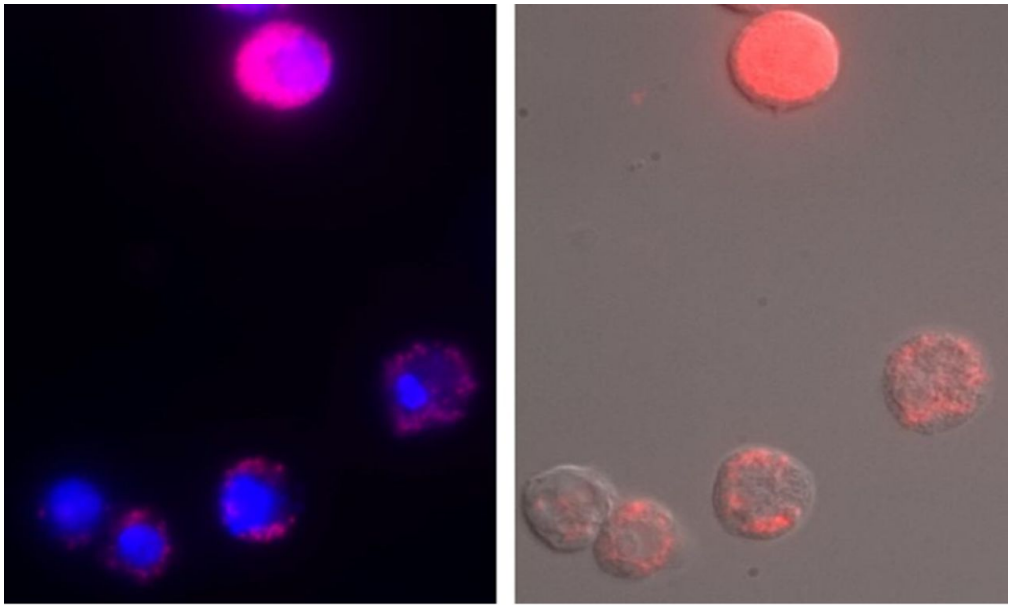

Figure 3.3: **Long-term *Wolbachia* infection in Drosophila S2 cells after coculture with infected JW18 cells in a transwell chamber.** Uninfected Drosophila S2 cells were seeded beneath *Wolbachia*-infected JW18 cells in a transwell insert. After coculture for 3 days, the transwell insert containing infected cells was removed, and new medium was added to the previously uninfected S2 cells. S2 cells were then cultured for an additional 18 days (21 days total), and *Wolbachia* infections were visualized by FISH and DIC. Red, *Wolbachia*; blue, nuclei stained with DAPI.

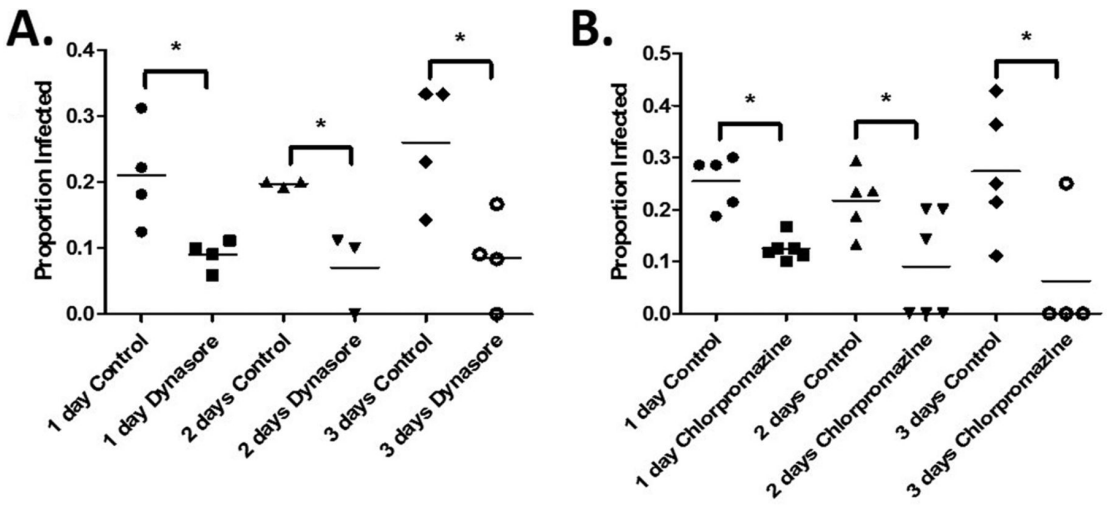

Figure 3.4: **Horizontal transfer of *Wolbachia* is clathrin mediated.** (A) Uninfected Drosophila S2 cells were pretreated with 80 μM dynasore or DMSO (control) for 1 h prior to seeding *Wolbachia*-infected Drosophila JW18 cells in a transwell insert above them. After being co-cultured for 1, 2, or 3 days, new *Wolbachia* infections in previously uninfected S2 cells were visualized by FISH in 3 to 7 fields of view for each group. Data are presented as proportion of infected cells ± SEM and were analyzed by t test to determine differences between control and dynasore-treated groups at each time point ($t = 2.96$, $df = 6$ at 1 day; $t = 3.58$, $df = 4$ at 2 days; $t = 3.05$, $df = 6$ at 3 days). Differences were deemed significant when the P value was <0.05 (indicated by an asterisk above the bracket). (B) Uninfected Drosophila S2 cells were pretreated with 10 μM chlorpromazine or DMSO (control) for 1 h prior to seeding *Wolbachia*-infected Drosophila JW18 cells in a transwell insert above them. After being co-cultured for 1, 2, or 3 days, new *Wolbachia* infections in previously uninfected cells were visualized by FISH and analyzed as described for panel A ($t = 5.73$, $df = 9$ at 1 day; $t = 2.44$, $df = 9$ at 2 days; $t = 2.51$, $df = 7$ at 3 days).

Nevertheless, these experiments demonstrate that *Wolbachia* use dynamin for horizontal transfer into new host cells. We hypothesized that *Wolbachia* cells entered through a clathrin-dependent mechanism. To test this, we used chlorpromazine to inhibit host clathrin [150, 151], a coat protein involved in the formation of vesicles. Similar to dynamin inhibition, inhibition of clathrin reduced infection from 25% in controls (n = 75) to 12% after 1 day of treatment (n = 64) (Figure 3.4B). After 2 days of treatment, the infection rate decreased from 22% in controls (n = 95) to 9% in treated cells (n = 35). As with dynasore, chlorpromazine produced the strongest effect after 3 days of treatment, reducing infection from 27% (n = 45) to 6% (n = 17). These results suggest that *Wolbachia* utilize clathrin-mediated endocytosis

pathways for entry during horizontal cell-to-cell transfer. We also used the inhibitors genistein and filipin to test the involvement of caveolin [151]. In these experiments, caveolin inhibition did not inhibit cell-to-cell transfer (J. E. Pietri, unpublished data).

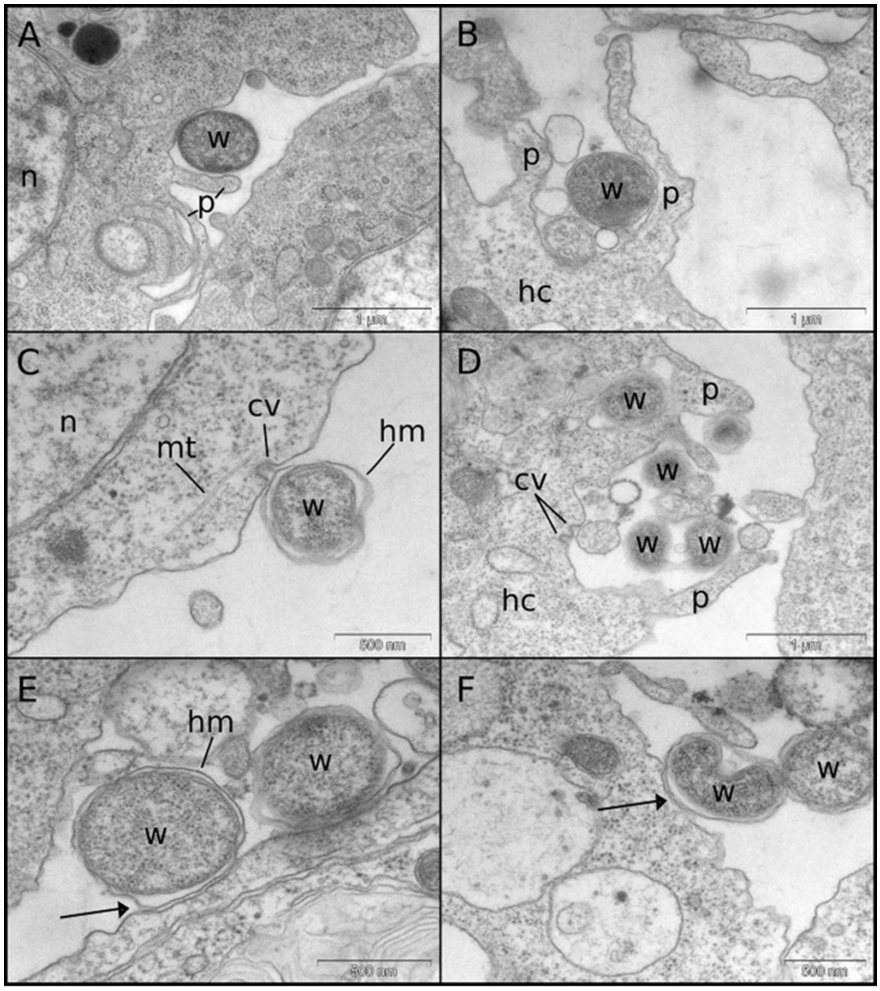

Figure 3.5: **Transmission electron micrographs of LDW/JW18 cells exposed to *Wolbachia* from cell lysates or infected JW18 cells.** (A and B) *Wolbachia* are frequently seen surrounded by phagocytic pseudopodium-like extensions of the host cell. (C and D) *Wolbachia* can be seen contacting what appear to be clathrin-coated pits, sometimes coinciding with pseudopodia (D). (E and F) The host-derived membrane surrounding the *Wolbachia* double membrane can be seen in close contact with the host cell membrane (arrows). cv, clathrin vesicle; hc, host cell; hm, host membrane; mt, microtubules; n, nucleus; p, pseudopodia; w, *Wolbachia*.

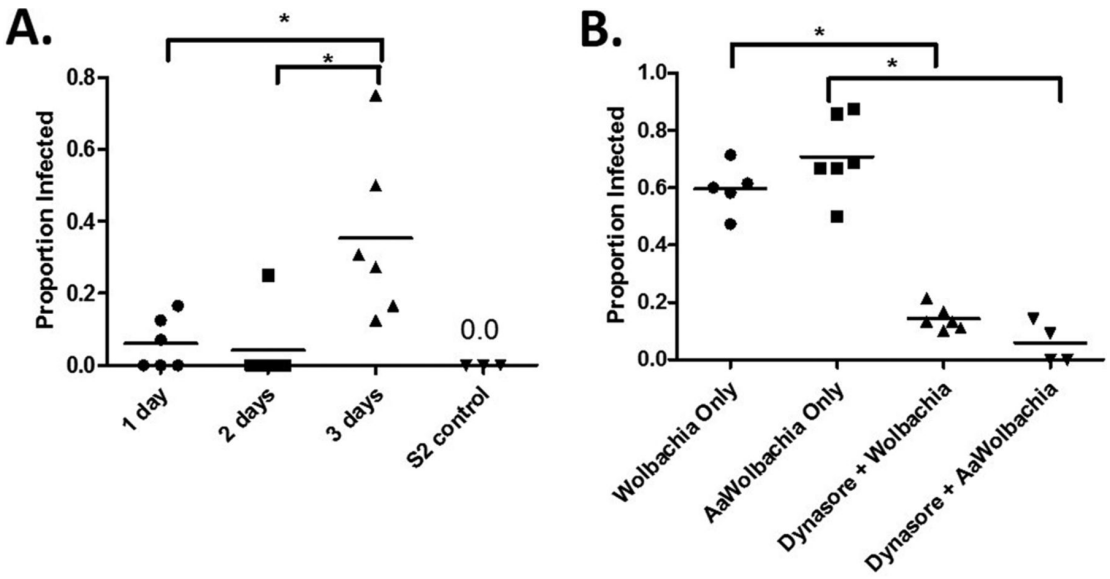

Figure 3.6: **Horizontal transfer of *Wolbachia* takes places between mosquito and Drosophila cells.** (A) Uninfected Drosophila S2 cells were seeded beneath *Wolbachia*-infected *A. albopictus* cells (C6/36) in a transwell insert. After being co-cultured for 1, 2, or 3 days, new *Wolbachia* infections in previously uninfected cells were visualized by FISH in 6 fields of view for each group. S2 cells plated in the absence of C6/36 cells served as a control for FISH staining. Data are presented as proportion of infected cells ± SEM and were analyzed by one-way ANOVA, followed by Newman-Keuls multiple-comparison test to determine differences between time points ($F = 7.78$, $R2 = 0.509$, $df = 17$). Values were deemed significant when $P < 0.05$ (indicated by an asterisk above the bracket). (B) Pretreatment of JW18-DOX cells with dynamin prior to the addition of crude *Wolbachia* preparations from infected Drosophila JW18 cells or mosquito C6/36 cells (*w*AlbB) for 24 h resulted in a reduced ability of Wolbachia to invade cells. Data are presented as proportion of infected cells ± SEM and were analyzed by one-way ANOVA, followed by Newman-Keuls multiple-comparison test to determine differences between groups ($F = 61.4$, $R2 = 0.912$, $df = 20$). Values were deemed significant when the P value was <0.05 (indicated an asterisk above the bracket).

Host cells internalize *Wolbachia* via engulfment

Finding that clathrin and dynamin are involved in *Wolbachia* uptake prompted us to examine the interaction between *Wolbachia* and host cells at the ultrastructural level. Transmission electron microscopy (TEM) revealed that *Wolbachia* uptake by host cells appears to be accomplished by engulfment via extensions of the cytoplasm similar to those of phagocytic pseudopodia (Figure 3.5A and B). The bacteria were observed in contact with putative clathrin-coated pits (Figure 3.5C and D), which in some cases were associated with

pseudopodia (Figure 3.5D). Internalization via membrane fusion may also contribute to transfer rates, as the host-derived membrane of extracellular *Wolbachia* was often seen in close contact with the host membrane (Figure 3.5E and F).

Horizontal transfer of *Wolbachia* takes place efficiently between cells of divergent hosts

Having implicated components of the host endocytic and phagocytic pathways in horizontal transfer, we sought to determine if a species barrier to horizontal transfer exists. We predicted that if this were the case, horizontal transfer of *Wolbachia* between cells of different insect species would be reduced or inhibited altogether. We examined this possibility by analyzing horizontal transfer rates between infected C6/36 cells from the mosquito *Aedes albopictus* and uninfected *Drosophila* S2 cells in our transwell assay (Figure 3.6A). Despite *Wolbachia* infection rates in C6/36 and *Drosophila* JW18 cells being very similar (Figure 3.7), cell-to-cell transfer of *Wolbachia* from these cells to *Drosophila* S2 cells was somewhat lower. The proportion of newly infected cells after 1 day of coculturing was a mere 6% and decreased to 4% on day 2. Although new infections increased to 35% after 3 days of coculturing, this rate was lower than that observed between *Drosophila* cells (Figure 3.2B), suggesting that while horizontal transfer can take places between cells from different species, it may be less efficient. To rule out the effect of differences in *Wolbachia* exocytosis rates in mosquito and *Drosophila* cells, we pretreated JW18-DOX cells with dynasore and incubated them with crude *Wolbachia* preparations derived from fly or mosquito cells. In these experiments, *Wolbachia* infection rates in cells treated with *Wolbachia* derived from mosquito cells and *Drosophila* cells were not different, regardless of pretreatment (Figure 3.6B). That is, within 24 h of incubation with *Wolbachia* from *Drosophila* cells, 60% of previously uninfected cells became infected (n = 63). This proportion was reduced to 14% by pretreating the cells with dynasore (n = 75). Similarly, when *Wolbachia* from *A. albopictus* cells were used, 71% (n = 63) of previously uninfected cells became infected. After

kpretreatment of the cells with dynasore, infection was almost completely blocked, as only 6% of the cells became infected (n = 55). Thus, reliance of Wolbachia on components of the endocytic pathway for cell-to-cell transfer appears to be conserved across species.

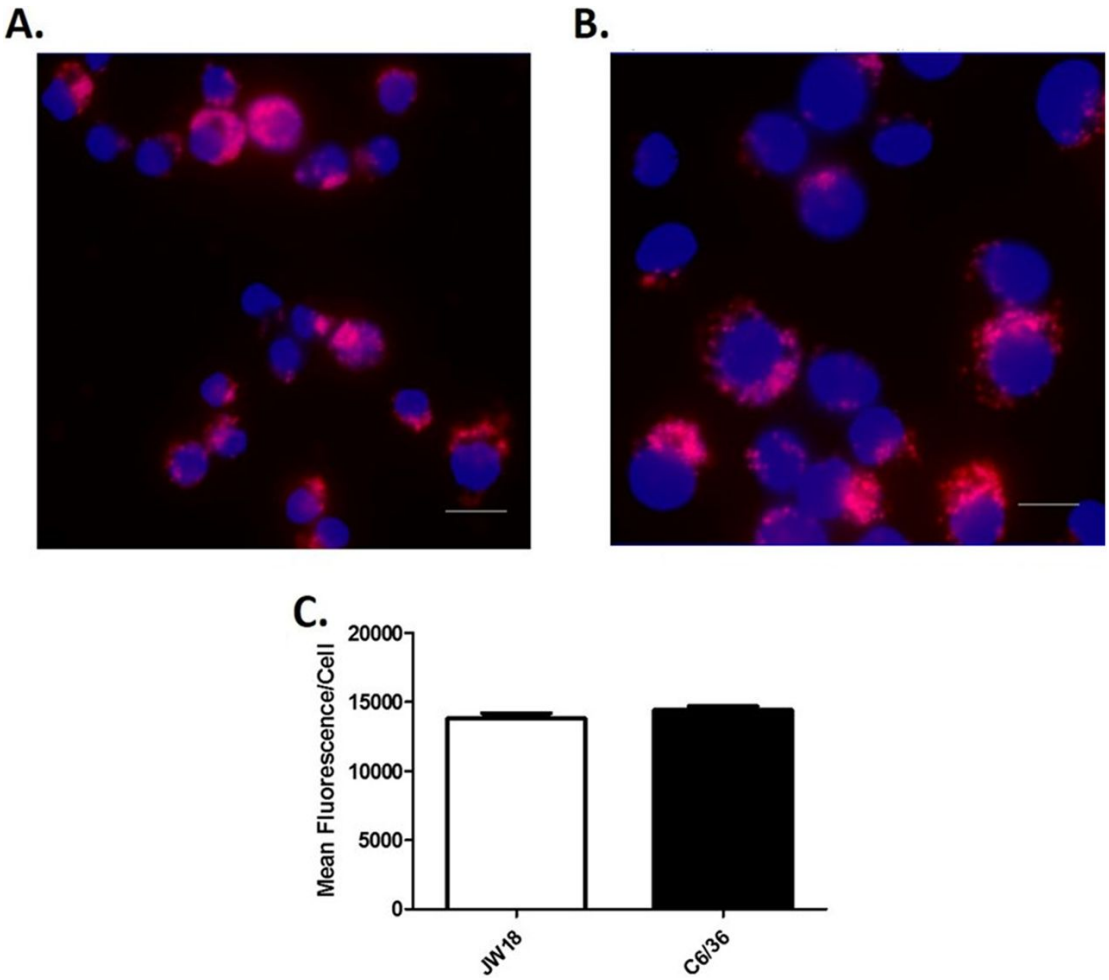

Figure 3.7: ***Wolbachia* infection in Drosophila and *A. albopictus* cells.** Cells were seeded on glass coverslips for 24 h and subsequently fixed with 8% paraformaldehyde for detection of *Wolbachia* by FISH (red) in Drosophila JW18 cells (A) and *A. albopictus* C6/36 cells (B). DAPI was used as a counterstain for cell nuclei (blue). Bar, 10 μm. (C) *Wolbachia* infection in JW18 and C6/36 cells was quantified by measurement of red fluorescence intensity. Data were analyzed by t test, and no significant differences between the two groups were found ($P = 0.223$, $t = 1.25$, $df = 18$).

3.4 Discussion

In our study, we documented the horizontal transfer of *Wolbachia* between *Drosophila* cells in culture and demonstrate that this process occurs through components of the host phagocytic and endocytic pathways. As such, our work directly demonstrates horizontal transfer of Wolbachia between cells while identifying a potential mechanism.

Our finding that horizontal transfer takes place between infected and uninfected cells when cultured together (Figure 3.1) or separated by transwells (Figure 3.3) suggests that cell-to-cell contact is not required to achieve efficient transfer. Nonetheless, cell-to-cell contact may play some role in horizontal transfer, as we observed several instances of *Wolbachia* transferring between cells in direct contact with each other (Figure 3.1C). However, a large proportion of horizontally acquired infections can be accounted for by transfer through the culture medium (Figure 3.2). *Wolbachia* can achieve a >50% infection rate through this route, implicating it as the prevalent mechanism for horizontal transfer. Nonetheless, a fair proportion of bacteria invading through this method may not survive, as reduced infection levels between 6 and 24 h in our transwell assay suggest that perhaps some horizontally acquired *Wolbachia* are digested or killed by the host cell.

Transfer through the culture medium likely takes place via uptake after *Wolbachia* are exocytosed from infected cells. The release of *Wolbachia* after cell lysis may make some minor contribution to horizontal transmission. However, it is unlikely that these infrequent cell death events account for the high rates of infection transfer observed in our short-term assays, given that infected JW18 cells can be maintained in culture without passaging for 7 to 10 days without notable cell lysis occurring (J. E. Pietri, unpublished data).

Our experiments using dynasore and chlorpromazine to block dynamin and clathrin activity in uninfected cells reveal the particular pathways of endocytosis coopted by *Wolbachia* after their release from infected cells (Figure 3.4A). Reduced horizontal transfer following inhibition of dynamin and clathrin, but not caveolin, argues against the possibility that *Wolbachia* enter cells exclusively through a process such as passive membrane fusion.

Further, while *Drosophila* S2 and JW18 cells are passively phagocytic to some extent, the use of clathrin and dynamin in transfer suggests a bacterially induced mode of entry, such as the zipper method [54]. However, clathrin has been reported to be involved in some forms of phagocytosis in *Drosophila* (e.g., references [152-154]), preventing us from excluding this as a mechanism of uptake with these data alone.

It is possible that *Wolbachia* use an active mode, such as the zipper method, and a passive method, such as phagocytosis, for uptake, as is the case for several other invasive bacteria. For instance, *Chlamydia* can specifically trigger phagocytosis for entry into in HeLa cells, as demonstrated by experiments comparing the internalization rate of this bacterium with those of *Escherichia coli* and polystyrene beads [155]. However, in the same cell type (i.e., HeLa cells), and in human endometrial gland epithelial cells, *Chlamydia* can be observed in coated pits and vesicles, indicative of endocytosis [156]. Similarly, *Listeria* has been shown to enter cells through multiple mechanisms depending on the cell type being invaded. For instance, traditional phagocytosis and a formin-dependent phagocytosis-like process [157] have been demonstrated in vascular endothelial cells, while a clathrin-mediated process [155] appears to be critical in HeLa cells.

In addition, we suggest that *Wolbachia* may bind to a variety of host cell receptors to gain entry into host cells. This is consistent with results of studies of other invasive intracellular bacteria, which demonstrate that while the machinery for endocytosis is often conserved, a variety of receptors can be used. For instance, although *Listeria* and *Neisseria* both enter through clathrin-coated pits [155-160], *Listeria* utilizes the hepatocyte growth factor receptor (met) [160], while *Neisseria* uses the asialoglycoprotein receptor (ASGP-R) [159]. Similarly, microorganisms may make use of the same receptors but achieve entry through different mechanisms. For example, both *Salmonella* and *Candida* bind to the epidermal growth factor receptor (EGFR) [161, 162], but they make use of phagocytosis and clathrin-mediated pathways, respectively [54, 163]. The receptor(s) that *Wolbachia* bind prior to entry remain undetermined. However, the conservation of horizontal transfer across species suggests that

this receptor and its ligand(s) may be highly conserved, as *Wolbachia* derived from the C6/36 and JW18 cells used as *Wolbachia* donors in our experiments harbored *w*AlbB and *w*Mel, respectively.

The processes of phagocytosis and endocytosis are intrinsically linked to the actin cytoskeleton [164]. Intriguingly, a number of microbes rely on host actin for invasion and are able to manipulate its structure through the use of secreted effectors [55]. The same appears to be true for *Wolbachia*, which was recently shown to rely on host actin for efficient maternal transmission [165]. *Wolbachia* also encodes a secreted effector, WD0830, which interacts with the host cytoskeleton [166]. This is particularly important, as it suggests that the horizontal transfer process may not be passive and host driven but, rather, induced by *Wolbachia* through the secretion of effector proteins that drive cytoskeletal changes for engulfment. This mode of transfer might explain cortical actin rearrangements that are associated with *Wolbachia* migration during filarial nematode development [106].

Differences in *Wolbachia* exocytosis rates may play some role in controlling horizontal transmission, as entry of *Wolbachia* extracted from mosquito cells from crude extractions was not inhibited compared to *Wolbachia* extracted from *Drosophila* cells (Figure 3.6B), despite our transwell assay in which lower rates of horizontal transfer were found (Figure 3.6A). It is unlikely that the reduced titer in mosquito cells plays a role in this discrepancy between assays, as infection levels in mosquito cells were equal to those in *Drosophila* cells (Figure 3.7). Likewise, genotype-specific differences in bacterial surface factors are likely not involved given the different strains of *Wolbachia* harbored by JW18 and C6/36 cells. However, differences in recipient cell properties, such as the presence or absence of particular receptors, may contribute to differences in the efficiency of horizontal transfer and should be explored further.

Ultimately, the results of our work significantly advance our understanding of how *Wolbachia* is transmitted both vertically and horizontally. During early embryogenesis in filarial nematodes, *Wolbachia* segregates exclusively to the lineage producing the hypodermal

chords, somatic tissues that provide nutrients to developing germ line cells. Occupation of the germ line for eventual vertical transmission requires cell-to-cell transfer from the chords [106]. The relevance of somatic to germ line cell-to-cell transfer for vertical transmission is further illuminated by images of *Wolbachia*-infected oocytes from recently captured wild *Drosophila* [113]. Egg chambers were identified in which *Wolbachia* was not present in many of the early developing oocytes, but all of the mature oocytes were infected. The absence of *Wolbachia* early in oogenesis is likely a direct result of its failure to segregate to the differentiating daughter cell during germ line stem cell division. The fact that these empty oocytes eventually become infected suggests that *Wolbachia* present in the surrounding somatic follicle cells eventually enter the oocyte using cell-to-cell transfer as a backup mechanism to ensure vertical transmission [167].

Our findings also shed some light on possible routes of horizontal transmission of *Wolbachia* infection in nature. Previous work showed that *Wolbachia* in the hemolymph of adult flies can migrate to the germ line across multiple somatic tissues [48]. This is likely mediated by cell-to-cell transfer between various tissues and suggests that *Wolbachia,* which enters a new host through the gut or a wound may use cell-to-cell transfer to establish both a somatic and stable (germ line) infection.

While more specifics regarding the mechanisms of horizontal transfer remain to be uncovered, our transwell fluorescence *in situ* hybridization (FISH) assay is a simple and tractable system for further probing cell exit and entry of *Wolbachia*, as it allows for the separate manipulation of recipient (uninfected) and donor (infected) cells while providing several advantages over antibody-based staining by increasing specificity and reducing background fluorescence. Our system is also highly biologically relevant, as *Wolbachia* that infect through this method can achieve proper localization inside the host cell (Figure 3.1; Figure S1) and also appear highly stable, surviving for at least 21 days (Figure 3.3).

Chapter 4

Reliance of *Wolbachia* on High Rates of Host Proteolysis Revealed by a Genome-Wide RNAi Screen of *Drosophila* Cells

4.1 Abstract

Wolbachia are gram-negative, obligate, intracellular bacteria carried by a majority of insect species worldwide. Here we use a *Wolbachia*-infected *Drosophila* cell line and genome-wide RNA interference (RNAi) screening to identify host factors that influence *Wolbachia* titer. By screening an RNAi library targeting 15,699 transcribed host genes, we identified 36 candidate genes whose depletion dramatically reduced *Wolbachia* titer and 41 whose depletion increased *Wolbachia* titer. Host gene knockdowns that reduced *Wolbachia* titer spanned a broad array of biological pathways including genes that influence mitochondrial function and lipid metabolism. In addition, knockdown of seven genes in the host ubiquitin and proteolysis pathways significantly reduced *Wolbachia* titer. To test the *in vivo* relevance of these results, we found that drug and mutant inhibition of proteolysis reduced levels of *Wolbachia* in *Drosophila* oocytes. The presence of *Wolbachia* in either cell lines or oocytes dramatically alters the distribution and abundance of ubiquitinated proteins. Functional studies revealed that maintenance of *Wolbachia* titer relies on an intact host Endoplasmic Reticulum (ER)-associated protein degradation (ERAD) pathway. Accordingly, electron microscopy studies demonstrated that *Wolbachia* is intimately associated with the host ER and dramatically alters the morphology of this organelle. Given that *Wolbachia* lack essential amino acid biosynthetic pathways, the reliance of *Wolbachia* on high rates of host proteolysis via ubiquitination and the ERAD pathway may be a key mechanism for provisioning *Wolbachia* with amino acids. In addition, the reliance of *Wolbachia* on the ERAD pathway and *Wolbachia* disruption of ER morphology suggest a previously unsuspected mechanism for *Wolbachia's* potent ability to prevent RNA virus replication.

4.2 Introduction

Wolbachia is a bacterial endosymbiont present in insects and filarial nematodes [6, 7]. *Wolbachia* resides in both somatic and germ line cells of its male and female insect hosts [146]. The evolutionary success of *Wolbachia* depends on efficient vertical transmission through the female germ line. This is facilitated by *Wolbachia* localization to the posterior pole of the oocyte, ensuring its incorporation into the germ line of the next generation. To achieve this, *Wolbachia* rely on host microtubules, motor proteins, and an interaction with host pole plasm components [39, 83, 84]. The success of *Wolbachia* also requires regulation of bacterial abundance within host somatic and germ line cells. Underreplication of *Wolbachia* in the oocyte results in inefficient vertical transmission and overreplication of *Wolbachia* results in disruption of critical host cellular functions [95, 165]. Cytological and PCR-based studies demonstrate that recently caught wild strains of *Drosophila* exhibit tremendous variability in *Wolbachia* titer [168]. These variations not only occur from one individual to another but also between tissues within an individual [40, 169].

Wolbachia abundance is influenced by a combination of host and *Wolbachia* factors as well as the environment. For example, in the *Drosophila* oocyte, *Wolbachia* rely on normal host microtubule organization and the Gurken dorsal signaling complex to maintain titer [83, 95]. Additional evidence for the influence of host factors on *Wolbachia* titer comes from the finding that the same *Wolbachia* strain in *D. simulans* and *D. melanogaster* exhibits dramatically different titers in the mature oocyte [84, 170]. Evidence that factors intrinsic to *Wolbachia* influence its titer comes from the identification of the *Wolbachia* variant, *w*MelPop. The *w*MelPop strain exhibits extremely high titers in the central nervous system relative to other *Wolbachia* strains, independent of the host strain or species in which it resides [171]. Finally, extrinsic environmental factors such as temperature and diet dramatically influence *Wolbachia* titer [4, 172]. These changes are moderated in part through the host insulin signaling pathway [4].

To comprehensively identify host factors that influence *Wolbachia* titer, we employed a genome-wide RNA interference (RNAi) screen using a *Drosophila* cell line infected with *Wolbachia*. Our approach was motivated by the success of a number of previous cell-based screens using *Drosophila* cell lines [60]. Using *Drosophila* cells, genome-wide RNAi screens were performed to identify host genes that alter *Listeria monocytogenes*, *Mycobacterium fortuitum*, *Chlamydia caviae*, and *Francisella tularensis* infection and proliferation [61-64]. We specifically assayed for RNAi-mediated gene knockdowns that either up- or down-regulate *Wolbachia* titer. The cell line used was created from primary embryonic cultures of *Drosophila melanogaster* infected with *w*Mel *Wolbachia* strain [1]. *Wolbachia* is stably maintained in these cultures and exhibits a close association with microtubules as found in *Drosophila* somatic and germ line tissues [39, 40]. The cell line expresses a transgene encoding GFP-tagged Jupiter, a microtubule-associated protein that labels microtubules and facilitates high-throughput, cell-based screening approaches [41]. The *Wolbachia*-infected cells were originally employed for high-throughput, cell-based screens to identify small molecule inhibitors of *Wolbachia* [1, 173]. By combining genome-wide RNAi approaches with automated microscopy, we were able to screen the majority of the *Drosophila* genome for those genes that influence *Wolbachia* titer. As described below, this analysis yielded a number of host genes critical for regulating intracellular *Wolbachia* titer and revealed that the host ubiquitin and proteolysis pathways play an especially critical role in maintaining *Wolbachia* titer.

4.3 Results

A genome-wide RNAi cell-based screen yields host genes that either enhance or suppress *Wolbachia* titer

To identify host components that influence *Wolbachia* infection of insect cells, we took advantage of the ability to perform genome-wide RNAi screens in *Drosophila* tissue culture cells. Because *Drosophila* cell lines are particularly amenable to RNAi-based screening, this

approach has been successfully used for studying a number of cellular processes including the cellular basis of host–pathogen interactions [174]. Here we used a well-characterized *Wolbachia*-infected cell line known as JW18 [1]. Our analysis revealed that 90% of the JW18 host cells are infected and *Wolbachia* have no obvious effects on cell viability or division [1]. Quantification of *Wolbachia* infection was based on fluorescent images of *Wolbachia*-infected and cured JW18 cell lines using automated microscopy and journaling software (Figure 4.1). By using the JW18 cell line in the 384-well plate format, we screened an RNAi library that targets 15,699 *Drosophila* protein-encoded genes [175]. *Wolbachia*- infected JW18 cells were plated into individual wells, each containing a unique dsRNA, and allowed to incubate for 5 days. Robotics and automated microscopy were used to fix, stain, and image the cells (see Methods). The JW18 cell line expresses a GFP-Jupiter fusion protein that labels the cytoskeleton [41], thus highlighting the entire cytoplasm and indicating cell boundaries. Anti-histone staining labeled the host nuclei, and DAPI was used to stain both host nuclei and cytoplasmic *Wolbachia*. Through customized journaling software, the overlap of anti-histone and DAPI nuclear staining enabled digital removal of the nucleus. This facilitated quantification of cytoplasmic DAPI, representing *Wolbachia* density per cell (Figure 4.1) [1]. Each cell was scored as *Wolbachia* positive or negative based on a predetermined cytoplasmic DAPI intensity cut-off value. Ten images per well were recorded and analyzed, and two independent screens of the RNAi library were performed. RNAi knockdowns that significantly reduced or increased the proportion of *Wolbachia*-infected cells per well without dramatically altering cell viability in both independent replicates were scored as hits (Figure 4.2). Because we are starting with a population in which 90% or more of the cells are infected, RNAi-induced alterations in the ability of *Wolbachia* to infect cells are expected to exert only a minor impact on titer.

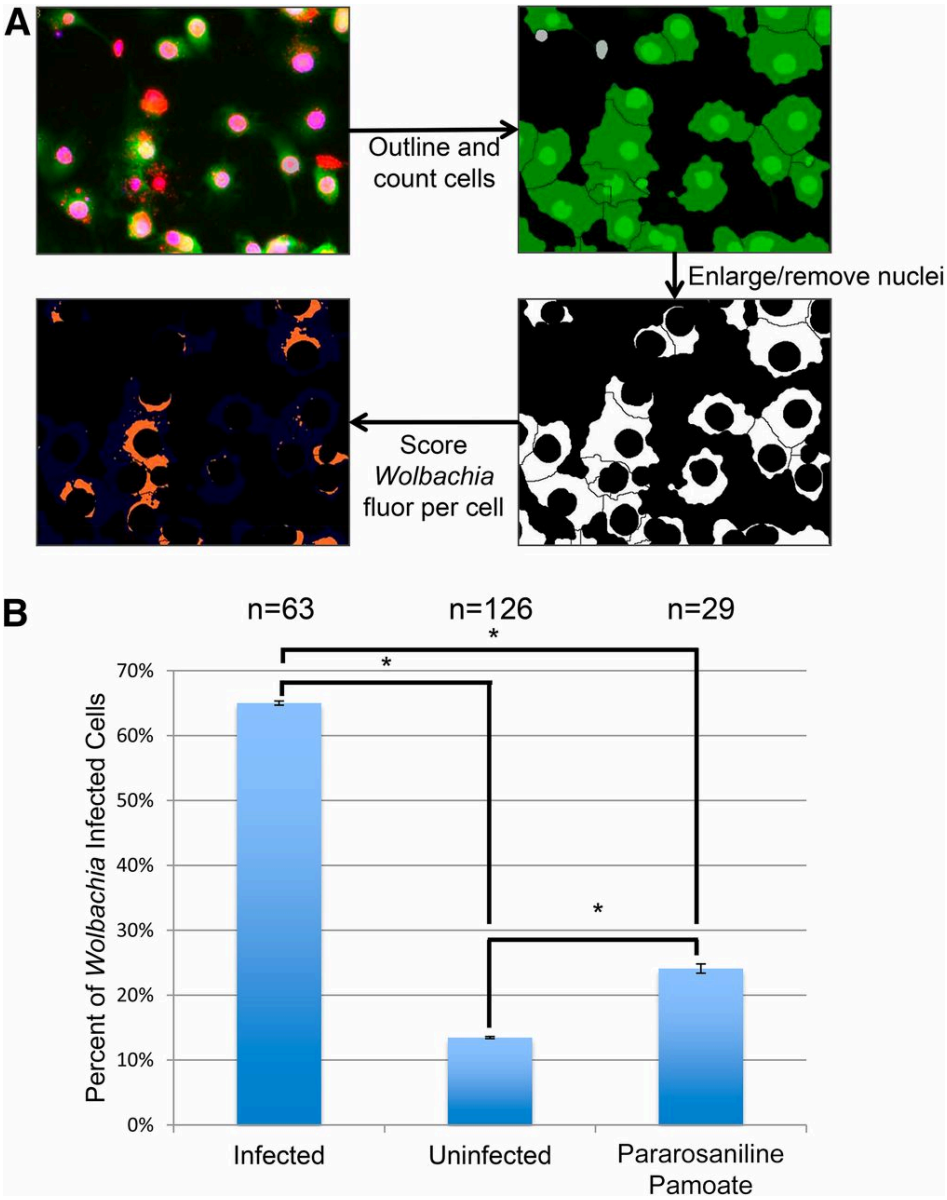

Figure 4.1: **Automated microscope-based quantification of *Wolbachia* titer.** (A) Flow chart showing screening methodology. Top left panel: *Wolbachia*-infected JW18 cells showing fluorescence from the markers DAPI (blue) and anti-histone (red), and the GFP-Jupiter (green). Top right panel: The journaling algorithm outlines cell borders based upon Jupiter-GFP. Bottom right panel: The algorithm digitally removes the nucleus from each cell based upon anti-histone staining. Bottom left panel: The total cytoplasmic DAPI signal in each cell is scored. (B) Graph depicts the percentage of cells scored by this algorithm as "*Wolbachia*-infected" in control JW18 cells, cured JW18 cells, and pararosaniline pamoate-treated JW18 cells. Though the algorithm can mis-identify fluorescent debris in the well as "infected cells," there are consistent significant differences by ANOVA between all of the control conditions tested ($P < 0.0001$). Error bars represent the SEM.

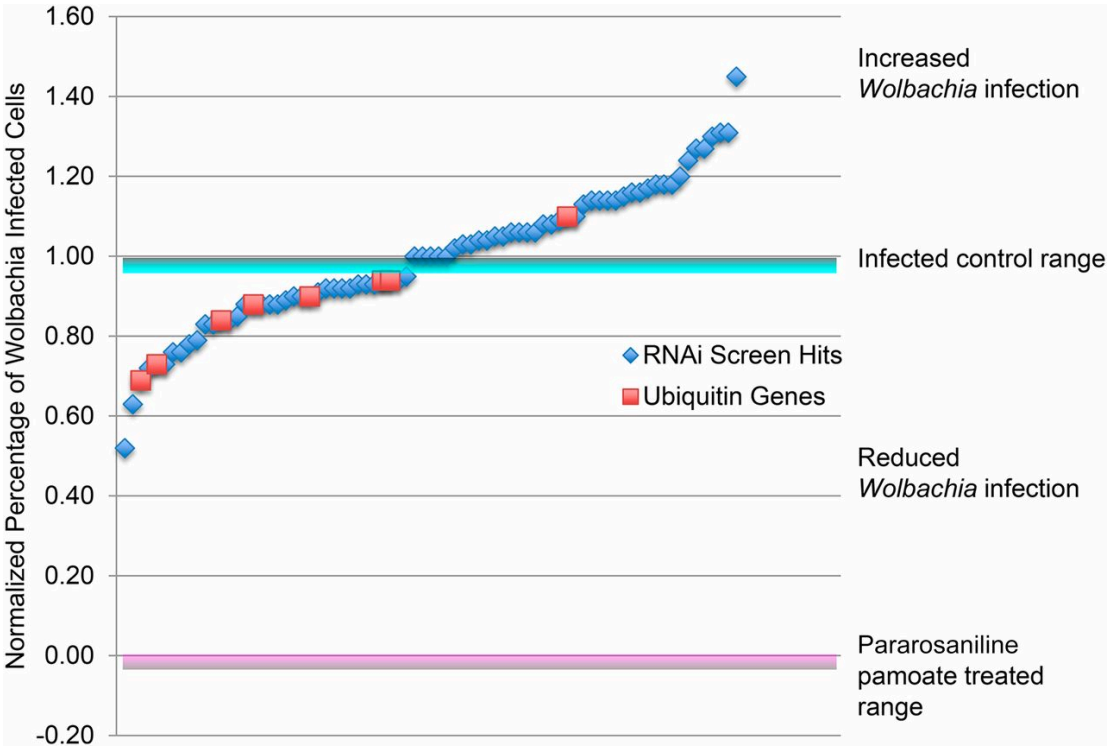

Figure 4.2: **RNAi knockdowns that decreased or increased *Wolbachia* infection rate.** Of 15,699 transcribed host genes, 36 candidate genes were identified that dramatically reduced *Wolbachia* titer and 41 that increased *Wolbachia* titer when knocked down via RNAi. Blue diamonds below or above the infected control range indicates dsRNA treatments targeting a single host gene that reduced or increased the proportion of *Wolbachia*-infected tissue culture cells. Red boxes indicate ubiquitin-related dsRNA treatment outcomes

The screen yielded 36 host genes that when knocked down through RNAi resulted in a significant drop in *Wolbachia* titer. These included hits in two genes involved in host lipid metabolism: CG9243, a phospholipase D; and CG1718, a gene involved in sterol uptake and esterification. In addition, hits in three mitochondrial metabolism components were recovered: CG3214, an NADH dehydrogenase; CG14757, a succinate dehydrogenase; and CG18324, a mitochondrial transporter. Knockdown of host genes encoding ATPases, GTPases, and ribosomal proteins also reduced titer (Table 4.1 and Table 4.2).

Particularly striking, the screen yielded eight hits in the ubiquitin-related pathways, seven of which reduced the proportion of *Wolbachia*-infected tissue culture cells. DsRNA targeting the

Ubiquitin-60S ribosomal protein L40 (CG2960), lingerer (CG8715), Ubiquitin-5E (CG32744), the ubiquitin transferase mei-P26 (CG12218), Ubiquitin-like protein 5 (CG3450), Ubiquitin-conjugating enzyme Ubc6 (CG2013), and Ubiquitin-like protein (CG12725) reduced infection, and targeting of the ubiquitin transferase CG31807 increased infection (Table 4.1 and Table 4.3). Ubiquitin is a small protein with a variety of functions including the marking of proteins for degradation and is targeted by a number of intracellular bacteria [176]. Previous inspection of the *Wolbachia* genome revealed that *Wolbachia* lack the ability to synthesize key amino acids and thus rely on the host as a source [30, 177]. Thus, it is possible that

Table 4.1: **List of host genes that reduce *Wolbachia* infection rates when knocked down**

CG#	Effect on Titer	Gene Name	Normalized Value	Functional Category	Additional Functional Category
CG14835	Reduced	CG14835	0.52		
HDC10201	Reduced	HDC10201	0.63		
CG12725	Reduced	CG12725	0.69	Ubiquitin	
CG9777	Reduced	CG9777	0.72		
CG12218	Reduced	mei-P26	0.73	Ubiquitin Transferase	Ligase
HDC05374	Reduced	HDC05374	0.73		
CG1527	Reduced	RpS14b	0.76	Ribosomal	
CG14579	Reduced	CG14579	0.76		
CG10970	Reduced	CG10970	0.78	Acylphosphatase	
CG13738	Reduced	CG13738	0.79		
CG2916	Reduced	Sep5	0.83	Septin	GTP-binding protein
CG14047	Reduced	PsGEF	0.83	RhoGEF	GTPase
CG2960	Reduced	RpL40	0.84	Ubiquitin	Ribosomal
CG32100	Reduced	CG32100	0.84		
CG30372	Reduced	Asap	0.85	ArfGap	GTPase activator
CG2958	Reduced	lectin-24Dd	0.88	C-type lectin	Carbohydrate Binding
CG3450	Reduced	ubl	0.88	Ubiquitin	
CG4688	Reduced	GstE14	0.88	Glutathione S-transferase	
CG32399	Reduced	CG32399	0.88		
CG7320	Reduced	CG7320	0.88	Hemocyanin	
CG12172	Reduced	Spn43Aa	0.89	Serpin	Endopeptidase Inhibitor
CG1344	Reduced	CG1344	0.90	Kinase	
CG3214	Reduced	ND-B17.2	0.90	Mitochondrial	NADH Dehydrogenase
CG2013	Reduced	Ubc6	0.90	Ubiquitin	Ubiquitin Conjugating Enzyme
HDC15882	Reduced	HDC15882	0.91		
CG33196	Reduced	dpy	0.92	EGF domain	Structural Constituent
CG18324	Reduced	CG18324	0.92	Mitochondrial Carrier	Transport
CG14757	Reduced	CG14757	0.92	Mitochondrial	Succinate Dehydrogenase
CG12807	Reduced	Spn85F	0.92	Serpin	Endopeptidase Inhibitor
CG1070	Reduced	Alh	0.93	Transcription	
CG1332	Reduced	CG1332	0.93	Endocytosis	
CG1718	Reduced	CG1718	0.93	ABC Transporter	ATPase
CG8715	Reduced	lig	0.94	Ubiquitin	
CG32744	Reduced	Ubiquitin-5E	0.94	Ubiquitin	
CG1394	Reduced	CG1394	0.94		
CG43345	Reduced	CG43345	0.95	Phospholipase D	Catalytic Activity

Hits are ordered from strongest at the top to weakest at the bottom.

Table 4.2: **List of host genes that significantly alter *Wolbachia* infection rates ordered by function**

	CG#	Effect on Titer	Gene Name	Normalized Value	Functional Category	Additional Functional Category
ATP/GTP	CG1718	Reduced	CG1718	0.93	ABC Transporter	ATPase
	CG30372	Reduced	Asap	0.85	ArfGap	GTPase activator
	CG14047	Reduced	PsGEF	0.83	RhoGEF	GTPase
	CG2916	Reduced	Sep5	0.83	Septin	GTP-binding protein
	CG1657	Increased	CG1657	1.20	GTPase activating	activates Rab GTPases
Kinase	CG1344	Reduced	CG1344	0.90	Kinase	
	CG5813	Increased	chif	1.14	Kinase	DBF zinc finger
Mitochondrial	CG3214	Reduced	ND-B17.2	0.90	Mitochondrial	NADH Dehydrogenase
	CG14757	Reduced	CG14757	0.92	Mitochondrial	Succinate Dehydrogenase
	CG18324	Reduced	CG18324	0.92	Mitochondrial Carrier	Transport
Ribosomal	CG2960	Reduced	RpL40	0.84	Ubiquitin	Ribosomal
	CG1527	Reduced	RpS14b	0.76	Ribosomal	
Serpin	CG12172	Reduced	Spn43Aa	0.89	Serpin	Endopeptidase Inhibitor
	CG12807	Reduced	Spn85F	0.92	Serpin	Endopeptidase Inhibitor
Ubiquitin	CG2960	Reduced	RpL40	0.84	Ubiquitin	Ribosomal
	CG8715	Reduced	lig	0.94	Ubiquitin	
	CG32744	Reduced	Ubiquitin-5E	0.94	Ubiquitin	
	CG3450	Reduced	ubl	0.88	Ubiquitin	
	CG2013	Reduced	Ubc6	0.90	Ubiquitin	Ubiquitin Conjugating Enzyme
	CG12725	Reduced	CG12725	0.69	Ubiquitin	
	CG12218	Reduced	mei-P26	0.73	Ubiquitin Transferase	Ligase
	CG31807	Increased	CG31807	1.10	Ubiquitin Transferase	RING finger domain
Ungrouped	CG10970	Reduced	CG10970	0.78	Acylphosphatase	
	CG1629	Increased	mal	1.04	Aminotransferase	MOSC domain
	CG2958	Reduced	lectin-24Dd	0.88	C-type lectin	Carbohydrate Binding
	CG33196	Reduced	dpy	0.92	EGF domain	Structural Constituent
	CG1332	Reduced	CG1332	0.93	Endocytosis	
	CG30361	Increased	mtt	1.31	G protein coupled receptor	
	CG4688	Reduced	GstE14	0.88	Glutathione S-transferase	
	CG7968	Increased	CG7968	1.03	Haemolymph juvenile hormone binding protein	
	CG7320	Reduced	CG7320	0.88	Hemocyanin	
	CG32005	Increased	CG32005	1.14	High Mobiligy Group Box	DNA binding
	CG43345	Reduced	CG43345	0.95	Phospholipase D	Catalytic Activity
	CG7988	Increased	CG7988	1.30	Regulation of Circadian Clock	
	CG4484	Increased	Slc45-1	1.45	Sucrose Transporter	
	CG1070	Reduced	Alh	0.93	Transcription	

Wolbachia require high levels of host proteolysis to supply sufficient amino acids for growth and reproduction.

The RNAi screen also yielded 41 host genes that when knocked down significantly increased the proportion of *Wolbachia*-infected cells. These included hits in: CG4484, a sucrose transporter; CG30361, a G-protein-coupled receptor; CG1657, a GTPase-activating protein (GAP); CG7968, a hemolymph juvenile hormone-binding protein. Of the 41 hits that increased *Wolbachia* titer, 32 were of unknown function. Unlike the hits that reduced titer, we did not recover multiple hits in known specific biological processes or pathways (Table 4.3).

Table 4.3: **List of host genes that increase *Wolbachia* infection rates when knocked down**

CG#	Effect on Titer	Gene Name	Normalized Value	Functional Category	Additional Functional Category
CG10589	Increased	CG10589	1.00	Domain of Unknown Function	
CG11231	Increased	CG11231	1.00		
CG14442	Increased	CG14442	1.00		
CG32736	Increased	CG32736	1.00	Uncharacterised protein family	
CG32718	Increased	CG32718	1.00		
CG15480	Increased	CG15480	1.02		
CG7968	Increased	CG7968	1.03	Haemolymph juvenile hormone binding protein	
HDC17458	Increased	HDC17458	1.03		
CG1629	Increased	mal	1.04	Aminotransferase	MOSC domain
CG34434	Increased	CG34434	1.04		
CG1971	Increased	CG1971	1.05		
HDC16920	Increased	HDC16920	1.05		
CG18656	Increased	CG18656	1.06		
CG4455	Increased	CG4455	1.06		
CG4631	Increased	CG4631	1.06	Domain of Unknown Function	
CG11260	Increased	CG11260	1.06		
CG32790	Increased	CG32790	1.08		
CG3568	Increased	CG3568	1.08	Domain of Unknown Function	
CG18404	Increased	CG18404	1.09		
CG31807	Increased	CG31807	1.10	Ubiquitin Transferase	RING finger domain
CG43117	Increased	CG43117	1.10		
CG14673	Increased	CG14673	1.13		
CG5813	Increased	chif	1.14	Kinase	DBF zinc finger
CG32005	Increased	CG32005	1.14	High Mobiligy Group Box	DNA binding
HDC12508	Increased	HDC12508	1.14		
HDC12757	Increased	HDC12757	1.14		
HDC19233	Increased	HDC19233	1.15		
CG9263	Increased	CG9263	1.16		
CG31819	Increased	CG31819	1.16		
CG31817	Increased	CG31817	1.17		
CG32988	Increased	CG32988	1.18		
CG31813	Increased	CG31813	1.18		
CG42749	Increased	CG42749	1.18		
CG1657	Increased	CG1657	1.20	GTPase activating	activates Rab GTPases
CG16852	Increased	CG16852	1.24		
CG4666	Increased	CG4666	1.27		
CG13365	Increased	CG13365	1.27		
CG7988	Increased	CG7988	1.30	Regulation of Circadian Clock	
CG30361	Increased	mtt	1.31	G protein coupled receptor	
CG16853	Increased	CG16853	1.31		
CG4484	Increased	Slc45-1	1.45	Sucrose Transporter	

Weakest to strongest hits are ordered from top to bottom

The presence of *Wolbachia* increases the quantity and distribution of ubiquitinated proteins in infected host cells and oocytes

Given RNAi knockdowns of host components involved in the ubiquitin/proteolysis pathway resulted in a reduction in *Wolbachia* titer, we examined whether the presence of *Wolbachia* might influence the ubiquitination state of host proteins. This was accomplished through

immunofluorescence analysis with an antibody that specifically recognizes ubiquitin-conjugated host proteins. The antibodies were developed to recognize the multi-ubiquitinated chains of polyubiquitinated proteins but not free ubiquitin (see Methods) [178, 179]. This analysis revealed a significant increase in the number of ubiquitin foci in the *Wolbachia*-infected cells compared to the uninfected controls (Figure 4.3). Figure 4.3B presents DAPI-stained nuclei (blue), microtubule-labeled cytoplasm (green), and ubiquitin foci (red) in JW18 infected and uninfected cells. The images reveal that the number, size, and intensity of the ubiquitin foci are much greater in the former. For example, 85% (n = 142) of the infected cells had one or more ubiquitin foci compared to 45% (n = 138) for the uninfected cells. Additionally, 51% of infected cells had five or more ubiquitin foci (n = 72), which was significantly different (P = 0.0001) compared to 7% of uninfected cells with that outcome (n = 10) (Figure 4.3A). Significance was determined using chi-square analysis.

We also performed this analysis on infected and uninfected *Drosophila* oocytes. The images shown in Figure 4.4 depict oocytes from infected and uninfected adult *D. melanogaster* females. PI (red) stains host nuclei in uninfected cells and both the host nuclei and *Wolbachia* in infected cells. The anti-ubiquitin antibody (green in top panels and black-and-white in bottom panels) stains the ubiquitin foci. Quantification was performed as previously described [4] (see Methods). Ubiquitin foci counts were accomplished by selecting a defined area at the posterior pole from an image of a medial section of each oocyte. This revealed an average of 10 ± 3 (n = 10) posterior ubiquitin foci in infected oocytes, in contrast to 3 ± 1 (n = 10) posterior ubiquitin foci detected in uninfected oocytes.

Drug-induced inhibition of the proteasome reduces *Wolbachia* titer in the *Drosophila* oocyte

To determine if the maintenance of *Wolbachia* titer relies on high levels of host proteasome activity, *Wolbachia*-infected *Drosophila* females were treated with Lactacystin, a proteasome inhibitor that targets the 20S subunit of the proteasome [180]. After being kept on a regular

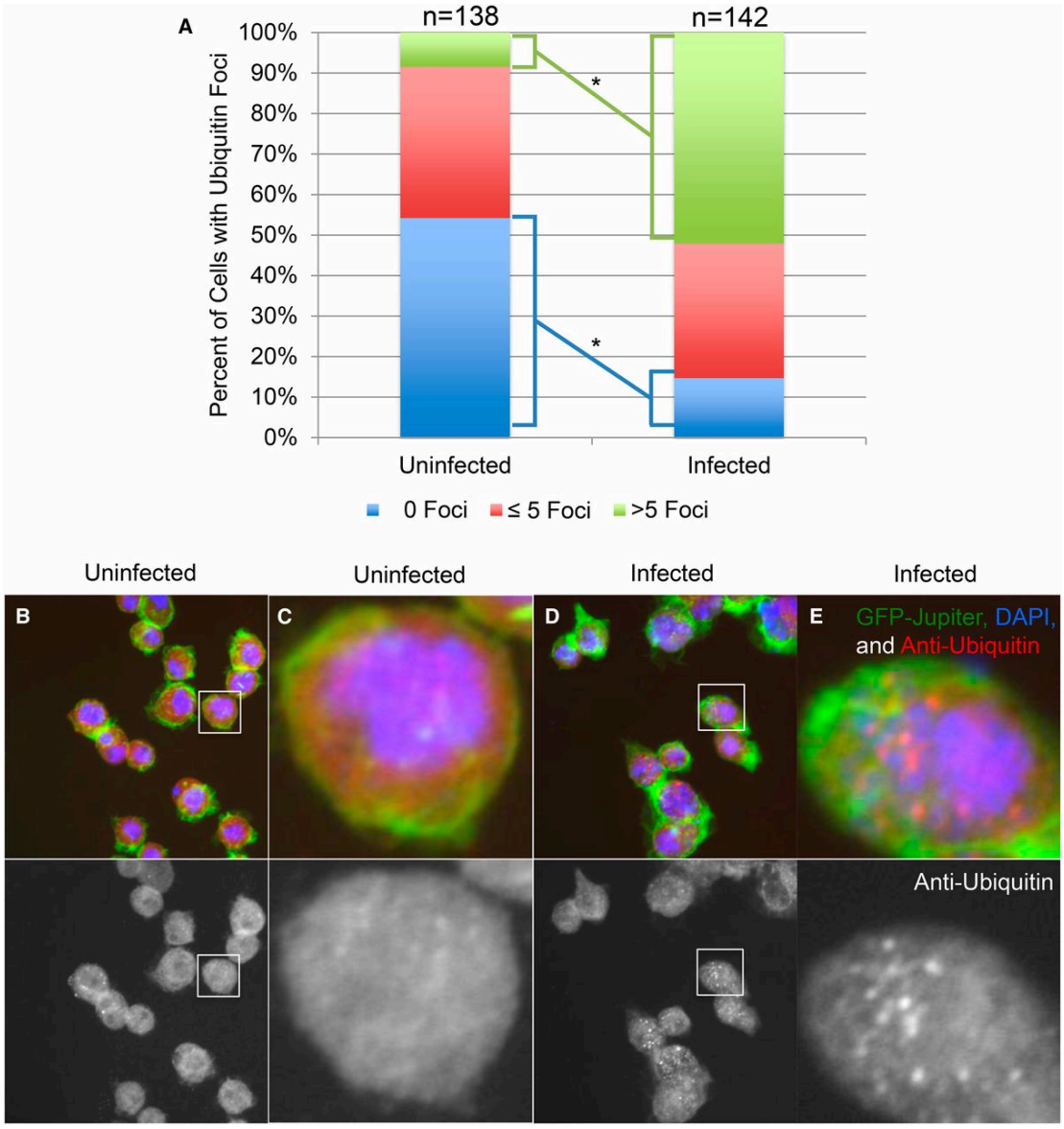

Figure 4.3: **Increase in ubiquitin foci in *Wolbachia*-infected tissue culture cells.** (A) Quantification of the number of ubiquitin foci in infected and uninfected cells. All P values were below 0.0001, and adjusted α value was 0083333. (B and C) Low and high magnification images of stained uninfected cells. (D and E) Low and high magnification images of stained Wolbachia-infected cells. Staining indicates DNA (blue), microtubules (GFP- Jupiter) (green), and ubiquitin foci (red). Significance was determined using chi-square analysis.

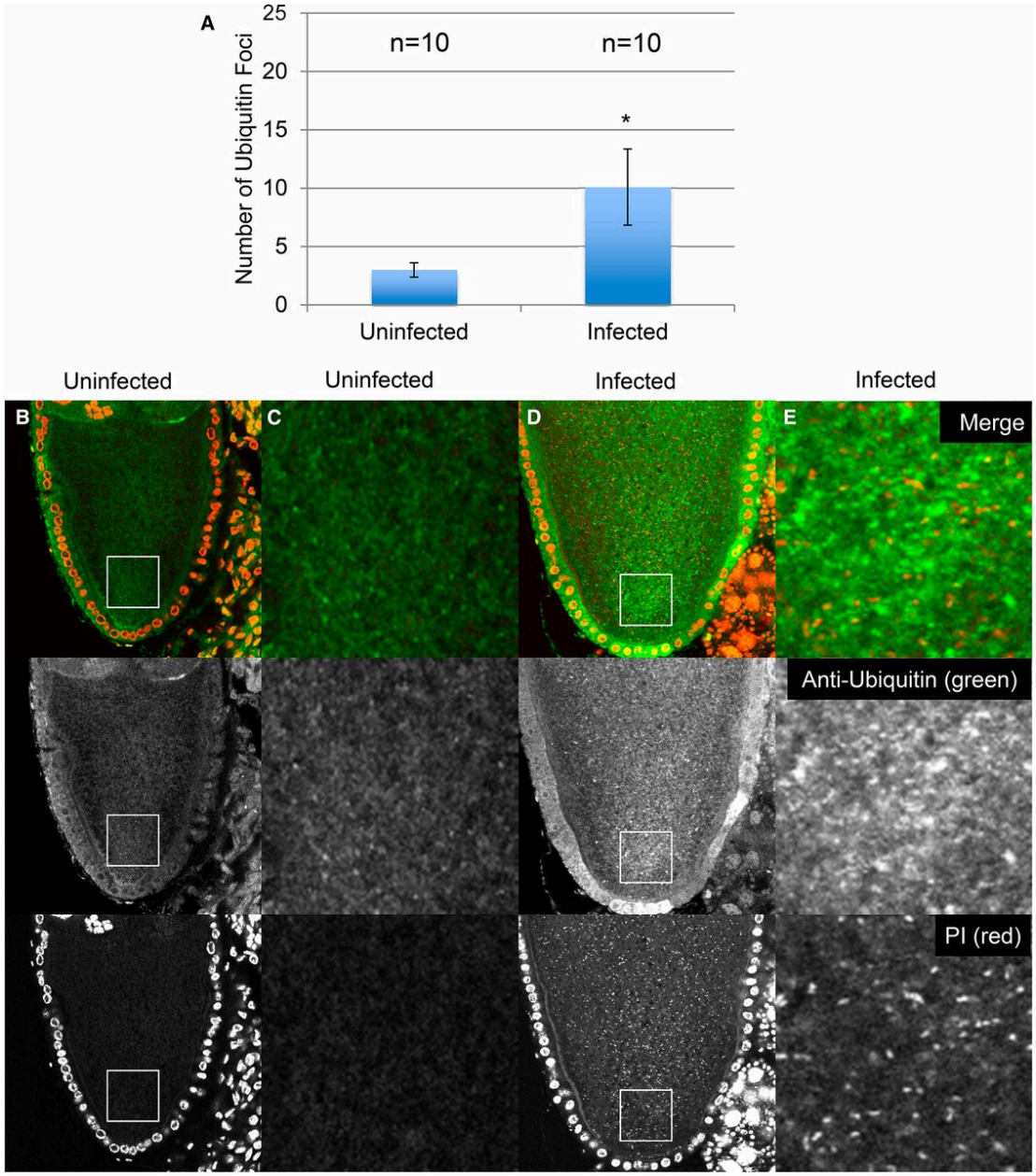

Figure 4.4: **Increase in ubiquitin foci in *Wolbachia*-infected Drosophila oocytes.** Immmunofluorescence analysis using an anti-ubiquitin antibody indicated more ubiquitin foci in *Wolbachia*-infected oocytes. (A) Quantification of ubiquitin foci per area in medial planes of infected and uninfected oocytes. Average values were significantly different according to ANOVA (P = 0.046). Error bars indicate SEM. (B and C) Low and high magnification images of uninfected oocytes. (D and E) Low and high magnification images of *Wolbachia*-infected oocytes. DNA (red) and ubiquitin foci (green).

diet for 2 days, the flies were exposed to food containing 100 µM lactacystin for 3 days. Control females were exposed to food with an equivalent amount of carrier DMSO. Ovarian tissues were dissected and stained with PI to label *Wolbachia* DNA. As previously described, *Wolbachia* abundance was determined by confocal imaging of the medial plane of PI-stained stage 10 oocytes [4] (see Methods). In these images, the PI stains the nuclei of the host follicle cells that border the oocyte and the *Wolbachia* nucleoids within the oocyte (Figure 4.5). This analysis indicated significant reduction in *Wolbachia* titer in lactacystin-treated oocytes compared to untreated control oocytes (Figure 4.5, A and B). Control oocytes averaged 700 ± 54 *Wolbachia* (n = 29), while the treated oocytes averaged 534 ± 35.0 (n = 29) (P = 0.012). Significance was determined using ANOVA.

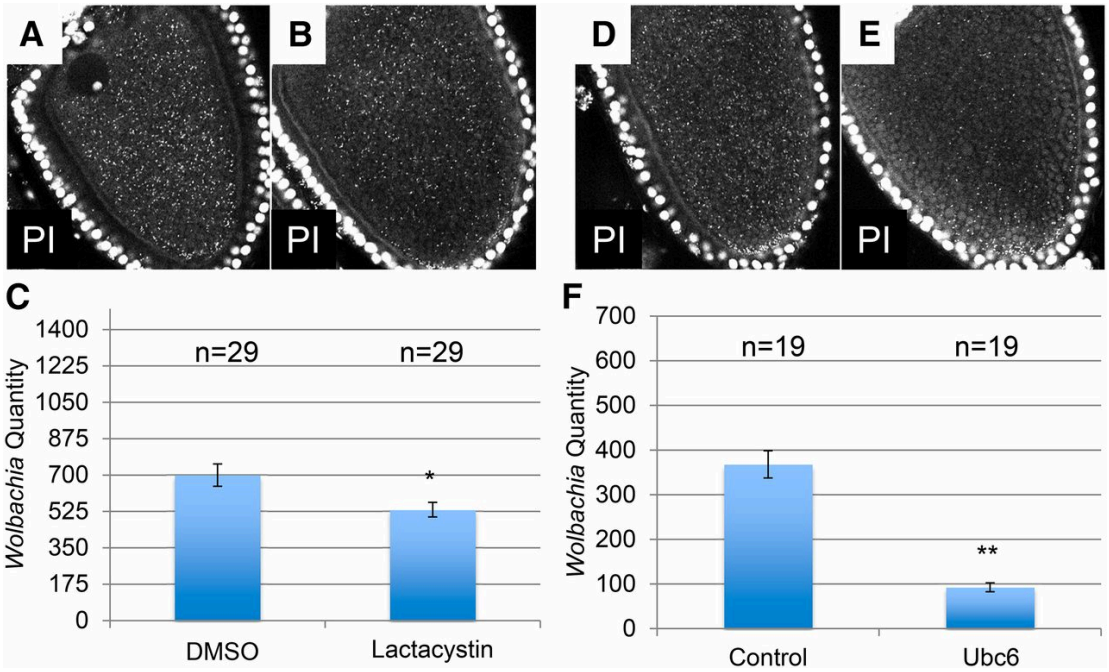

Figure 4.5: **Disruption of host proteasome reduces *Wolbachia* titer in the Drosophila oocyte.** Adult females were fed food containing either DMSO (A) or lactacystin (B). (C) Quantification of the Wolbachia in medial plane of stage 10 oocytes indicated a significant difference by ANOVA (P = 0.012). Control (D) and Ubc6 (E) knocked down using GAL4-UAS dsRNA expression. Quantification of oocyte titers (F) indicated a significant difference by ANOVA (P < 0.001). Error bars indicate SEM.

RNAi knockdown of proteasome component Ubc6 results in a dramatic decrease in *Wolbachia* titer in the oocyte

We next genetically tested the impact of the host ubiquitin/proteasome pathway on oocyte *Wolbachia* titer. We used the GAL4:UAS system to knockdown specific components of the ubiquitin/proteasome pathway in the female germ line (see Methods) [181]. Because *Wolbachia* is intimately associated with the ER in our cell lines (see next section), we focused on the host factor Ubc6 recovered in our screen (Table 4.1). Ubc6 is an ER integral membrane protein that functions as an E2 conjugating enzyme in the ERAD pathway: endoplasmic reticulum (ER)-associated degradation of mis-folded proteins [182]. Ubc6 is specifically required for the degradation of cytosolic domains of membrane proteins (ERAD-C) [183]. Previous studies have successfully knocked down Ubc6 using UAS Ubc6 RNAi fly lines [184]. By crossing in the maternal nanos-GAL4 driver into the UAS-Ubc6 RNAi line, we specifically knocked down the level of Ubc6 in *Drosophila* female germ line cells. This RNAi knockdown of Ubc6 in the *Drosophila* germ line resulted in an approximately fourfold reduction in oocyte *Wolbachia* titer (Figure 4.5). The wild-type oocytes averaged 368 ± 133 (n = 19) *Wolbachia* while the Ubc6 knockdowns averaged 93 ± 43 (n = 19) ($P < 0.01$) (Figure 4.5). These results suggest that a fully functional host ERAD pathway is required to maintain *Wolbachia* titer in the *Drosophila* oocytes and cell lines.

***Wolbachia* is closely associated with and alters the morphology of the ER**

Given the dependence of *Wolbachia* titer on ERAD, we performed ultrastructural analysis on the *Wolbachia*-infected cell lines to determine its subcellular localization. Ultrastructural images of the *Wolbachia*-infected cell line are shown in Figure 4.6 and Figure 4.7. The *Drosophila* cells are round with a mean diameter of 6–8 μm. *Wolbachia* (W), golgi (G), the endoplasmic reticulum cisternae (ERC), mitochondria (M), and nuclei (N) are readily visualized in these cells (Figure 4.6, A and B). *Wolbachia* tend to exhibit an approximate diameter of 0.5 μm and occasionally observe lengths >1 μm (Figure 4.6C). As previously

described, *Wolbachia* are often encompassed by a double membrane, enclosing the bacteria within a small vacuole [185, 186]. In some instances, multiple *Wolbachia* occupy the same vacuole. Dividing *Wolbachia* are depicted in Figure 4.6D. In this case, both daughter bacteria lie in the same vacuole although it is expected that each daughter bacterium will reside within its own host vacuole after completion of division (Figure 4.6D).

Our ultrastructural analysis reveals an intimate association between *Wolbachia* and the host ER. Figure 4.7A depicts an elaboration of the ER extending from the nuclear envelope to a

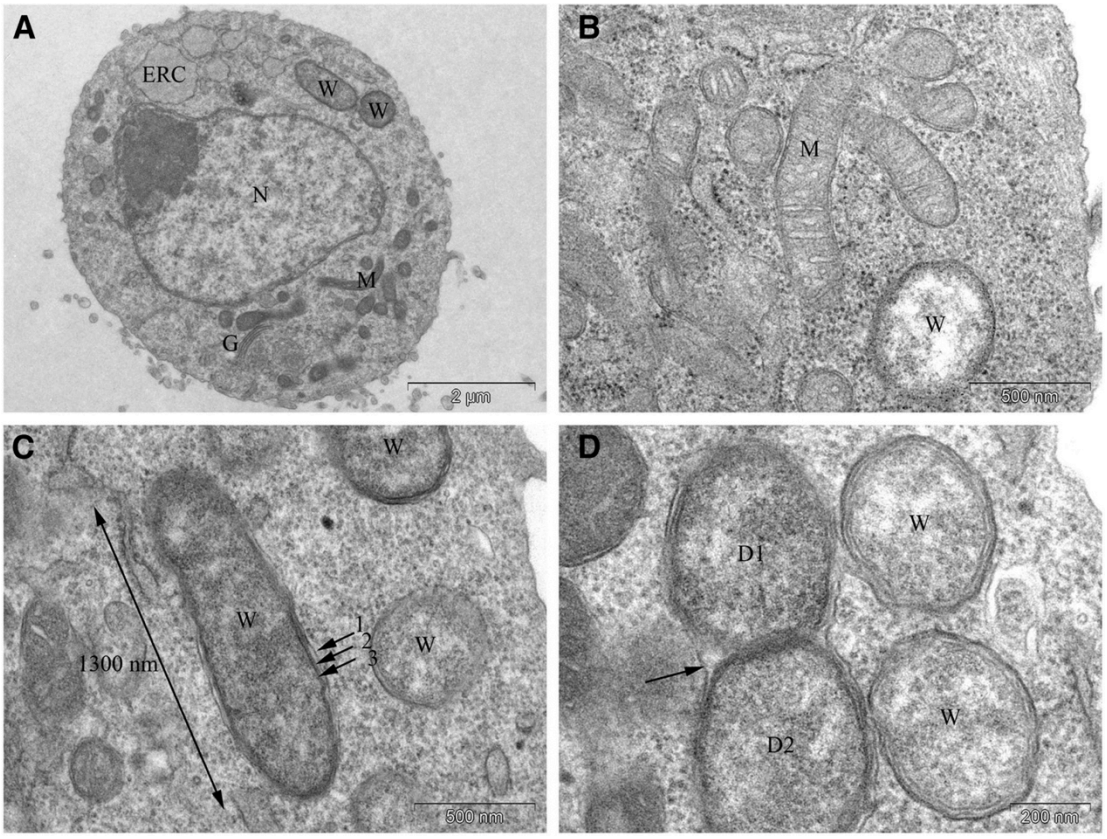

Figure 4.6: **Ultrastructural analysis of *Wolbachia* in Drosophila cultured cells.** (A) Cross-section of a *Wolbachia*-infected Drosophila cell in which the nucleus (N), endoplasmic reticulum cisternae (ERC), golgi (G), mitochondria (M), and *Wolbachia* (W) are readily visualized. Cells are spherical with a mean diameter of 6–8 µm. (B) Mitochondria and *Wolbachia* are readily distinguished as the former exhibit distinct internal tubular structures and are narrower in width. (C) The maximum size observed for *Wolbachia* is a 1300 nm length and 460 nm width. Each *Wolbachia* bacterium is encompassed by three membranes, the outermost derived from the host (arrows 1, 2, 3). (D) Image of dividing *Wolbachia*. The two daughter cells (D1 and D2) lie in the same vacuole (arrow), which ultimately will abscise.

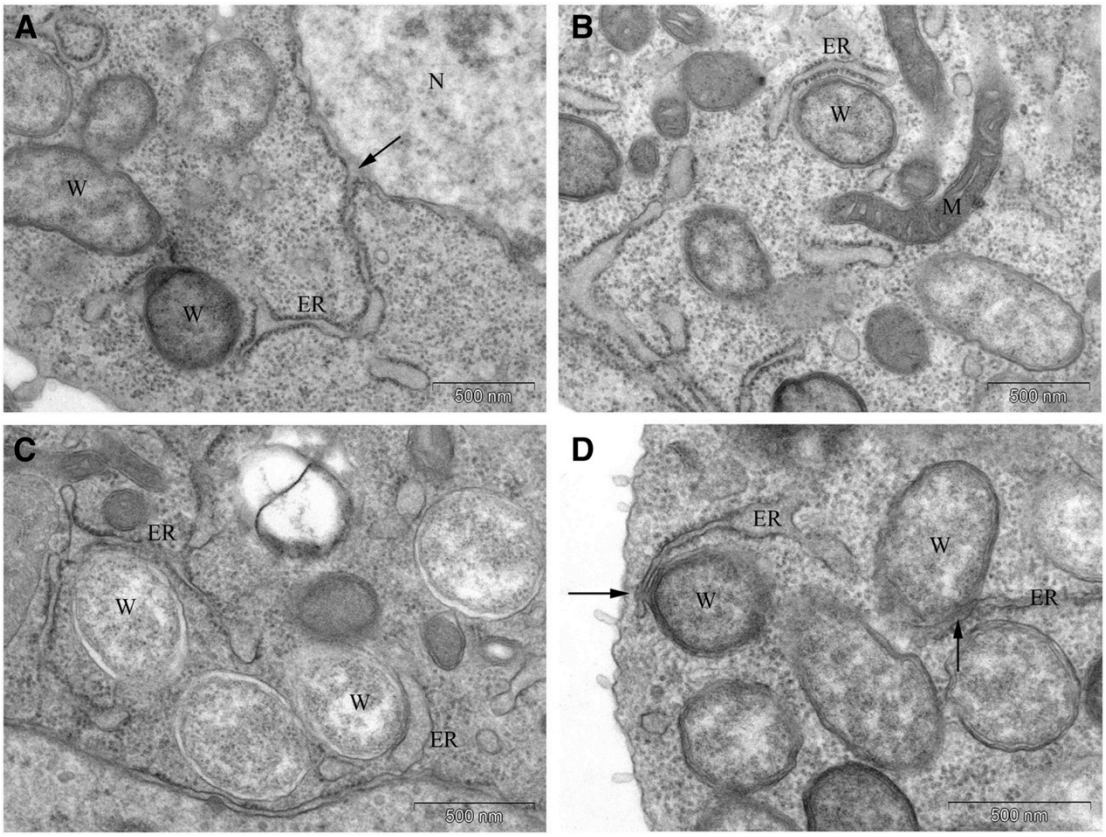

Figure 4.7: ***Wolbachia* closely associate and alter the morphology of the ER.** (A) The presence of *Wolbachia* results in an ER extension from the nuclear envelope (arrow) to *Wolbachia*. (B and C) Examples of ER extensions wrapping around and in close association with *Wolbachia*. (D) In some instances, *Wolbachia* appear to communicate with the ER lumen (arrows). W, *Wolbachia*; ER, endoplasmic reticulum; N, nucleus; M, mitochondria.

Wolbachia located in the cytoplasm. Figure 4.7, B and C depict similar ER extensions that encompass individual *Wolbachia*. In some instances, there is a direct contact and continuity between the host ER and *Wolbachia* membrane vacuole. This is especially evident in Figure 4.7D. These images suggest that *Wolbachia* are connected to the luminal space of the ER. In addition to the intimate association between *Wolbachia* and the ER, we find that the presence of *Wolbachia* induces dramatic alterations in ER morphology. In the uninfected cell line, the ER exhibits classic tubule morphology with ribosomes decorating its entire length (Figure 4.8, A and B). By contrast, in the *Wolbachia*-infected cells, the ER is highly

elaborated forming a complex network of extensions (Figure 4.8, C and D). In addition, the ER tubules have expanded to form large cisternae. As seen in the images, *Wolbachia* are often associated with these cisternae. To quantify the effect of *Wolbachia* on ER morphology, we analyzed randomly selected EM images from *Wolbachia*-infected and cured cell lines (n = 128 and 121, respectively) (Figure 4.9). Quantification revealed a dramatic increase in all classes of abnormal ER morphology, including the ER network extensions, ER swelling, and formation of large ER cisternae. Particularly striking is the 10-fold increase in the formation of ER cisternae in *Wolbachia*-infected cells (Figure 4.9).

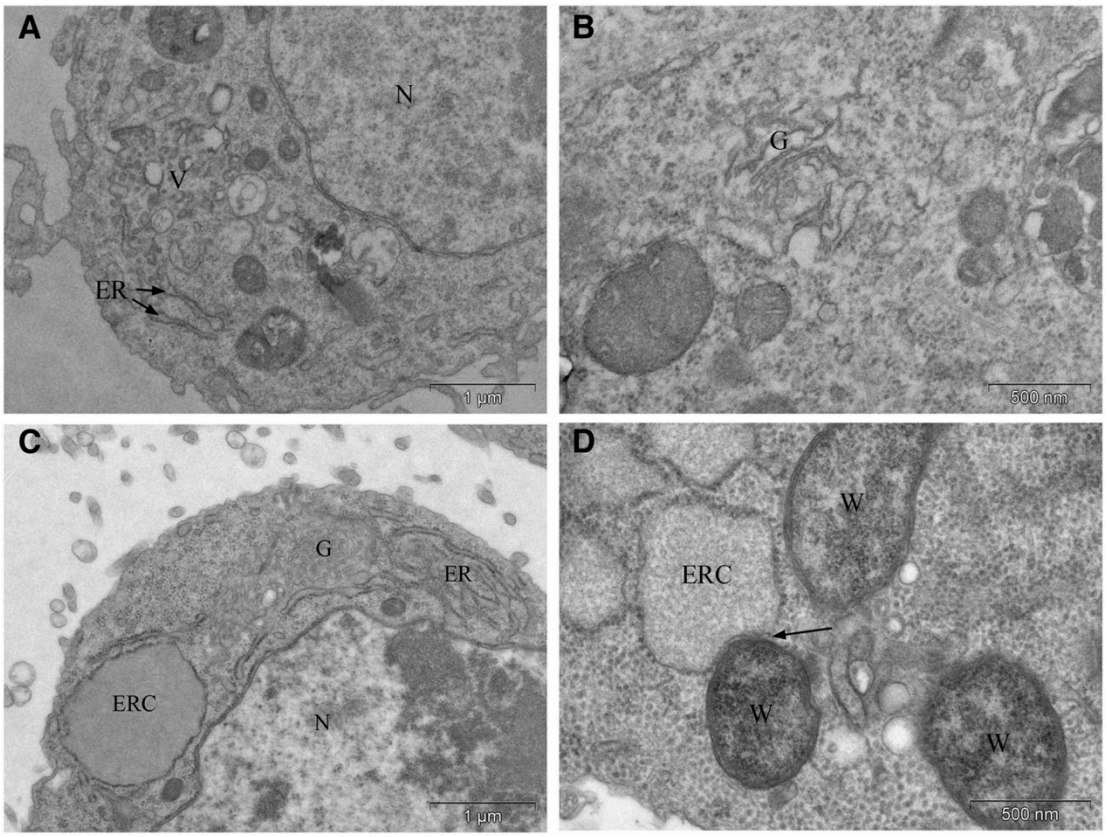

Figure 4.8: ***Wolbachia* alter the morphology of the ER.** (A and B) Images from uninfected (doxycycline cured) *Drosophila* cell lines. Under these conditions, the ER compartments exhibited a normal tubular and discrete shape. Additionally, only few Golgi bodies were found. (C and D) Images from *Wolbachia*-infected *Drosophila* cell lines. (C) The presence of *Wolbachia* resulted in the swelling of the ER to form either ER cisternae or a highly elaborate complex of ER extensions and golgi. (D) *Wolbachia* are often observed in close contact with enlarged ER cisternae (ERC, arrow). W, *Wolbachia*; ER, endoplasmic reticulum; N, nucleus; V, vesicles; G, golgi.

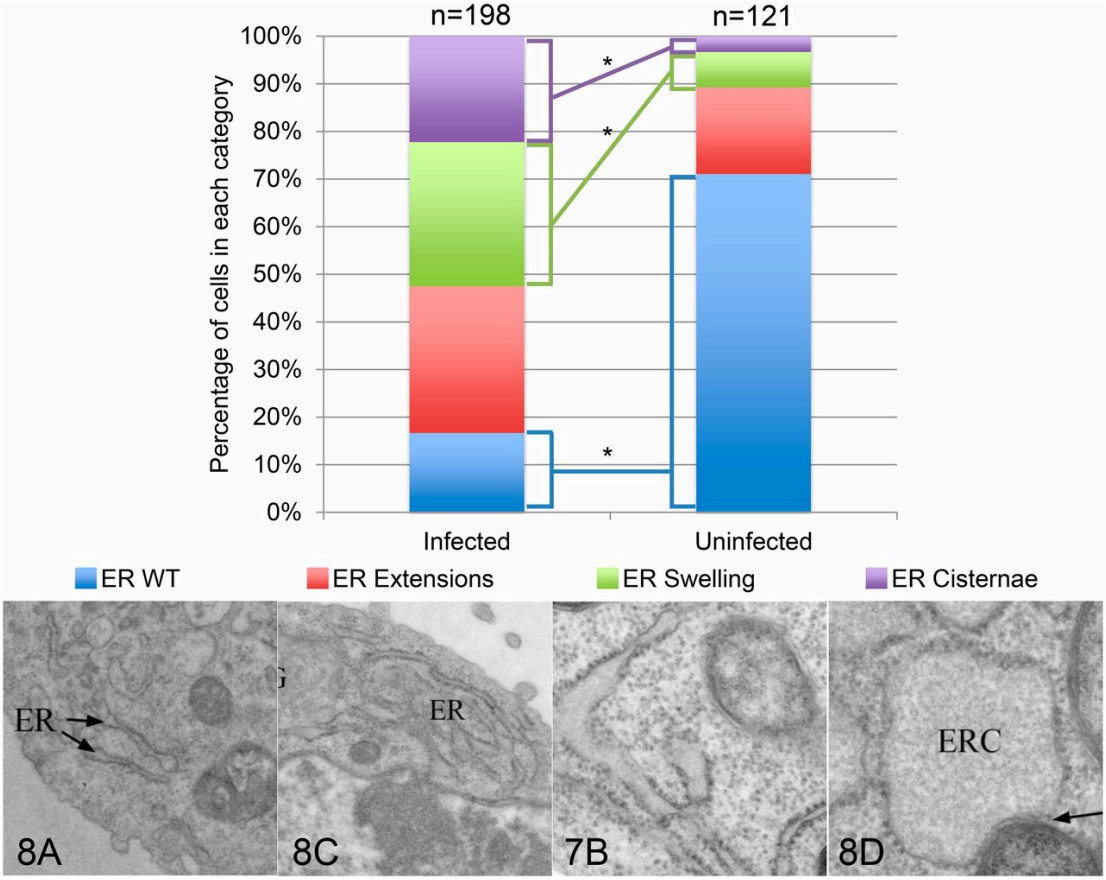

Figure 4.9: **Quantification of ER morphology in *Wolbachia*-infected and cured cells.** ER morphology in randomly selected EM sections from 198 *Wolbachia*-infected cells and 121 cured cells was classified into four distinct categories of ER morphology: wild type (WT), extensions, swelling, and cisternae. Quantification revealed the presence of *Wolbachia* significantly decreased the percentage of cells exhibiting wild-type ER and significantly increased the percentage of cells exhibiting ER swelling and ER cisternae ($P < 0.0001$ for all, with adjusted $\alpha = 0.00625$). Significance was determined using chi-square analysis. Images below illustrate each category. The number and letter in the bottom left of the images indicate which previous figure the image originated from. The ER and ER cisternae (ERC) are labeled where appropriate.

4.4 Discussion

Performing the genome-wide, cell-based RNAi screen enabled us to comprehensively identify host factors that influenced *Wolbachia* titer. Of the 15,699 targets tested by RNAi disruption [175], the screen yielded 36 RNAi treatments that decreased *Wolbachia* titer and 41 RNAi treatments that increased titer, implicating 77 host genes. The fact that only a small fraction

of the RNAi knockdowns influenced titer suggests that *Wolbachia* possesses robust mechanisms of maintaining specific intracellular titers. Not surprisingly, hits that reduced *Wolbachia* titer spanned a broad array of cellular functions including host transcriptional and translational machinery, mitochondrial proteins, cell signaling, and metabolism (Table 4.1).

Of the 77 gene knockdowns that significantly altered *Wolbachia* titer, eight genes were involved in the ubiquitin/proteolysis pathway. These included RpL40, lig, Ubiquitin-5E, ubl, Ubc6, mei-P26, CG12725, and CG31807. These studies indicate that maintenance of *Wolbachia* titer requires fully functional host ubiquitin and proteolysis pathways. A likely explanation for this dependence comes from genomic studies demonstrating that *Wolbachia* lacks many of the pathways for amino acid production [177, 187]. A robust ubiquitin/proteasome pathway would ensure an adequate pool of amino acids in order for *Wolbachia* to thrive. Similarly, RNAi screens in *Drosophila* infected with *L. monocytogenes*, *M. fortuitum*, and *F. tularensis* revealed that bacteria titer uptake and proliferation was highly dependent on the ubiquitin and proteasome pathways [61, 63, 64].

We used immunofluorescence to determine if the presence of *Wolbachia* influenced the ubiquitination state of proteins in these cells by taking advantage of an antibody that broadly recognizes mono and poly-ubiquitinated proteins [179]. Our analysis of ubiquitin staining in tissue culture cells and *Drosophila* oogenesis revealed significantly more foci in the *Wolbachia*-infected conditions than uninfected conditions. Previous studies using an antibody that broadly recognizes poly-ubiquitinated proteins revealed that the herpes simplex virus immediate-early protein ICPO induces proteasome-dependent degradation of host proteins and results in a similar increase in the number and extent of ubiquitin foci, which are interpreted as sites of concentrated poly-ubiquitinated proteins [179].

Function disruption tests also support a role for the ubiquitin-proteasome system in regulating *Wolbachia* titer in *Drosophila* oogenesis. Disruption of proteasome activity with the small molecule inhibitor lactacystin also significantly reduced oocyte *Wolbachia* titer, indicating that maintenance of *Wolbachia* titer in oogenesis is dependent on host proteasome activity. We

also knocked down Ubc6, an E2 conjugating enzyme involved in the ERAD pathway [183]. Ubc6 is specifically associated with the ERAD-C complex that monitors the folding state of the cytosolic domains of membrane proteins. These results suggest that *Wolbachia* preferentially rely on the ERAD-C protein degradation pathway as an amino acid source. In support of this conclusion, our EM analysis of *Wolbachia*-infected tissue culture cells reveals that *Wolbachia* exhibits a particularly close association with the ER (Figure 4.6, Figure 4.7, and Figure 4.8).

Our results are in accord with proteomic and genomic studies indicating that *Wolbachia* in Aedes and *B. malayi* must rely on host-derived amino acids [30, 188]. In addition, studies demonstrate that amino acids may be limiting because *Wolbachia* competes with its host for amino acids [189]. Our findings are also in line with work demonstrating that mosquito cell lines newly infected with *Wolbachia* exhibit up-regulation of the host 26S proteasome and a general increase in ubiquitinated proteins [190]. However, a key difference between these studies in mosquito cells and our work in *Drosophila* is the timeline of the effects. Differences in the proteasome and ubiquitination levels were not observed between long-term *Wolbachia*-infected and cured mosquito cell lines, nor was it observed in cured cell lines reinfected with *Wolbachia*. This suggests that the up-regulation was a transient host response to new infection. In contrast, we found that up-regulation of the proteasome occurs in *Drosophila* cell lines and oocytes with long-term *Wolbachia* infections. Whether this is the result of a difference in the fundamental biology of mosquito and *Drosophila* cells is unclear.

Our ultrastructural studies of the infected cell lines demonstrate a close association between *Wolbachia* and the ER. As shown in Figure 4.6 and Figure 4.7, *Wolbachia* shares membrane with the ER and is often found embedded in the ER. A similar close association between *Wolbachia* and the ER has been documented in early *Drosophila* embryos [185], nurse cells [95], and in the central nervous system [191]. These observations are intriguing in light of our finding that the ERAD pathway is required for maintaining *Wolbachia* titer both in cells lines

and *Drosophila* oocytes. By being embedded in the ER, *Wolbachia* is in prime position to utilize the products derived from ERAD-mediated protein degradation.

An alternative interpretation of these results is based on studies of apicoplasts, organelles present in apicomlexan parasites including *Toxoplasma gondii* and *Plasmodium falciparum*. This organelle originated from an alga that under- went secondary endocytosis [192]. Apicoplasts have many properties in common with *Wolbachia* including maternal inheritance, multiple membranes, and a close association with the ER [192]. In apicoplasts, the ERAD pathway has been usurped and modified to facilitate import of key required proteins from the host cytoplasm [193]. Strikingly, it also relies on the ubiquitin pathway marking proteins for import to the apicoplast. These findings raise the intriguing possibility that *Wolbachia* may also rely on the ERAD pathway for import of host cytoplasmic proteins.

Two other functional categories have been validated *in vivo* in addition to Ubiquitin: "ATP/GTP" and "Mitochondrial." Five hits were identified in the ATP/GTP functional category. We found that knockdown of protostome-specific GEF (CG14047) in the *Drosophila* germ line significantly decreased oocyte titer (Figure S1A). Three hits were also recovered in mitochondrial metabolism: a NADH dehydrogenase (CG3214), a succinate dehydrogenase (CG14757), and a mitochondrial carrier protein (CG18324). We found that knockdown of CG3214 and CG18324 in the *Drosophila* oocyte resulted in significant increases and decreases in *Wolbachia* titer, respectively (Figure S1, C and D). We suspect that the reduction of cellular ATP levels expected from knockdown of these genes limits the ability of *Wolbachia* to replicate within the cells. Alternatively, because specific *Wolbachia* and mitochondrial strains have coevolved, *Wolbachia* may be highly sensitive to functional changes in its companion mitochondria [194]. It should be pointed out that some of these RNAi hits might be false positives because secondary screens have not confirmed them.

Two hits that reduced *Wolbachia* titer were in genes regulating lipid metabolism. CG9243 encodes phospholipase D that catalyzes breakdown of phosphatidylcholine to phosphatidic acid and choline. CG1718 is an ABC transporter that functions in sterol uptake and

esterification. This reliance on host lipid metabolism to maintain titer may be due to the fact that *Wolbachia* is encompassed by an outer host-derived membrane and lacks key fatty acid and cholesterol metabolic pathways [177, 185]. Thus, replication of *Wolbachia* is likely to place exceptional demands on host lipid metabolism. Our results are also in accord with a recent study demonstrating that the presence of *Wolbachia* significantly alters lipid metabolism of *Aedes albopictus* mosquito cells [195]. Significantly, the titer of *Spiroplasma*, another maternally inherited insect endosymbiont, is also limited by the levels of host lipids [196]. In addition, replication of mammalian pathogens *M. tuberculosis* and *C. trachomatis* requires host-derived lipids [197, 198].

It is now well documented that the presence of *Wolbachia* confers resistance against a number of positive-strand RNA viruses including dengue and Zika [199]. There is evidence that multiple host mechanisms may be involved in inhibiting viral replication including synthesis of reactive oxygen and cholesterol and induction of host autophagy [200-203]. Our finding that Wolbachia dramatically alters host ER morphology and relies on the ERAD pathway to maintain titer suggests the involvement of a previously unsuspected mechanism in preventing the replication of positive-strand RNA viruses. For a number of positive-strand RNA viruses, the ER is the preferred site of replication and assembly [204]. Viral targeting of host ER induces dramatic changes in the morphology of the ER including invaginations of the ER membrane, swelling of the ER into large cisternae, and formation of virus-containing vesicles in the lumen [204]. These alterations are believed to create membrane-based sites of viral replication and assembly. Particularly striking are the recent findings that positive-strand RNA viruses specifically target and subvert the ERAD pathway to facilitate replication and assembly [205]. For example, the ERAD pathway was identified in a recent genome-wide CRISPR (clustered regularly interspaced short palindromic repeats) screen to identify host factors essential to the dengue virus [206]. Our finding that *Wolbachia* also relies on the ERAD pathway for replication and produces dramatic alterations in ER morphology suggests that *Wolbachia* and positive-strand RNA viruses may be competing for the same intracellular

niche. The intimate association between *Wolbachia* and the ER may physically prevent viruses from associating with ERAD sites. Alternatively, the extensive disruption in ER morphology may nonspecifically prevent the interactions necessary for viral replication. A satisfying aspect of this explanation of viral suppression is that it readily explains the ability of *Wolbachia* to suppress RNA viruses, and not DNA viruses, which preferentially replicate in the nucleus [207]. A number of other intracellular bacteria also exhibit a close association with the ER [208, 209]. It will be of great interest to determine whether these also suppress positive-strand RNA viral replication.

Chapter 5

The Impact of Host Diet on *Wolbachia* Titer in *Drosophila*

5.1 Abstract

While a number of studies have identified host factors that influence endosymbiont titer, little is known concerning environmental influences on titer. Here we examined nutrient impact on maternally transmitted *Wolbachia* endosymbionts in *Drosophila*. We demonstrate that *Drosophila* reared on sucrose- and yeast-enriched diets exhibit increased and reduced *Wolbachia* titers in oogenesis, respectively. The yeast-induced *Wolbachia* depletion is mediated in large part by the somatic TOR and insulin signaling pathways. Disrupting TORC1 with the small molecule rapamycin dramatically increased oocyte *Wolbachia* titer, whereas hyper-activating somatic TORC1 suppressed oocyte titer. Furthermore, genetic ablation of insulin-producing cells located in the *Drosophila* brain abolished the yeast impact on oocyte titer. Exposure to yeast-enriched diets altered *Wolbachia* nucleoid morphology in oogenesis. Furthermore, dietary yeast increased somatic *Wolbachia* titer overall, though not in the central nervous system. These findings highlight the interactions between *Wolbachia* and germ line cells as strongly nutrient-sensitive, and implicate conserved host signaling path- ways by which nutrients influence *Wolbachia* titer.

5.2 Introduction

Microbial endosymbionts have a profound impact on host metabolism and there are numerous examples in which microbes provide essential nutrients to the host [209-224]. In contrast, considerably less is known regarding how host metabolism and nutrition affect resident endosymbionts. To date, there is evidence that restricting the supply of host carbon, nitrogen and phosphorous significantly limits the number of *Chlorella* endosymbionts of green hydra and dinoflagellate endosymbionts of cnidarians [209]. Researchers have also

observed that exposure to high levels of exogenous thiamine monophosphate suppresses the titer of *Sodalis* and *Wigglesworthia* endosymbionts in tsetse flies [221, 222]. In this largely unexplored area, many outstanding questions remain: What are the host and endosymbiont metabolic and signaling pathways involved in nutrient sensing? To what extent do endosymbionts exhibit tissue-specific responses to nutrient availability? How are the rates of endosymbiont replication and cell death influenced by host metabolism and nutrients?

The symbiosis between *Wolbachia* and *Drosophila* is an excellent system to experimentally address these issues. *Wolbachia* are obligate intracellular endosymbionts carried by an estimated 40% of all insect species, including the established model organism *Drosophila melanogaster* [6, 7, 225, 226]. Though *Wolbachia* endosymbionts are naturally carried within germ line cells of both male and female insects, *Wolbachia* are ultimately removed from sperm prior to completion of spermatogenesis [6, 7, 227-231]. Thus, *Wolbachia* rely upon transmission through the maternal germ line for their success. In addition to its functional importance in *Wolbachia* transmission, the well-characterized molecular and cell biology of *Drosophila* oogenesis has provided considerable contextual information and experimental tools that can be applied to studies of *Wolbachia*-host interactions [6, 96, 181, 232-234].

The primary developmental units of the ovary that carry *Wolbachia* are referred to as egg chambers [96, 234]. In each egg chamber, an outer layer of somatic follicle cells encapsulates an interconnected cyst of germ line cells, comprised of 15 nurse cells and an oocyte. *Wolbachia* are initially loaded into these developing cysts during the first mitotic division from a Wolbachia-infected germ line stem cell [6, 83]. This germ line *Wolbachia* population is amplified over time by binary fission and likely to some extent by exogenously invading *Wolbachia* [48, 83, 95, 113, 167, 235]. *Wolbachia* persist in the germ line throughout oogenesis, and a subset of the bacteria concentrate at the oocyte posterior pole during mid- to late oogenesis [83, 84, 103]. This ensures incorporation of *Wolbachia* into germ line progenitor cells that form at the posterior pole of the embryo, perpetuating maternal

germ line transmission cycle [236]. Thus, maintenance of a sufficient *Wolbachia* titer in germ line cells is important for success of the germ line-based transmission strategy.

Here we examined how host diet affects *Wolbachia* titer in *Drosophila melanogaster*. Our findings demonstrate that yeast-enriched diets suppress *Wolbachia* titer and lead to altered nucleoid morphology during oogenesis. Genetic and chemical disruptions indicate that the somatic insulin and TORC1 pathways (Figure 5.1) are required for yeast-based suppression of oocyte *Wolbachia* titer. Our findings also indicate that sucrose-enriched diets increase oocyte *Wolbachia* titer, with little impact on nucleoid morphology. We observed that yeast-enriched diets substantially increase somatic *Wolbachia* titers, though this was not the case in the central nervous system (CNS). These studies demonstrate that *Wolbachia*, and likely other bacterial endosymbionts, exhibit distinct, tissue-specific responses to host nutrients that involve conserved signaling and metabolic pathways.

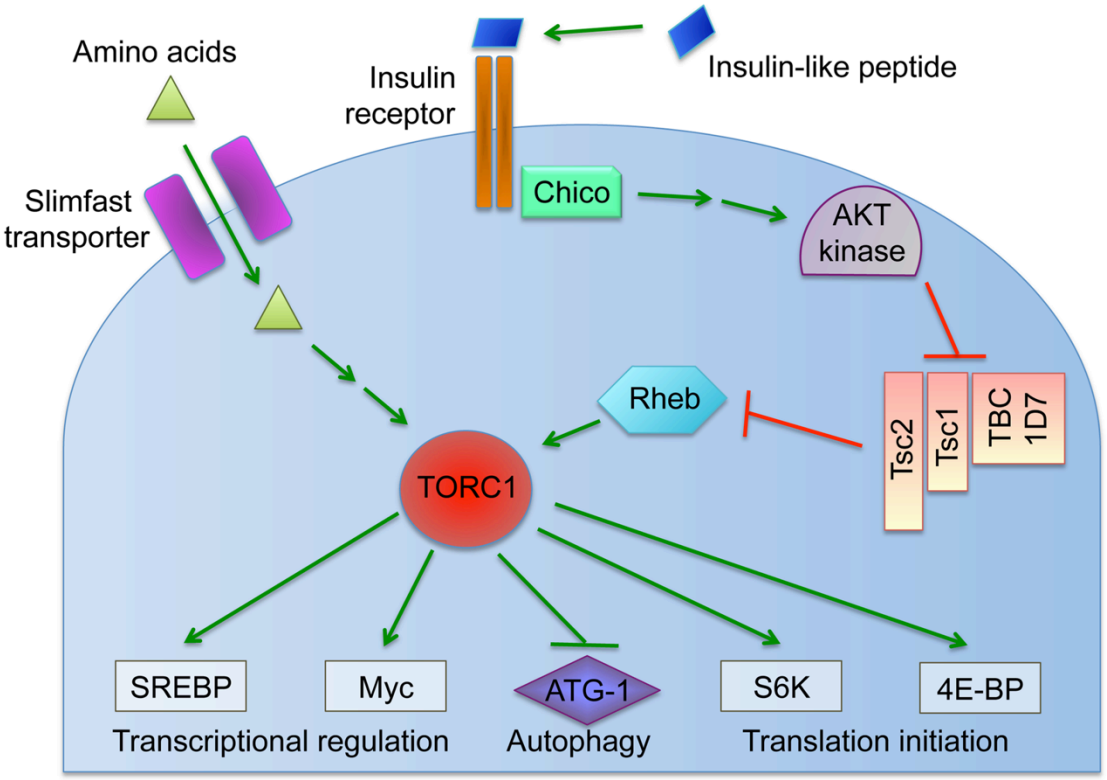

Figure 5.1: **Overview of the nutrient-induced TORC1 signaling pathway.**

5.3 Results

Exposing *Drosophila* to a yeast-enriched diet suppresses germ line *Wolbachia* titer

Nutrient availability strongly affects the life cycle of cultured bacteria, raising questions about how host nutrient conditions affect intracellular *Wolbachia* bacteria. As *D. melanogaster* in nature preferentially consume yeast [237-242], we tested the effect of dietary yeast on *Wolbachia* titer *in vivo*. Female flies were aged first for two days on standard food, then fed yeast paste for 3 days, and examined for *Wolbachia* titer in oogenesis. Ovarian tissues were stained with propidium iodide to label *Wolbachia* DNA, and the *Wolbachia* nucleoids imaged in oocytes of stage 10 egg chambers by confocal microscopy [84]. This analysis demonstrated that yeast paste-fed oocytes carried far fewer *Wolbachia* than control oocytes (Figure 5.2A-B) (S1 Table). *Wolbachia* were further quantified within single oocyte focal planes to determine the relative titer for each condition [95]. This revealed that *Wolbachia* titer in yeast paste-fed oocytes was at 27% of the control level. Oocytes treated with standard fly food exhibited an average of 229 +/- 21.1 *Wolbachia* puncta (n = 30), as compared to yeast paste-fed oocytes that carried 62.6 +/- 4.33 *Wolbachia* (n = 29) ($p < 0.001$) (Figure 5.2C). This indicates that host exposure to yeast paste significantly reduces *Wolbachia* titer in oogenesis.

One possibility is that yeast paste diets reduce oocyte titer because other critical nutrients provided by standard fly food are unavailable. To address this issue, 2-day old *Drosophila* were fed with either standard food diluted 1/3 with water, thereafter referred to as “control food”, or fed with standard food diluted 1/3 with yeast paste, thereafter referred to as “yeast-enriched food” (S1 Table). After 3 days of exposure to these conditions, the titer was assessed in oogenesis. The yeast-enriched condition exhibited 55% of the control titer level, with controls displaying 124 +/- 10.8 *Wolbachia* (n = 58), compared to yeast-enriched oocytes carrying 68.7 +/- 5.12 *Wolbachia* (n = 35) ($p = 0.001$) (Figure 5.2D). To further assess whether this is due to differences in food hydration between control and yeast-enriched conditions, we also exposed flies to a 1/3 dilution of corn syrup into standard fly food (S1

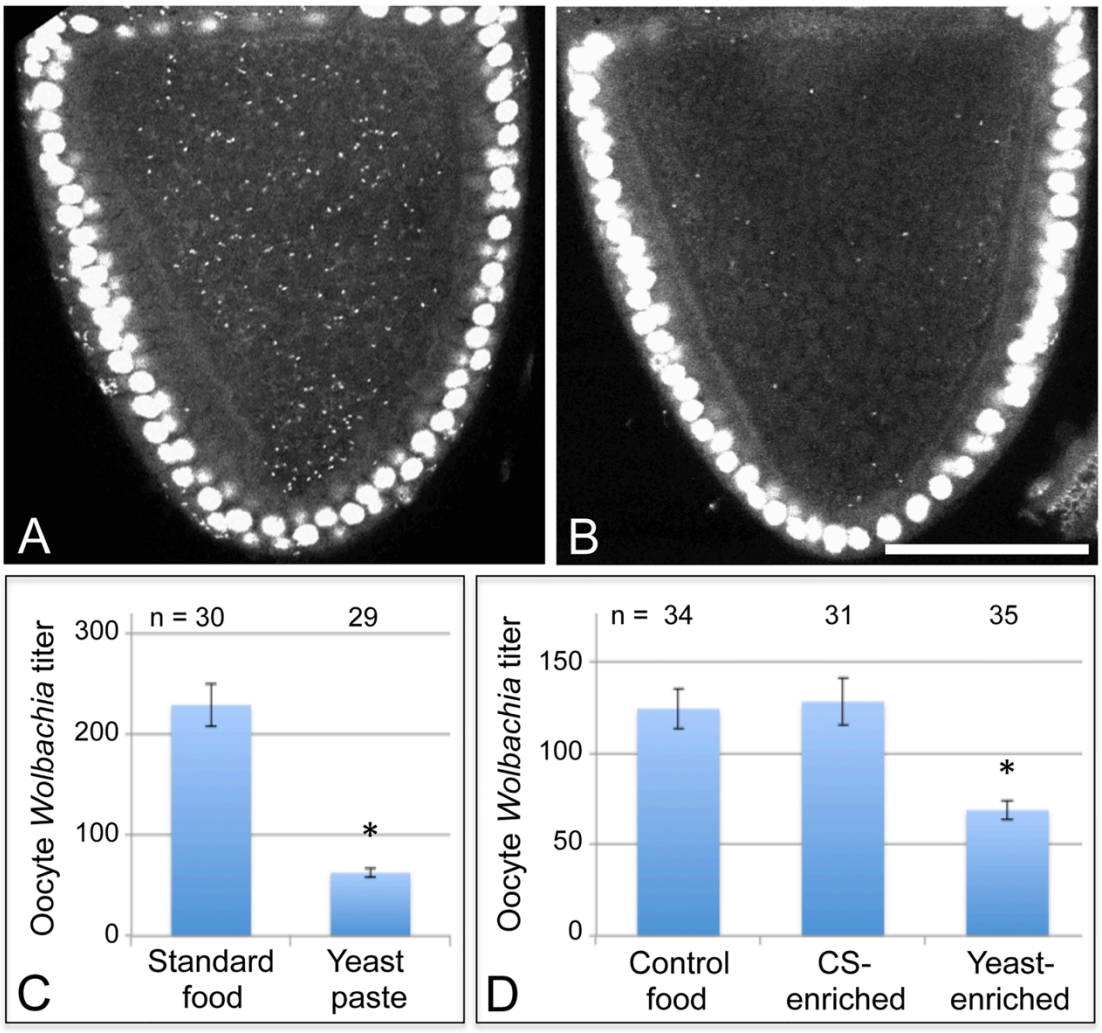

Figure 5.2: **Host diet significantly impacts *Wolbachia* titer in Drosophila oogenesis.** Stage 10A oocytes are outlined in red. Propidium iodide indicates Drosophila nuclei as large circles and *Wolbachia* as small puncta. A) *D. melanogaster* oocyte exposed to standard fly food. B) *D. melanogaster* oocyte exposed to yeast paste. Graphs indicate the average number of *Wolbachia* nucleoids within single focal planes of stage 10A oocytes. C) Oocyte *Wolbachia* titer comparison between control food and yeast paste conditions. D) *Wolbachia* titer response in *D. melanogaster* to 1:3 dilutions of water, corn syrup (CS), or yeast paste into standard food. Scale bar: 50 μm.

Table). Although corn syrup-enriched food is less hydrated than control food, it resulted in similar oocyte titer measurements as the control, with an average of 128 +/- 12.9 *Wolbachia* visible per oocyte (n = 31) (Figure 5.2D). These data together suggest that yeast-induced

titer reduction is not due to depletion of specific nutrients or water available in standard food. Rather, the data indicate that dietary yeast is responsible for reducing *Wolbachia* titer carried by oocyte cells.

To determine whether dietary yeast can induce a similar oocyte titer response in wild insects as seen in laboratory fly stocks, *Drosophila melanogaster* and *Drosophila simulans* were collected from nature. These flies were exposed to yeast-enriched food and assessed for *Wolbachia* titer in oogenesis. We found that oocyte *Wolbachia* titer in the yeast-enriched condition was at 47% of the control level, with an average of 94.8 +/- 21.8 *Wolbachia* detected in control oocytes (n = 12), versus 44.6 +/- 6.52 *Wolbachia* detected in the yeast-enriched condition (n = 13) ($p = 0.029$) (S1 Fig). Thus, yeast-enriched diets suppress oocyte *Wolbachia* titer in wild-caught *Drosophila* analogous to laboratory *D. melanogaster* strains.

To further investigate the basis for yeast-associated *Wolbachia* depletion in oocytes, *Wolbachia* titer was examined in the germ line-derived nurse cells associated with the oocyte. It is currently unclear in *Drosophila* when or how frequently *Wolbachia* travel through the ring canals between the nurse cells and oocyte. Thus, it is possible that *Wolbachia* depletion in oocytes could be due to preferential retention in the nurse cells. To investigate this, we imaged *Wolbachia* in equivalent focal planes of nurse cells and oocytes within single egg chambers and analyzed their *Wolbachia* titer [95]. Overlaid images showing a planar reconstruction of egg chambers indicated fewer *Wolbachia* throughout the germ line cells of yeast-exposed organisms (Figure 5.3A-B). Quantitation of the yeast-enriched condition indicated that nurse cells carried 27% of the control titer level (Figure 5.3C). Specifically, 52.6 +/- 4.93 *Wolbachia* per nurse cell were detected in the control (n = 20), in contrast to 14.4 +/- 1.65 *Wolbachia* per nurse cell in the yeast-enriched condition (n = 20) ($p < 0.001$) (Figure 5.3C). Furthermore, oocyte titer in the yeast-enriched condition was 14% of the control level, with 420 +/- 44.6 *Wolbachia* detected in control oocytes (n = 17), versus 59.0 +/- 11.1 *Wolbachia* in oocytes from the yeast-enriched condition (n = 20) ($p < 0.001$) (Figure 5.3D). These data indicate that *Wolbachia* redistribution between germ line cells is not

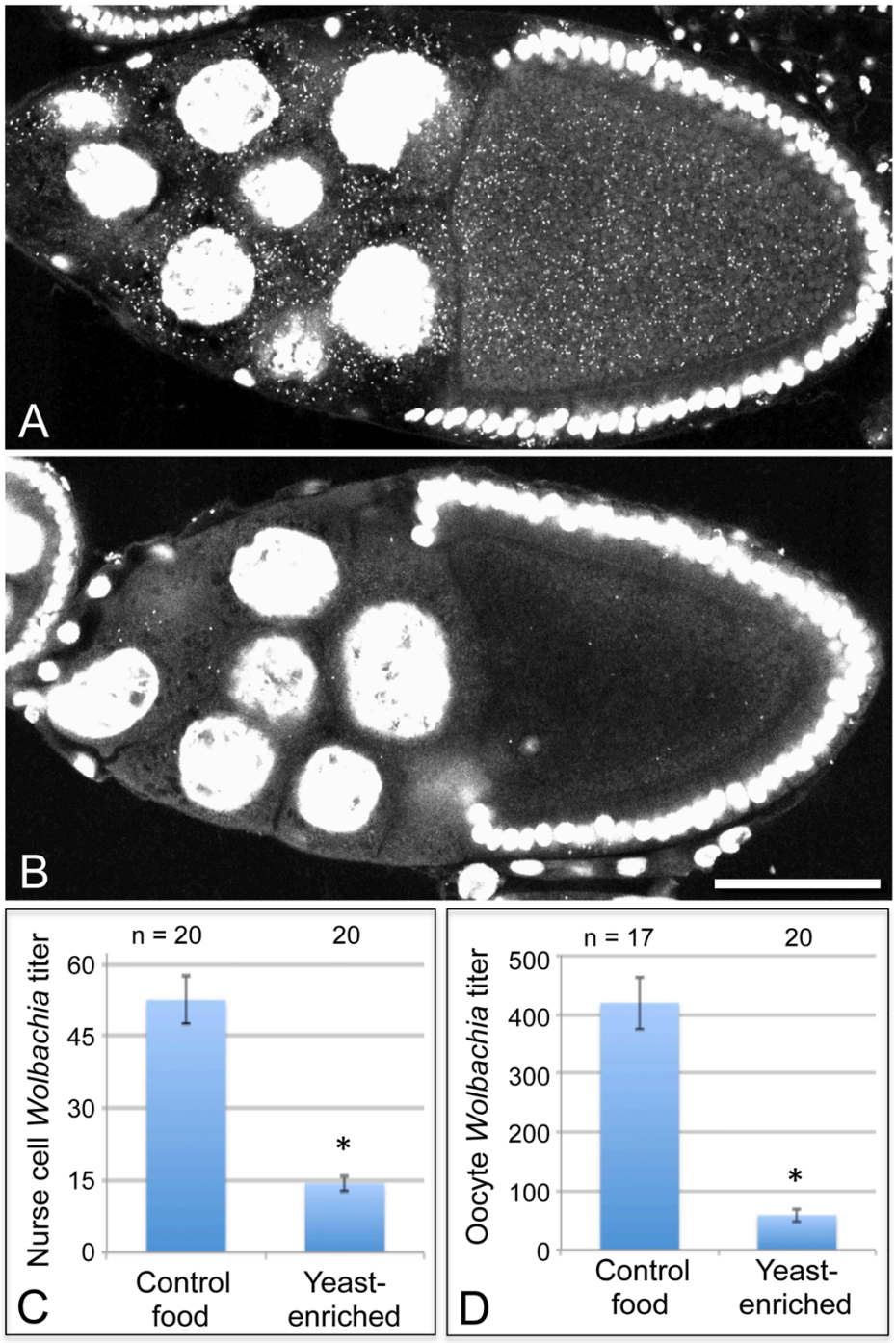

Figure 5.3: **Dietary yeast affects *Wolbachia* titer in nurse cells as well as oocytes.** Merged images show a full cross section from egg chambers raised on A) control food and B) yeast-enriched food. C-D) Average *Wolbachia* titer was determined for control vs. yeast-enriched conditions within a single egg chamber focal plane. C) Nurse cell titer values. D) Oocyte titer values from the same focal plane. Scale bar: 50 μm.

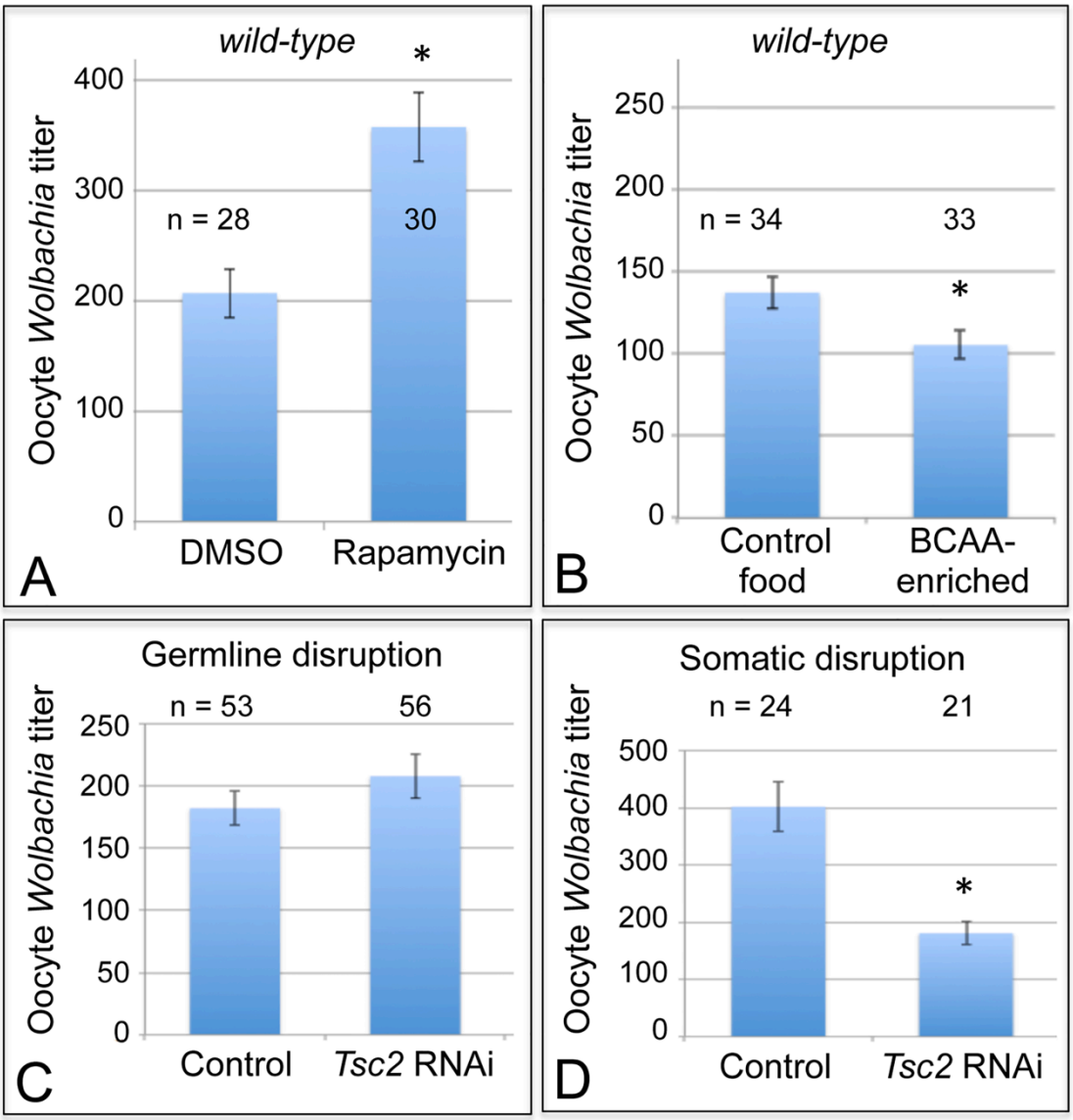

Figure 5.4: **Somatic TORC1 activity affects *Wolbachia* titer in oogenesis.** A) Average *Wolbachia* titer in oocytes treated with control DMSO or the mTORC1 inhibitor, Rapamycin. B) Titer was assessed in oocytes exposed to BCAA-enriched food. C-D) *Wolbachia* titer was also tested in flies carrying disruptions of the Tsc2 gene, expected to elevate TORC1 activity. C) Genotypes used for germ line Tsc2 disruption: Control: (nos-GAL4)/+; (nos-GAL4)/+. Tsc2 RNAi: (nos-GAL4)/+; (nos-GAL4)/(UAS-Tsc2 dsRNA). D) Genotypes used for somatic Tsc2 disruption: Control: (da-GAL4)/+. Tsc2: (da-GAL4)/(UAS-Tsc2 dsRNA). * indicates a significant change in titer.

responsible for the low oocyte titer observed in yeast-exposed organisms. Rather, yeast-enriched food induces similar *Wolbachia* depletion in nurse cells and oocytes.

The nutrient-responsive kinase complex, TORC1, affects oocyte *Wolbachia* titer

Cells coordinate intracellular events in response to exogenous nutrients using multiple signaling pathways that converge upon the Target of Rapamycin kinase complex 1 (TORC1) (Figure 5.1) [243]. TORC1 can be activated by an amino-acid dependent signaling mechanism, or by insulin signaling (Figure 5.1) [243-245]. To test whether TORC1 activity affects oocyte *Wolbachia* titer, flies were exposed to standard food containing the TORC1 inhibitor, rapamycin [246-249]. This experiment indicated that rapamycin treatment drove a 1.7-fold increase in oocyte *Wolbachia* titer (Figure 5.4A). The average titer from control oocytes, exposed to DMSO-containing standard food, was 207 +/- 22.1 *Wolbachia* (n = 28). By contrast, oocytes exposed to rapamycin-containing standard food had 357 +/- 31 *Wolbachia* (n = 30) ($p < 0.01$) (Figure 5.4A). Since rapamycin exposure leads to higher oocyte *Wolbachia* titer, this suggests that a normal consequence of TORC1 activity is suppression of oocyte *Wolbachia* titer.

If TORC1 function normally leads to decreased oocyte *Wolbachia* titer, then hyper-activation of TORC1 would be expected to drive a further reduction of oocyte titer. Branched chain amino acids (BCAAs) taken up through the Slimfast transporter can induce up-regulation of TORC1 (Figure 5.1) [250-255]. Therefore, we fed flies a slurry of BCAAs diluted 1/3 into standard food (S1 Table), and assessed *Wolbachia* titer in oogenesis. *Wolbachia* titer in the BCAA condition was reduced to 77% of the control (Figure 5.4B). This was indicated by an average of 137 +/- 9.71 *Wolbachia* in control oocytes (n = 34) versus 105 +/- 8.48 *Wolbachia* in oocytes from the BCAA condition (n = 33) ($p = 0.015$) (Figure 5.4B). The data suggest that TORC1 stimulation with BCAAs drives oocyte titer reduction, opposite to the effect of the TORC1 inhibitor, Rapamycin.

To further investigate a possible role for TORC1, we genetically manipulated a key regulator of TORC1 activity. Tsc2, known as Gigas in *Drosophila*, is downstream of the insulin receptor (Figure 5.1) [256-261]. If Tsc2 function is suppressed by any means, this allows TORC1 to become active (Figure 5.1) [243, 261-265]. Therefore, we tested the impact of Tsc2 on oocyte *Wolbachia* titer by expressing Tsc2 dsRNA under the control of germ line- and soma-specific GAL4 drivers [266-269]. This investigation revealed different oocyte *Wolbachia* titer responses to tissue-specific Tsc2 RNAi knockdowns. Our efforts to manipulate Tsc2 dosage in germ line cells had no impact on oocyte titer (Figure 5.4C). An average of 182 +/- 13.5 *Wolbachia* were detected in control oocytes (n = 53), which was not significantly different from the 207 +/- 17.7 *Wolbachia* detected in response to germ line Tsc2 RNAi (n = 56) (Figure 5.4C). By contrast, Tsc2 RNAi knockdowns in all somatic cells reduced oocyte *Wolbachia* titer to approximately 50% of the control level (Figure 5.4D). Control oocytes exhibited an average of 402 +/- 43.4 *Wolbachia* (n = 24). However, oocytes in somatic Tsc2 knockdown flies exhibited an average of 181 +/- 19.8 oocyte *Wolbachia* (n = 21) ($p < 0.001$) (Figure 5.4D). These data implicate somatic Tsc2, and thus somatic TORC1 signaling, in regulation of oocyte *Wolbachia* titer.

Yeast suppression of oocyte *Wolbachia* titer is mediated by insulin-TORC1 signaling

A role for somatic TORC1 in regulating oocyte *Wolbachia* titer raised the question of whether dietary yeast stimulates TORC1. This could occur through either protein- or insulin-based mechanisms (Figure 5.1). As yeast is a major source of protein for *D. melanogaster*, perhaps its amino acid content stimulates TORC1 to ultimately suppress oocyte *Wolbachia* titer. To test this possibility, we exposed flies to food enriched in Bovine Serum Albumin, prepared specifically to match the protein content of yeast-enriched food (S1 Table). Oocyte *Wolbachia* titer was similar for control and BSA-enriched conditions, with the control exhibiting 1260 +/- 102 *Wolbachia* (n = 26), and the BSA-enriched condition exhibiting 1190

+/- 48.2 *Wolbachia* (n = 18) (S2 Fig). This suggests that amino acid availability in the host diet has little impact on oocyte *Wolbachia* titer.

An alternate possibility is that yeast-enriched diets affect oocyte *Wolbachia* through insulin stimulation of TORC1. It was previously shown that dietary yeast stimulates insulin-producing cells (IPCs) the brain to release the insulin-like-peptides (Dilps) into the hemolymph [270, 271]. To test whether yeast acts through somatic Dilp secretion to affect oocyte *Wolbachia* titer, we ablated the IPCs in the brain of fully mature *Drosophila* females. This can be achieved using a dilp2: Gene-Switch-GAL4, UAS: Reaper system that specifically kills the brain IPCs in response to a 2-week mifepristone treatment [271].

We first investigated whether mifepristone on its own modulates the yeast effect in wild-type flies. After completing a 2-week exposure to either DMSO or mifepristone, flies were exposed to either control or yeast-enriched food for 3 days, and their oocyte titer levels were assessed. DMSO-treated flies exhibited substantial oocyte titer depletion in response to yeast-enriched food, down to 30% of the titer in the control condition (Figure 5.5A). This was indicated by 785 +/- 64.8 *Wolbachia* per oocyte in the DMSO-control food condition (n = 24), in contrast to 191 +/- 26.9 *Wolbachia* in the DMSO-yeast-enriched condition (n = 25) ($p < 0.001$) (Figure 5.5A). Mifepristone-treated flies showed a similar titer reduction after exposure to yeast, exhibiting 21% of the titer seen in the control food condition (Figure 5.5B). This was indicated by 896 +/- 77.2 *Wolbachia* per oocyte in the mifepristone-control food condition (n = 23), versus 264 +/- 39.5 *Wolbachia* in the mifepristone-yeast-enriched condition (n = 25) (Figure 5.5B) ($p < 0.001$). Therefore, mifepristone alone has no effect on yeast-based suppression of oocyte *Wolbachia* titer.

Next, the same treatment regimens were performed on flies with the dilp2: Gene-Switch-GAL4, UAS: Reaper genotype. In this experiment, DMSO-treated flies, which retained functional IPCs, exhibited a severe oocyte *Wolbachia* depletion in response to yeast-enriched food, exhibiting only 7% of the oocyte titer seen on DMSO-control food (Figure 5.5C). This was indicated by the presence of 999 +/- 116 *Wolbachia* per oocyte in the

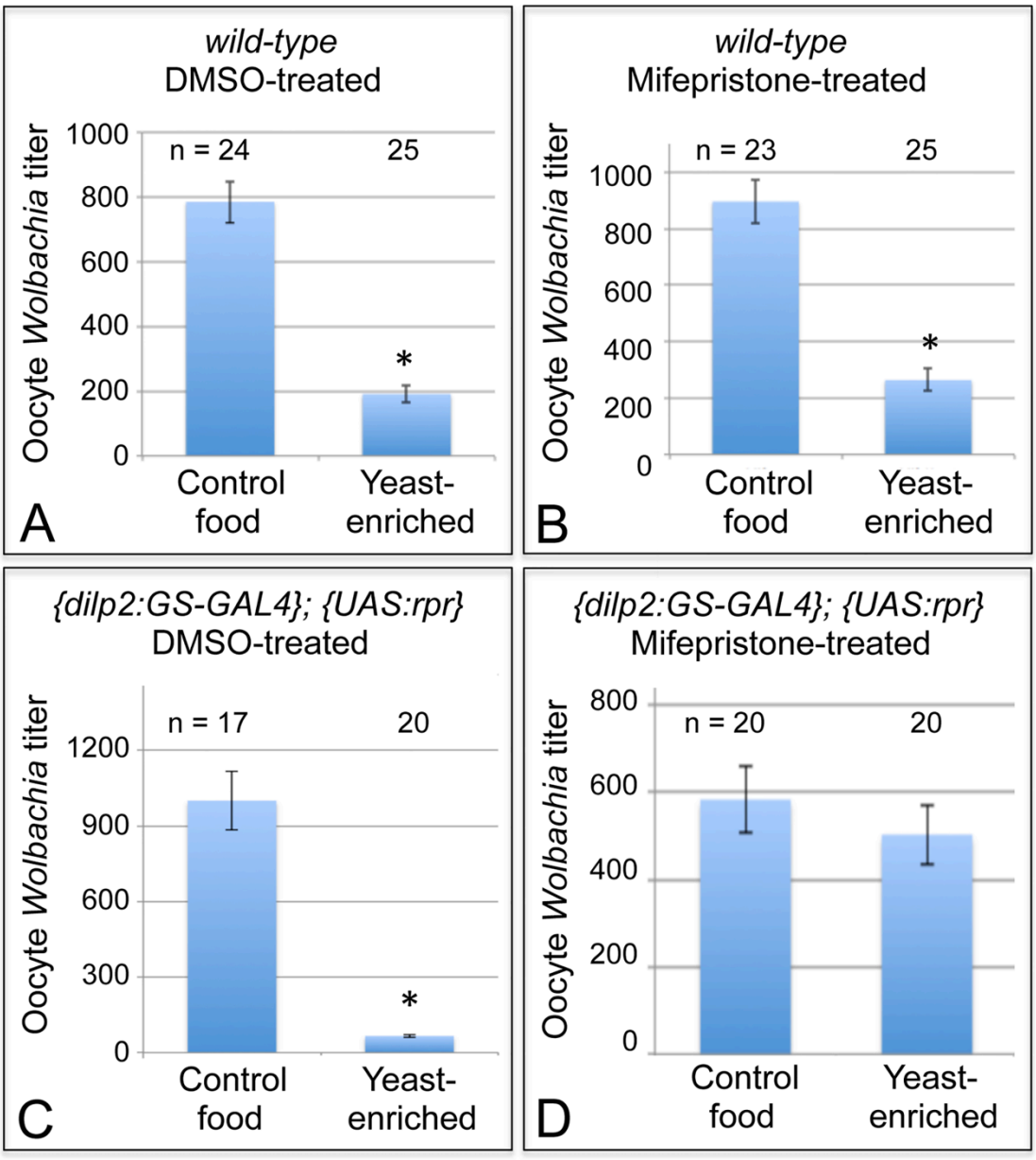

Figure 5.5: **Nutrients affect germ line *Wolbachia* titer through the somatic insulin pathway.** Dietary impact on oocyte *Wolbachia* titer was tested in flies that either carried or lacked functional IPCs in the brain. Wild-type flies were A) treated with DMSO or B) induced with Mifepristone over a 14-day period as a control. (dilp2: GS-GAL4); (UAS-rpr) flies were also C) treated with DMSO as a control, or D) induced with Mifepristone over a 14-day period to drive IPC lethality. * indicates significant changes in titer.

DMSO-control food condition (n = 17), versus 66.5 +/- 6.61 *Wolbachia* in the DMSO-yeast-enriched condition (n = 20) ($p < 0.001$) (Figure 5.5C). In stark contrast, mifepristone-treated flies that had lost their IPCs exhibited no oocyte titer change after exposure to yeast (Figure 5.5D). This was indicated by detection of 583 +/- 72.6 *Wolbachia* per oocyte in the mifepristone-control food condition (n = 20), versus 503 +/- 68.0 *Wolbachia* in the mifepristone-yeast-enriched condition (n = 20) (Figure 5.5D). Since mifepristone in combination with the dilp2: Gene-Switch-GAL4, UAS: Reaper system specifically prevented yeast from affecting oocyte *Wolbachia* titer, this demonstrates that somatic IPCs mediate *Wolbachia* titer suppression by dietary yeast.

Dietary sucrose elevates oocyte *Wolbachia* titer in an insulin-dependent manner

To further investigate the sensitivity of oocyte *Wolbachia* titer to somatic insulin signaling, we also examined the effect of a sucrose-rich, high sugar diet. High sugar diets have been shown to induce insulin resistance in *Drosophila* [272, 273]. This may be due in part to increased expression of NLaz [272], which in mammals is known to suppress Akt function within the insulin signaling pathway (Figure 5.1) [274-276]. To test the impact of sucrose-enriched diets on oocyte *Wolbachia* titer, 2-day old *D. melanogaster* were fed standard food diluted 1/3 with saturated sucrose solution, hereafter referred to as “sucrose-enriched food” (S1 Table). After 3 days of exposure to this diet, *Wolbachia* titer was assessed in oogenesis. Oocytes from the sucrose-enriched condition exhibited a 2.4-fold increase in *Wolbachia* (Figure 5.6A). Unlike oocytes raised on control food, which exhibited an average of 165 +/- 22.2 *Wolbachia* (n = 24), *D. melanogaster* oocytes exposed to sucrose-enriched food exhibited 392 +/- 25.3 *Wolbachia* (n = 26) ($p < 0.001$) (Figure 5.6A). These data indicate that a high sugar diet significantly elevates oocyte *Wolbachia* titer, possibly via an insulin-related mechanism.

A sucrose-based impact on oocyte *Wolbachia* titer is surprising, as corn syrup-enriched food did not induce a similar effect (Figure 5.2D). Notably, sucrose is a disaccharide, composed

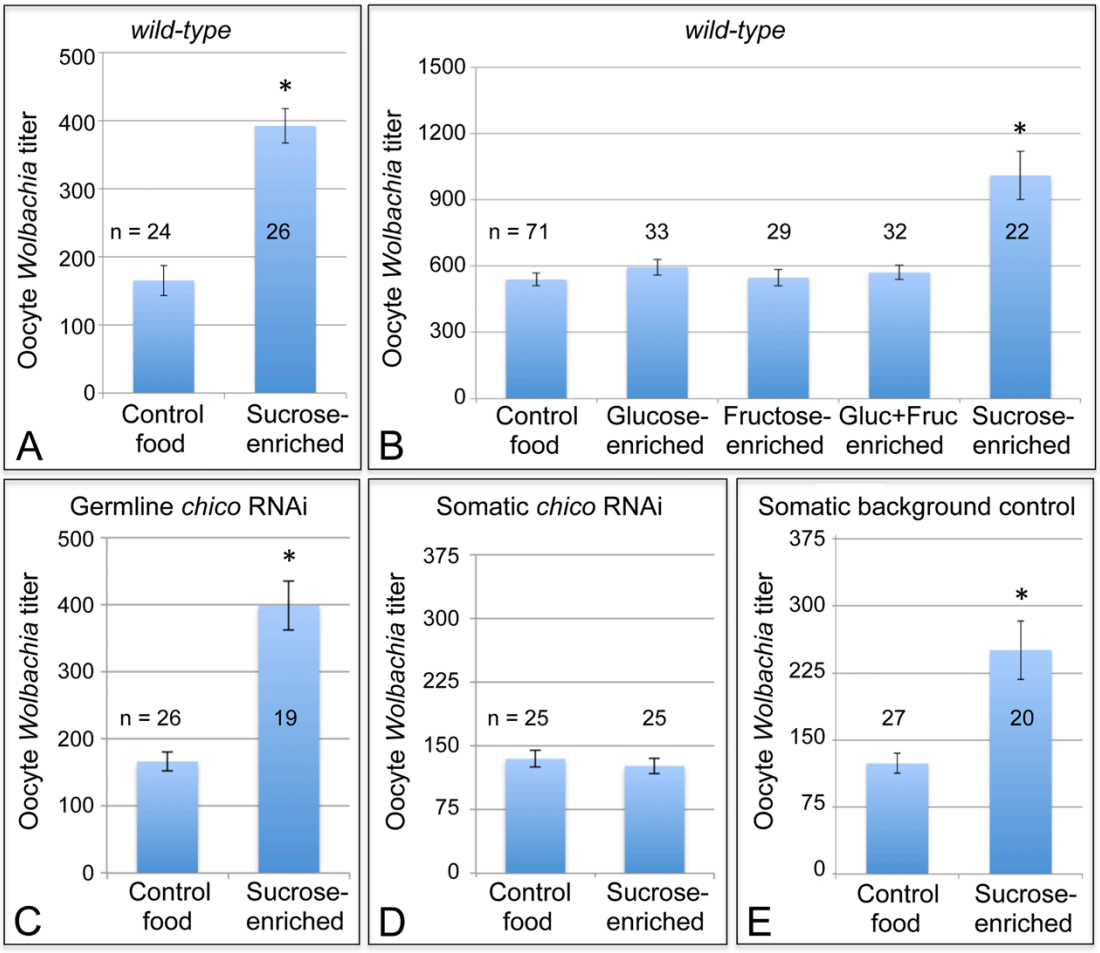

Figure 5.6: **Sucrose-enriched food elevates oocyte *Wolbachia* titer in a chico-dependent manner.** *Wolbachia* were quantified within single focal planes of oocytes exposed to control food or sucrose-enriched food. The average titer detected per nutrient condition is shown. A) Impact of sucrose on oocyte *Wolbachia* titer in wild-type *D. melanogaster*. B) Comparison of oocyte *Wolbachia* titers between control food and other foods enriched in glucose, fructose, a mixture of glucose and fructose, or sucrose. C-E) Sucrose impact on oocyte *Wolbachia* titer in flies that carry tissue-specific chico RNAi disruptions. Genotypes used: C) (nos-GAL4)/+; (nos-GAL4)/(UAS-chico dsRNA). D) (da-GAL4)/(UAS-chico dsRNA). E) (da-GAL4)/+.

of glucose and fructose, whereas corn syrup consists mainly of glucose. To elucidate the basis for sucrose-induced titer effects in oogenesis, food enriched for glucose and fructose were also tested. However, none of the monosaccharide-enriched conditions significantly affected oocyte *Wolbachia* titer (Figure 5.6B). Control food yielded an average oocyte titer of

478 +/- 27.6 *Wolbachia* per oocyte (n = 71). Similarly, oocytes in the glucose-enriched condition displayed 520 +/- 31.1 bacteria (n = 33), the fructose-enriched food condition resulted in 478 +/- 33.0 *Wolbachia* (n = 29), and a mixture of glucose + fructose yielded 499 +/- 28.0 *Wolbachia* (n = 32). By contrast, oocytes from the sucrose-enriched condition presented 883 +/- 95.4 *Wolbachia* (n = 22) ($p < 0.001$) (Figure 5.6B). This confirms that disaccharide sucrose molecule specifically elicits *Wolbachia* titer increases in oogenesis.

To further test the possibility that insulin signaling mediates sucrose impact on ovarian *Wolbachia* titer, we coupled genetic disruptions of the insulin pathway with sucrose-enriched food. Chico is a *Drosophila* homolog of the Insulin Receptor Substrate that relays signals from the Insulin Receptor to AKT kinase, and thus ultimately TORC1 (Figure 5.1) [277, 278]. Germ line and soma-specific GAL4 drivers were used to drive expression of chico dsRNA [266-269], and oocyte *Wolbachia* titer was assayed in control and sucrose-enriched conditions. This test did not indicate any effect of germ line chico RNAi on sucrose-induced oocyte titer elevation, with sucrose-enriched food corresponding to 2.4-fold higher oocyte titer than the control (Figure 5.6C). Germ line chico RNAi oocytes exhibited 125 +/- 10.6 *Wolbachia* when exposed to regular food (n = 26) as compared to 299 +/- 27.2 *Wolbachia* in response to sucrose-enriched food (n = 19) ($p < 0.001$) (Figure 5.6C). By contrast, somatic chico RNAi eliminated sucrose-induced titer effects in oogenesis (Figure 5.6D). Oocytes from somatic chico RNAi flies exhibited 180 +/- 12.9 *Wolbachia* in the control condition (n = 25), as compared to 169 +/- 12.5 *Wolbachia* per oocyte in the sucrose-enriched condition (n = 25) (Figure 5.6D). Analysis of sibling controls further indicated that the genetic background for the somatic chico RNAi experiment was not responsible for differential oocyte titer responses to sucrose (Figure 5.6E). In flies carrying the somatic da-GAL4 driver used for this experiment, the sucrose-enriched condition continued to exhibit 2-fold more *Wolbachia* than the control food condition. An average of 124 +/- 11.1 *Wolbachia* were detected in control oocytes (n = 27) as compared to 251 +/- 32.8 *Wolbachia* detected in oocytes from the sucrose-enriched condition (n = 20) ($p < 0.001$) (Figure 5.6E). Though the complete

mechanistic implications of somatic chico disruption remain unclear, these data demonstrate that sucrose acts through somatic insulin signaling to elevate oocyte *Wolbachia* titer.

Oocyte *Wolbachia* titer responses are independent of ovary productivity

These data raise the fundamental question of why diet-modulated insulin signaling affects *Wolbachia* titer so strongly in germ line cells. One possibility is that these titer responses are an indirect result of nutrient-induced changes in ovary size and productivity [273]. Yeast-rich diets and insulin signaling are known to drive formation of larger, more productive ovaries [257, 273, 277, 279-288], while high-sucrose diets have the opposite effect [273-276]. To test the contribution of ovary size and productivity variables on oocyte *Wolbachia* titer, we manipulated ovary productivity by controlling female mating. Mating stimulates ovary development, resulting in a moderately sized, productive ovary. By contrast, virgin females exhibit very large ovaries, filled mainly by mature eggs [289-293]. Oocytes from mated versus virgin females revealed similar oocyte *Wolbachia* titers, however (S3 Fig). The mated condition displayed 449 +/- 27.5 *Wolbachia* per oocyte (n = 26), while the virgin female condition that carried 470 +/- 40.6 *Wolbachia* per oocyte (n = 24) (S3 Fig). These data suggest that ovary size and productivity do not serve as primary determinants of oocyte *Wolbachia* titer.

***Wolbachia* nucleoid morphology responds to dietary yeast**

To further investigate the effects of host diet on *Wolbachia*, we examined *Wolbachia* nucleoid morphology. Other studies indicate that nucleoid morphology can serve as a proxy indicator of replication-associated changes in cell shape, or stress-induced DNA compaction [106, 294, 295]. Multiple, zoomed-in images of *Wolbachia* stained with propidium iodide were projected as a single image, and nucleoid shape was measured. The images indicated that *Wolbachia* nucleoid shape differs between nutrient conditions (S4 Fig). To specifically analyze changes in nucleoid length, 120 nucleoids were selected at random from each

treatment condition and their lengths were compared. This analysis indicated that 50% of nucleoids in the control condition exceeded 2 μm in length (S4 Fig). The sucrose-enriched condition was similar, with 53% of nucleoids exceeding 2 μm. In the yeast-enriched condition, however, only 37% of nucleoids exceeded this measure ($p < 0.05$). Thus, yeast-enriched food significantly shortened *Wolbachia* nucleoids. We further determined an elongation index (EI), representing bacterial length divided by width, for the same 120 nucleoids per treatment condition as above. This analysis indicated that 50% of nucleoids measured in the control condition had an EI greater than 2 um. In the sucrose-enriched condition, only 33% of nucleoids showed an EI greater than 2 um ($p < 0.05$). In the yeast-enriched condition, even fewer nucleoids showed this degree of elongation, with only 22% of nucleoids exceeding this EI ($p < 0.001$) (S4 Fig). These data indicate that dietary conditions, and especially exposure to yeast-enriched food, alter *Wolbachia* nucleoid morphology in oogenesis. This is consistent with a bacterial physiological response to host diet.

Wolbachia titers are regulated in a tissue-specific manner

The striking impact of dietary nutrients on oocyte *Wolbachia* titer raised the question of whether *Wolbachia* titer in other tissues is responsive to nutrient conditions. *Wolbachia* are present in insect somatic cells, and the *Drosophila* brain is particularly amenable to assessment of somatic *Wolbachia* titer [171, 296]. To take advantage of this, we imaged *Wolbachia* in the central brain of *D. melanogaster* exposed to different nutrient conditions. This analysis revealed that *D. melanogaster* on control food already carry very low *Wolbachia* titer in the central brain (Figure 5.7A, A', n = 3), and flies fed with either yeast-enriched or sucrose-enriched food were indistinguishable in appearance from the control (Figure 5.7B, B', n = 3) (Figure 5.7C, C', n = 3). Thus, *Wolbachia* titer in *D. melanogaster* brain does not appear to be affected by the dietary conditions used in this study. An alternative possibility, however, is that the overall low *Wolbachia* titer detected under these conditions hampered our ability to assay nutrient-induced changes in titer.

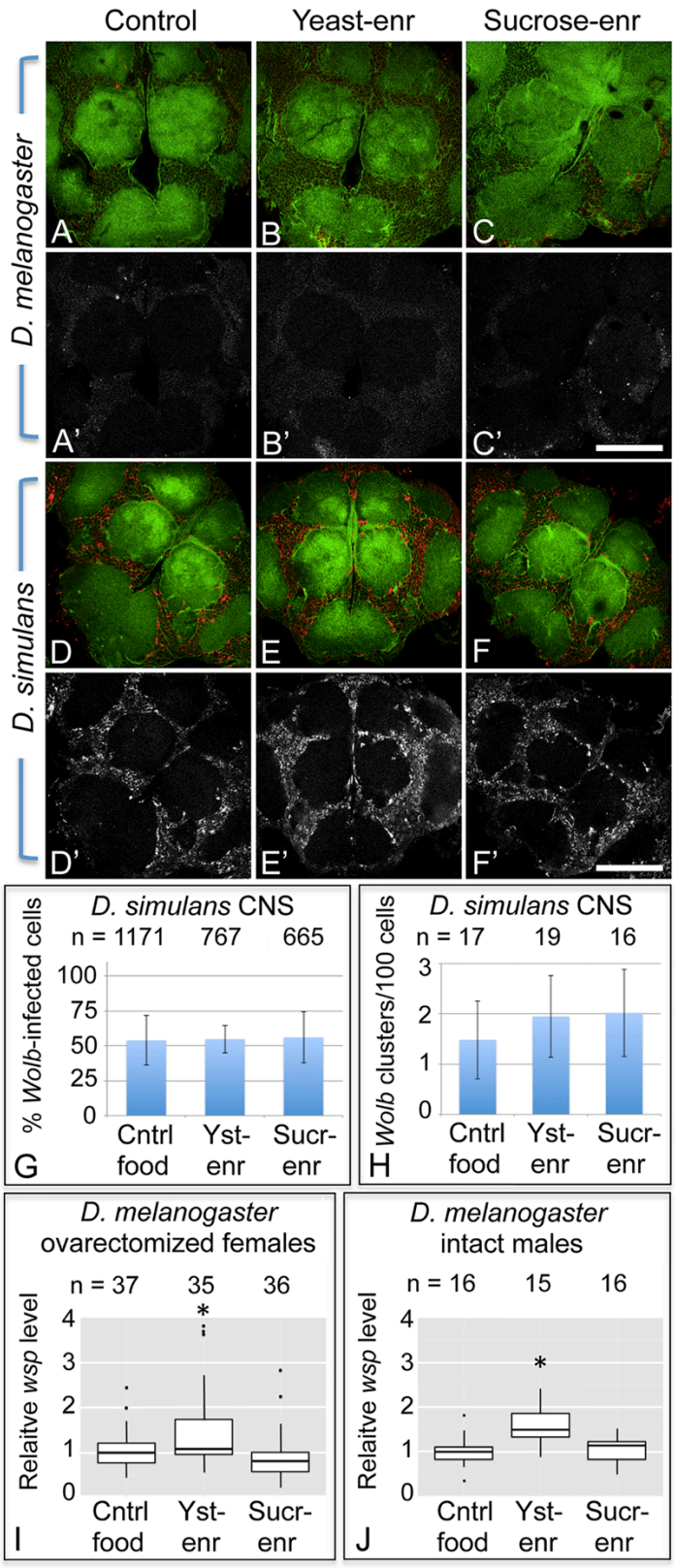
Control
Yeast-enr
Sucrose-enr
D. melanogaster
D. simulans
A
B
C
A'
B'
C'
D
E
F
D'
E'
F'
D. simulans CNS
n = 1171 767 665
% Wolb-infected cells
100
75
50
25
0
Cntrl food
Yst-enr
Sucr-enr
G
D. simulans CNS
n = 17 19 16
Wolb clusters/100 cells
3
2
1
0
Cntrl food
Yst-enr
Sucr-enr
H
D. melanogaster
ovarectomized females
n = 37 35 36
Relaitve wsp level
4
3
2
1
0
*
Cntrl food
Yst-enr
Sucr-enr
I
D. melanogaster
intact males
n = 16 15 16
Relaitve wsp level
4
3
2
1
0
*
Cntrl food
Yst-enr
Sucr-enr
J

Figure 5.7: **Host diet has tissue-specific effects on somatic *Wolbachia* titer.** A-F') *Wolbachia* in the central brain of female flies. Columns from left to right: Control food, Yeast-enriched, Sucrose-enriched. In merged images, red shows Anti-Wsp to indicate *Wolbachia*, and green shows phalloidin to indicate actin. Grayscale images show only Anti-Wsp. A-C, A'-C') *D. melanogaster* brains. Little Wsp signal is detected under each feeding condition. D-F, D'-F') Brains from *D. simulans*. These show similarly high Wsp immunoreactivity under all feeding conditions. G) Percentage of *Wolbachia*-infected *D. simulans* brain cells. H) Frequency of large *Wolbachia* clusters per 100 *D. simulans* brain cells. I-J) qPCR analysis of relative *Wolbachia* levels from flies exposed to nutrient-altered diets. The Y-axis shows relative quantitation of genomic wsp. Flies used: I) ovarectomized *D. melanogaster* females. J) intact *D. melanogaster* males. Values are normalized to the control flies in each panel. * indicates a significant change in titer. Scale bars: 150 μm.

To pursue this further, the impact of nutrient-altered food was tested in the closely related *D. simulans* species, known for carrying high *Wolbachia* titer in its brain cells [296]. Flies exposed to control food exhibited a high titer of *Wolbachia* in the central brain overall (Figure 5.7D, D', n = 7). Similarly high *Wolbachia* titer was detected in the brain after exposure to yeast- and sucrose-enriched food (Figure 5.7E, E', n = 5) (Figure 5.7F, F', n = 4). Further quantification of *Wolbachia* infection frequency did not reveal any differences between nutrient conditions (Figure 5.7G). In control food, yeast-enriched, and sucrose-enriched conditions, 55–56% of brain cells exhibited *Wolbachia* infection (n = 1171, 767, and 665 cells, respectively). No differences were seen in formation of large *Wolbachia* aggregates either (Figure 5.7H). Brain samples reared on control food, yeast-enriched, and sucrose-enriched conditions all exhibited between 16–19 large bacterial clusters per hundred cells. This indicates that *Wolbachia* titer in the *D. simulans* brain is unresponsive to the nutrient-altered conditions used in this study.

To address the possibility that *D. simulans* tissues are generally unresponsive to nutrients, we also assessed *D. simulans* oocyte titer in response to nutrient-altered food. In contrast to the brain, *D. simulans* oocytes exhibited a clear nutrient-dependent *Wolbachia* titer response (S5 Fig). Control oocyte images carried 293 +/- 49.9 *Wolbachia* (n = 10). By contrast, oocyte titer from the yeast-enriched condition was at 40% of the control level, with an average of 116

+/- 20.1 bacteria detected per oocyte (n = 10) (p = 0.004). Furthermore, the sucrose-enriched condition exhibited 2.3-fold higher titer than the control, with 662 +/- 73.6 *Wolbachia* detected per oocyte (n = 10) (p = 0.001) (S5 Fig). Thus, *D. simulans Wolbachia* titers are capable of responding similarly to nutrient conditions as D. melanogaster.

To further probe the impact of host diet on somatic *Wolbachia* titer, we analyzed relative amounts of *Wolbachia* versus host DNA in ovarectomized female flies. In this analysis, females were exposed to nutrient-altered diets, dissected to remove ovarian tissues, and analyzed by qPCR. The results indicate the relative level of *Wolbachia* per host genome copy number. This analysis indicated that yeast-enriched dietary conditions led to higher levels of *Wolbachia* than the control food condition (Figure 5.7I). Control samples exhibited a mean relative level of *Wolbachia* of 0.989 (n = 37), whereas the yeast-enriched condition displayed a mean relative level of *Wolbachia* of 1.28 (n = 35) ($p < 0.05$). Females exposed to sucrose-enriched diets were not significantly different from the control, however, exhibiting a mean *Wolbachia* relative level of 0.792 (n = 36) (Figure 5.7I). This titer response profile differs from analyses of *Wolbachia* titer in the ovary as well as the brain. This suggests that host diet affects *Wolbachia* titers in a tissue- specific manner.

As host nutrition has a different impact on ovarian versus somatic *Wolbachia* titers, this raised the question of what would happen in organisms lacking ovarian tissue altogether. To address this issue, qPCR analysis was performed on intact male flies. This indicated that bodywide *Wolbachia* titer also increases in response to yeast-enriched food, although not sucrose-enriched food (Figure 5.7J). The control food condition carried a mean *Wolbachia* relative level of 1 (n = 16), in contrast to the yeast-enriched condition, which displayed a mean *Wolbachia* relative level of 1.545 (n = 15) ($p < 0.05$). Sucrose-enriched diets corresponded to a mean *Wolbachia* relative level of 1.027 (n = 16). This analysis confirms that the profile of bodywide titer responses in males is equivalent to ovarectomized females. This suggests that somatic *Wolbachia* titers overall respond to host dietary conditions in a consistent manner.

5.4 Discussion

The major finding of this study is that dietary intake by *Drosophila* strongly influences *Wolbachia* titer in the host female germ line: a high yeast diet decreases *Wolbachia* oocyte titer and a high sucrose diet increases *Wolbachia* oocyte titer. This finding adds to a small but growing literature on the impact of host diet on endosymbionts [209, 221, 222]. Prior studies of *Wolbachia* suggest that this endosymbiont relies heavily upon host provisioning of amino acids and carbohydrates [177, 189, 297]. A very recent study analyzing the *Drosophila* midgut and ovary surprisingly indicated that neither dietary yeast nor sucrose had any affect on the *Wolbachia*:host genomic ratio in those tissues [298]. The image-based analyses of this study demonstrate that yeast and sucrose affect germ line *Wolbachia* titer at the cellular level, however. It is unclear why *Wolbachia* titer in the oogenesis should be particularly sensitive to diet and whether this is an adaptive response to changes in the host metabolic environment. The evolutionary success of *Wolbachia* depends on its ability to localize at the posterior pole of the oocyte, the site of germ line formation. Significantly, we find that *Wolbachia* localize to the posterior pole regardless of whether the host is exposed to the low titer, yeast-enriched diet, or the high titer, sucrose-enriched diet. This suggests the previously described microtubule and motor protein based mechanisms driving posterior localization of *Wolbachia* [84] are robust, even in the face of dramatic titer changes caused by nutrient-altered diets.

Insight into the mechanism of yeast-induced titer suppression comes from our functional studies demonstrating that this response is mediated through TORC1. Genetic up-regulation of TORC1 suppresses oocyte *Wolbachia* titer, whereas drug-based inhibition of TORC1 increases titer. This finding creates the basis for a sensible functional connection between intracellular *Wolbachia* and host diet, as both amino acids and insulin signaling are known to drive TORC1 activity [243]. Our finding that BSA-enriched food had no effect on oocyte *Wolbachia* titer argues that yeast protein content is not the major determinant of germ line titer suppression, and alternatively suggests a role for insulin signaling. Prior work has

shown that yeast-rich diets trigger insulin signaling in *Drosophila*, and that *Wolbachia* interact with host insulin signaling processes [285, 286]. Our finding, that loss of somatic IPCs eliminates yeast impact on oocyte *Wolbachia* titer, confirms that insulin signaling facilitates the titer-suppressing effects of yeast. Furthermore, disrupting the somatic insulin receptor substrate, Chico, suppressed the impact of dietary sucrose on oocyte *Wolbachia* titer. This suggests that both dietary yeast and sucrose affect germ line *Wolbachia* titer via antagonistic impacts on somatic insulin signaling (Figure 5.8).

In considering the mechanism of insulin-based impact on germ line *Wolbachia* titer, one possibility is that changes in ovary productivity are responsible. Diet-modulated insulin signaling affects the relative rates of germ line stem cell division, germ line cell survival and

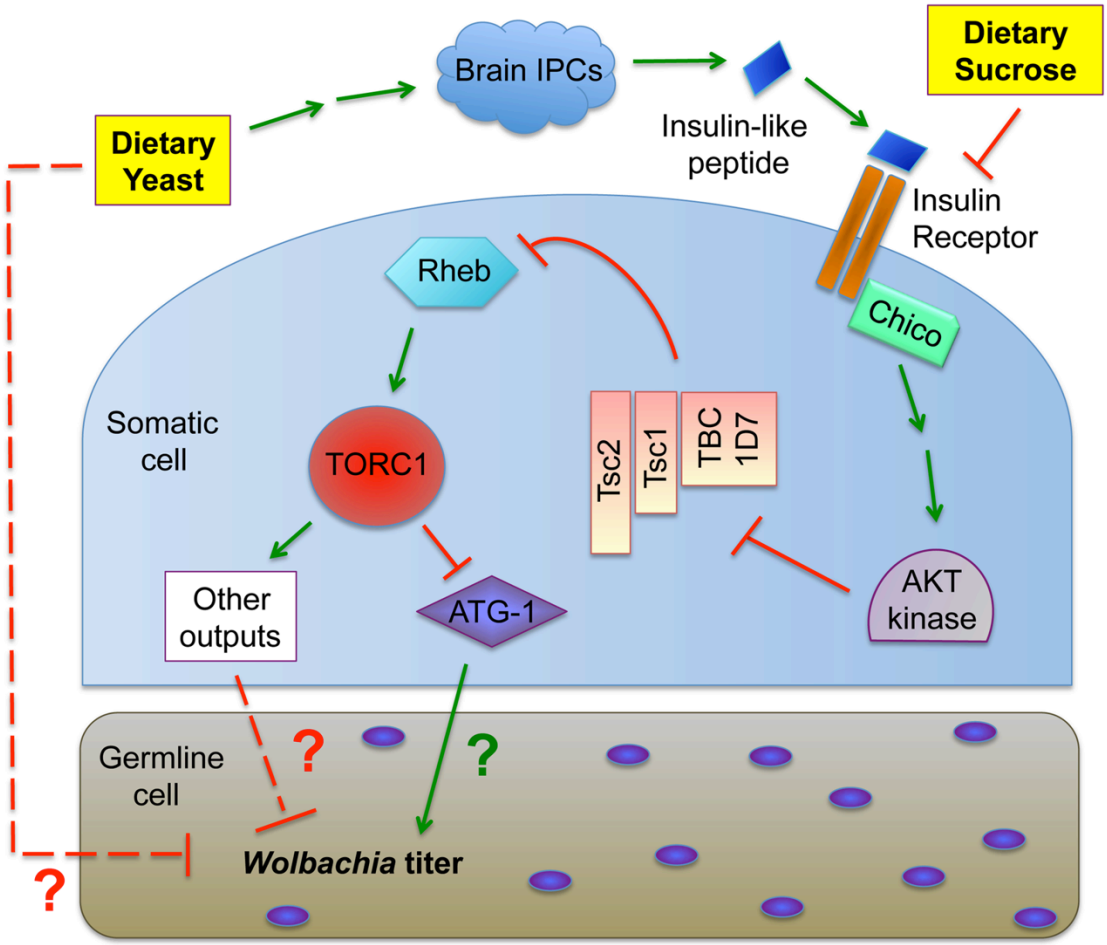

Figure 5.8: **Model for the impact of host diet on germ line *Wolbachia* titer.**

egg chamber development [257, 273, 277, 279-288]. If *Wolbachia* are unresponsive to nutrient-induced adjustments in germ line cell growth and development, significant titer changes in oogenesis would be expected. However, oocyte *Wolbachia* titers were very similar in mated and virgin females, despite the different rates of germ line stem division expected for each type of flies [273, 280, 283, 284, 287-293]. Another possibility is that yeast-induced insulin signaling affects *Wolbachia* physiology in oogenesis. The "rounded" *Wolbachia* nucleoids visible in the yeast-enriched condition could indicate substantially slowed bacterial growth or a bacterial stress response, for example [106, 294, 295]. Insulin signaling has been shown to induce changes in cytoskeleton organization, proteasome activity, and chaperonin activity [299-303], any of which could affect *Wolbachia* physiology. It is also possible that dietary yeast in particular carries one or more bioreactive agents that are toxic to germ line *Wolbachia* (Figure 5.8).

The impact of somatic insulin signaling on germ line *Wolbachia* titer also raises the question of whether somatic *Wolbachia* titers are similarly affected by host nutrient conditions. Our initial findings that *Wolbachia* titers in the *Drosophila* brain are non-responsive to host diet suggested that nutrient-associated titer changes are restricted to the ovary. Analysis of sucrose-fed, ovarectomized females is further consistent with that interpretation. However, analysis of ovarectomized females also indicated that dietary yeast triggers somatic titer changes opposite of oogenesis. It is possible that this occurs by physical relocation of *Wolbachia* within the body, with dietary yeast driving *Wolbachia* egress from ovarian cells, followed by invasion of somatic target tissues. Alternatively, host dietary conditions may drive tissue-specific differences in the *Wolbachia* life cycle. Perhaps yeast-enriched diets favor *Wolbachia* replication and survival in specific somatic tissues while disfavoring the same in oogenesis. Support for this hypothesis comes from our finding that yeast-enriched food induces the same bodywide titer changes in male flies as seen in ovarectomized females. This demonstrates that ovarian *Wolbachia* titer responses are distinct from that of other tissues.

The pathways downstream and upstream of TORC1 that mediate yeast-based suppression of *Wolbachia* germ line titer are yet to be determined. An obvious possibility is the role of TORC1 in suppressing autophagy (Figure 5.8). There are numerous examples in which autophagy either enhances or suppresses intracellular bacteria titer [304]. Since TORC1 disruptions increase *Wolbachia* titer in oogenesis, it is possible that *Wolbachia* interact positively with autophagy, consistent with other endosymbionts [305, 306]. As insulin signaling is expected to down-regulate autophagy (Figure 5.1), the low *Wolbachia* titers seen in yeast-fed oocytes are further consistent with this possibility. However, the finding that dietary yeast also increases somatic *Wolbachia* titers implies that somatic autophagy is normally bactericidal in that context, consistent with another recent report [307]. These conflicting results may indicate that tissue-specific differences in autophagy regulation contribute to *Wolbachia* titer control, or that other mechanisms downstream or independent from autophagy are responsible (Figure 5.8). Perhaps responses from one or more other TORC1 effectors further contribute to *Wolbachia* titer regulation (Figure 5.1).

Wolbachia have been shown to suppress replication of RNA viruses in insects, including the human pathogens, Dengue Fever Virus and Chikungunya Virus [308-310]. This finding, together with the fact that *Wolbachia*-induced Cytoplasmic Incompatibility rapid spreads *Wolbachia* through insect populations [230, 311], has led to a novel strategy of combating these diseases by releasing *Wolbachia*-infected insect carriers of these viruses into afflicted regions [312, 313]. Although the mechanism of *Wolbachia*-induced viral suppression is unknown, several studies demonstrate that the higher the *Wolbachia* titer, the greater the viral suppression [314-318]. Our finding that host diet dramatically affects tissue-specific *Wolbachia* titers suggests that the natural diets of the released insects should be taken into account when evaluating the potential effectiveness of a *Wolbachia*-based viral suppression field study. Finally it will be of interest to determine whether diet has a similar effect on *Wolbachia* titer in disease-associated filiarial nematodes.

Chapter 6

Unpublished Screening Data

After publication of “A Cell-Based Screen Reveals that the Albendazole Metabolite, Albendazole Sulfone Targets *Wolbachia*” in Chapter 2, screening continued. The first library we screened contained 400 representative anti-malarial compounds were combined into the “Malaria Box.” There were 37 hits with a 9.25% hit rate when screening at 100 uM for 5 days. A hit is a compound that is at least 3 standard deviations from the average in at least 2 out of 3 replicates. 9 hits were in the uninfected range, which are compounds that fall within 3 standard deviations of the uninfected control average. Any hits that have a significantly reduced number of cells, which means less than two standard deviations from the average, in 2 out of 3 replicates was removed. Compounds that reduce the number of cells most likely will target the host, which is not of interest to us. 7 benzimidazoles comprise the largest class of hits, which correspond to results from the Spectrum and NCI screens. Additionally, 3 of the 9 uninfected hits are benzimidazoles. The results of this screen up until this point were published in 2016 in PLoS pathogens titled “Open Source Drug Discovery with the Malaria Box Compound Collection for Neglected Diseases and Beyond.” After publication, 5 of the 9 uninfected hits were tested in our *Brugia pahangi in vivo* screen: MMV011567, MMV665878, MMV665824, MMV665899, and MMV006937. These compounds were tested at 5 uM for 3 days. After which the *Brugia pahangi* ovaries were dissected, stained, and imaged using confocal microscopy and *Wolbachia* titer was quantified. Results indicate that treatment with MMV006937, which is not a benzimidazole, significantly reduces *Wolbachia* titer.

The “Pathogen Box” was screened next and was modeled after the “Malaria Box.” It contains 400 compounds that target neglected diseases of interest such as tuberculosis, cryptosporidiosis, and many more. There were 126 hits with a 31.5% hit rate when screening at 100 uM for 5 days. Same as the “Malaria Box” screen, hits are compounds that are at

least 3 standard deviations from the average in at least 2 out of 3 replicates. There were no hits in the uninfected range. The compounds were categorized based on the disease they target. Two different analyses were performed. First, the 126 hit compounds were grouped, normalized, and averaged based on the disease. The results of this analysis are listed from best to worse at reducing the number of *Wolbachia* infected cells with total number of hits in parenthesis: reference compounds (9), kinetoplastids (24), schistosomiasis (4), onchocerciasis (3), toxoplasmosis (5), malaria (40), cryptosporidiosis (6), tuberculosis (33), hookworm (1), and dengue (1). Second, the hit rate for each disease was calculated. The results of this analysis are listed from highest to lowest hit rate with the total number of hits listed first / the total number of compounds listed second = the hit rate listed last in parenthesis: hookworm (1 / 1 = 100%), cryptosporidiosis (6 / 11 = 55%), reference compounds (9 / 26 = 35%), kinetoplastids (24 / 70 = 34%), toxoplasmosis (5 / 15 = 33%), malaria (40 / 125 = 32%), schistosomiasis (4 / 13 = 31%), tuberculosis (33 / 116 = 28%), onchocerciasis (3 / 11 = 27%), and dengue (1 / 5 = 20%). Curiously, trichuriasis (0 / 1 = 0%), lymphatic filariasis (0 / 3 = 0%), and *Wolbachia* (0 / 3 = 0%) all had a 0% hit rate. Due to the high number of hits, I argue the best course forward is to screen the library at a lower concentration, which would remove some of the false positive hits and allow us to better choose which hits would be best to test in the *Brugia pahangi in vivo* screen.

Most recently, at UCSF's Small Molecule Discovery Center (SMDC), we screened the Chembridge library, which is composed of 30,000 compounds. This library is organized such that the compounds on each plate share structural similarity. Given our previous results, this particularly interested us. We tested the entire library in singlicate, which yielded 972 hits and a 3.27% hit rate. The library was screened at 10 uM concentration compared to the Spectrum, NCI, Malaria Box, and Pathogen Box which were screened at 100 uM concentration.

To narrow down our hits, 7 plates were chosen to be tested in duplicate. Combined with the initial screen, these plates were screened in triplicate. These 7 plates contained a higher

number of hits compared to the average and comprised 358 hits in the primary screen, which are 37% of the primary screen hits and a 16% hit rate overall on these plates. After the secondary screen, 116 compounds were hits (5.78% hit rate on these plates). Compounds that reduce the number of cells most likely will target the host, which is not of interest to us. The results from the secondary screen provided us with 20 compounds that reduce titer in 3 out of 3 replicates and 74 compounds that reduced titer in 2 out of 3 replicates. We also have 8 uninfected hits, which are compounds tested in the primary screen that fall within three standard deviations of the uninfected control average. Thus far, 16 out of 20-3 out of 3 hits and 8 out of 8 uninfected hits were tested in the *Brugia pahangi* ovary and 2 compounds significantly reduced titer (1-3 out of 3 hit and 1 uninfected hit). In total we have screened 36,231 compounds, which include NCI diversity, spectrum, malaria box, pathogen box, Celgene, and Chembridge libraries. Of those, 8 compounds efficiently reduce *Wolbachia* titer in nematode based screens.

Three papers have been published using albendazole combination therapy to treat *Wolbachia* causing diseases in humans since our 2012 publication [1]. Most recent results in Ute Klarmann-Schulz et al. 2017 show that treatment with albendazole for 3 days in combination with doxycycline for 3 weeks significantly reduces *Wolbachia* in 81.4% of adult female worms [319]. This combination was compared to doxycycline alone for 4 weeks (significantly reduces *Wolbachia* in 98.8%), doxycycline alone for 3 weeks (significantly reduces *Wolbachia* in 64.1%), and albendazole alone for 3 days (significantly reduces *Wolbachia* in 35.2%) [319]. These data suggest even though doxycycline alone for 4 weeks reduces Wolbachia more that there is an additive effect of albendazole for 3 days with doxycycline for 3 weeks. This paper has the shortest treatment time for albendazole at 3 days when the other papers list treatment times for albendazole at 7 days [320] and 12 days [321]. Treatment with albendazole for longer than 3 days in combination with doxycycline for 3 weeks would reduce *Wolbachia* further and be worth testing. Further, our hypothesis that

albendazole targets *Wolbachia* FtsZ was supported by a 2013 study that FtsZ is sensitive to albendazole [322].

A notable observation is that in the *Wolbachia* infected cell culture cells there are small particles that move. These cell-like particles are filled with *Wolbachia* and do not grow on agar plates (without antibiotics) which indicates that this is not contamination. They are always present in *Wolbachia* infected cultures and we have no idea what they are. They also increase when cells undergo an increased rate of apoptosis.

Chapter 7

Discussion

While my thesis work has addressed a number of outstanding issues regarding the interaction between *Wolbachia* and its host, it has also raised a number of new exciting questions that remain to be explored. Here I discuss these potential new avenues of research.

A key question raised by our small molecule anti-*Wolbachia* screens is what are the targets of our most promising hits. We suspect that the albendazole derivatives may be targeting FtsZ. FtsZ is an essential bacterial division protein and without it when *Wolbachia* divide cytokinesis does not occur. Elongated *Wolbachia* are visible with albendazole sufone treatment, which could suggest that FtsZ is the target of the albendazole derivatives. The known target of albendazole and other benzimidazoles is beta-tubulin, which disrupts microtubule polymerization. FtsZ is a bacterial homolog of tubulin further supporting this assertion. This results in Wolbachia that look like long sausages due to the mother and daughter bacteria remaining connected; these bacteria eventually die. *Wolbachia* rely on locating in a specific time and place within a cell and organism. This reliance on location means that they are highly dependent on host microtubules and actin for movement, which makes it a great potential target.

Although we are unsure of the targets, we have noticed that the best hits have consistently been compounds with simple core structures of two rings together composed of either a 5- and a 6-member ring or two 6-member rings. Compounds usually have nitrogens at the 1 and 3 positions with an R group at the 2 position. If the nitrogens are on the 5-member ring then there is usually only 1 R group. If the nitrogens are on the 6-member ring then there is usually another R group at the 4 position. Sometimes there is another R group or a sulfur

opposite the first R group on the other ring. If screening were to continue, it would be beneficial to test libraries of compounds that all fall into these criteria.

Another issue raised by our cell-based anti-*Wolbachia* screens is whether there is a more efficient way to execute the screening procedure. Given what I know now, if I were to approach the screen *de novo* I would change how *Wolbachia* are quantified. It would be beneficial to determine the number of *Wolbachia* per cell instead of relying on total fluorescence to determine if a cell is infected. The technology that is utilized for high-throughput screening is improving every day and while determining the number of *Wolbachia* per cell may not have been possible when screening began, I believe it is possible now and this research would greatly benefit from that knowledge.

After compounds are tested in the primary screen, compounds are tested in our secondary screening assay where we feed compounds to flies for 3 days to determine if *Wolbachia* titer decreases in the fly oocyte. The fly oocyte is a useful tool because flies are cheap and easy to grow in the lab. This contrasts with parasitic worms, which are expensive, difficult to get, and cannot grow to an adult without a mammalian host. I have found that the fly oocyte is a useful system, with some caveats. Titer reducing compounds in the fly oocyte usually translate and reduce titer in the worm. Usually these compounds are the strongest hits and reduce titer close to the same level as doxycycline. However, some compounds will not reduce titer in the fly oocyte, but will still reduce titer in the worm. These compounds tend to be our weaker hits with technically significant reduction in titer, but also significantly more titer then doxycycline treated worms. How effective and ineffective drugs are in each of these systems could be due to many things, but most likely is due to the difference in how these organisms get the drug into their system. The fly must consume the drug compared to the worm, which absorbs the drug through the cuticle. Overall, I think the fly oocyte is still a useful secondary assay.

After compounds are tested in *Drosophila* oocytes, hit compounds are tested in our tertiary assay where we dose *Brugia* with compounds of interest to determine if titer decreases in the

Brugia ovaries. By looking near the distal tip cell we can accurately find if compounds alter titer due to the consistent amount of *Wolbachia* in that area. In *Brugia Wolbachia* can also be found in the hypodermal chords, which we have not used. It would be interesting to figure out if that tissue can also be used to measure titer. It has not been used in the past due to massive differences in titer in different areas of the hypodermal chord. More basic research needs to be done on this tissue to answer some questions before we can use this tissue reliably. Some questions include: do *Wolbachia* replicate in the hypodermal chords? If so, do they always grow or do they only grow during specific stages? These questions need to be addressed because if it is found that *Wolbachia* do not grow in the hypodermal chords and the worms are treated with a compound targets *Wolbachia* growth, such as an FtsZ inhibiting drug, then one would not see the effects of the compound in the hypodermal chords. One easy way to begin answering these questions is to measure *Wolbachia* using qPCR in *Brugia* at every stage of *Brugia* development. Ovaries are further developed as a mature adult so if *Wolbachia* titer increases prior to ovary maturity you can determine that *Wolbachia* are growing in the hypodermal chord.

Another major issue raised by my studies is elucidating the mechanisms by which *Wolbachia* are able to undergo horizontal cell-to-cell transfer. In “Mechanisms of horizontal cell-to-cell transfer of *Wolbachia* spp. in *Drosophila melanogaster*” we developed a new method of testing cell-to-cell transfer. This showed that horizontal transmission of *Wolbachia* does occur, can take place in 12 hours or less, and uses both clathrin-mediated endocytosis and phagocytosis to gain entry into a cell. This new knowledge poses new questions including: what receptor do *Wolbachia* use for clathrin-mediated endocytosis? When do *Wolbachia* use endocytosis versus phagocytosis? How fast can endocytosis occur? What happens after *Wolbachia* gain entry into a cell? Using my knowledge of cell-to-cell transfer, high-throughput screening, and RNAi many of these question can be answered by designing a screen to determine host factors involved in cell-to-cell transfer. From our paper we know that clathrin and dynamin are needed for endocytosis, but there are numerous unidentified host factors

required for endocytosis. In addition to learning more about *Wolabchia*, studying endocytosis of endosymbionts like *Wolbachia* can teach us more about host cell physiology. One question not addressed in this paper is, how do *Wolbachia* exit the cell? My hypothesis is that *Wolbachia* use both apoptosis and exocytosis to exit the cell, utilizing specific receptors and exocytosis gene products. I would test this hypothesis *in vivo* using adult *Drosophila melanogaster*. Previous studies demonstrated that cell-to-cell transfer occurs, therefore *Wolbachia* is not only capable of cell-to-cell transfer, but is capable of targeting the female germ line stem cells over long distances [323]. Through a combination of cell specific gene knockdowns, one should be able to identify key host genes involved in both cell-to-cell transfer and long distance targeting. Promising candidate genes include epidermal growth factor receptor (EGFR) and hsp70.

Since Chapter 4 was published, more work has been done looking more into ERAD and its significance to *Wolbachia*. What role do other ERAD components play in regulation of *Wolbachia* titer? MG132 is a synthetic proteasome inhibitor and when fed to flies *Wolbachia* titer goes down in the oocyte. This result is consistent with the results from the proteasome inhibitor lactacystin published in the paper. To look further into ERAD, we used kifunensine, which is an ERAD inhibitor and inhibits the preparation of misfolded proteins upstream of ERAD. When kifunensine was fed to flies, *Wolbachia* titer in the oocyte decreased. This result is consistent with what was shown in the paper when ERAD-C component, ubc6, was knocked down and titer goes down [3]. To test the other branches of ERAD we looked at hrd1, which is an E3 ubiquitin ligase involved in ERAD-L and –M. We have found that when hrd1 is knocked down, titer goes up. At this point it is unclear why when ERAD-C is knocked down titer goes down and when ERAD-L and –M are knocked down titer goes up. Our hypothesis is that *Wolbachia* are utilizing the amino acids that output from ERAD-C therefore when ERAD-L and –M are turned off more proteins are degraded through ERAD-C, which benefits *Wolbachia*, but this has not been tested. Furthermore, when running a coomassie gel looking at *Wolbachia* infected versus uninfected cell culture cells we consistently found an

extra band in the *Wolbachia* infected lane at 70 kDa (P.M. White unpublished data). It was thought that this band might be hsp70, which plays a chaperone role in ERAD. The western blot however showed no difference in hsp70 between infected and uninfected cells. Even though the results were negative, I still think that hsp70 could be playing a role and it should be pursued further.

Our screen for host factors that, when knocked down, reduce *Wolbachia* titer also yielded knockdowns that increased titer. This latter class would be interesting to pursue as it may shed additional insight into factors that inhibit *Wolbachia*. Other interesting classes of hits that should be further pursued are lipids, mitochondria, and ATP/GTP. These categories could lead to new pathways utilized by *Wolbachia*.

"The Impact of Host Diet on *Wolbachia* Titer in *Drosophila*" in Chapter 5 was an instrumental step in beginning to understand how host dietary nutrients affect pathogens. However, with knowledge come more questions. First, food enriched with glucose, fructose, and glucose + fructose combined did not alter titer. Are there other sugars that alter titer besides sucrose? In figure 2, Camacho *et al.* 2017 show that galactose, lactose, maltose, and trehalose all increase titer and in figure 3 show that they all decrease ovary size as well [324]. Second, sucrose enriched food increases titer but decreases ovary size and yeast enriched food decreases titer but increases ovary size. Is the titer change a result of the change in size? In figure 4, Camacho *et al.* 2017 show that even though lactulose, erythritol, xylitol, aspartame, and saccharin decrease ovary size even though there is no change in titer [324]. This suggests that ovary titer and size are not linked. Third, when making the sugar enriched foods, the thick syrup is mixed with regular fly food. This made us wonder if the sugar-enriched foods caused the food to desiccate. Therefore, does desiccated food cause a change in titer? In figure 5, Camacho *et al.* 2017 show that when silica gel is added to fly food there is no change in titer indicating that desiccation does not cause a change in titer seen in sugar-enriched foods [324]. Last, how is titer and ovary size affected when flies are fed yeast and sugar enriched food combined? In figure 6, Camacho *et al.* 2017 show that

when yeast is fed in combination with sucrose, galactose, lactose, and maltose there is no significant change compared to control food and compared to yeast enriched food there is a significant increase [324]. However this is a different story when yeast is fed in combination with trehalose. There is a significant decrease compared to control food and no significant difference compared to yeast enriched food. Despite these results, all yeast and sugar enriched combinations had a normal ovary size that were not significantly different compared to the control and significantly decreased compared to the yeast enriched food. This suggests that the titer change caused by sucrose, galactose, lactose, and maltose act within the same mechanism yeast does, but that trehalose acts within an entirely different mechanism. Moving forward it would be interesting to parse the different mechanisms identified in this paper. Specifically the trehalose is the most interesting because it caused the greatest increase in titer but did not rescue the effects of yeast like the other sugars that increased titer did.

Another unexplored issue in the *Wolbachia* field is the reciprocal influences between *Wolbachia* and host cell on cell cycle regulation. Initially after treatment with doxycycline, division rate of cured cells is the same as infected cells. Over time however, the division rate of cured cells increases to five-times faster then infected cells, which always have the same division rate. This could be due to the fact that treatment with doxycycline has been shown to cause mitochondrial dysfunction [325]. This same change in division rate is seen comparing cells that are uninfected and have never been infected to *Wolbachia* infected cells, which can be made using an infection method similar to what was published in Chapter 4. This allows for the creation of *Wolbachia* infected S2 cells and when division rates are compared, again uninfected S2 cells divide five-times faster then *Wolbachia* infected S2 cells.

Chapter 8

Methods

Generation and maintenance of cultured cells

The JW18 cell line bearing the Jupiter-GFP transgene was generated according to the method described in [38, 41]. 2 to 15 hour old embryos derived from *Wolbachia*-infected flies carrying a Jupiter-GFP transgene were homogenized and plated in flasks. During the next 6 months of maintenance, 5 of the initial 20 seed flasks converted into immortal tissue culture lines. The JW18 cell line was selected for further pursuit due to its planar growth pattern and stable abundant *Wolbachia* infection. JW18 cells were maintained at 25–26°C in Sang and Shields media containing 10% fetal bovine serum, split weekly at a 1:2 dilution. A cured version of the JW18 line, referred to as JW18TET and JW18DOX, was generated by treating the cells with tetracycline and doxycycline respectively [26, 326, 327]. A Chi-square test was used to test for differences in the frequency of mitosis between JW18 and JW18TET cells. Electron microscopy was primarily performed on a second *Wolbachia*-infected cell line that expresses Jupiter-GFP and Histone-RFP (LDW1) generated and maintained as described above.

Stocks of uninfected *Drosophila* S2 cells and *Wolbachia*-infected *A. albopictus* C6/36 cells were maintained in Shields and Sang M3 insect medium (Sigma-Aldrich) supplemented with 10% fetal bovine serum (FBS) (Gibco) at a temperature of 25 to 26°C. JW18 and LDW1 cells are naturally infected with the *w*Mel strain of *Wolbachia* [1], while C6/36 cells were artificially infected with the *w*AlbB strain from Aa23 cells, as previously described [328].

Screening approach

Several small chemical libraries were used in this study. The Spectrum Collection (MicroSource Discovery Systems, Inc) of 2,000 compounds contains 1,000 drugs with known

pharmacological properties, 600 natural products, and 400 other bioreactive compounds. The NCI Diversity Set I contains 1,990 compounds selected for structural uniqueness and fewer than 5 rotatable bonds. The NCI Mechanistic Set contains 879 compounds, selected for their diversity of impact in human tumor cell line screened by the NCI. The NCI Challenge Set contains 57 compounds that stood out in the NCI tumor cell screens because of the unusual patterns of cell lethality and resistance induced by these compounds. The stock concentration of the compounds in these libraries was 10 mM. Furthermore, these libraries were reformatted into 384-well plates by the UCSC screening center. Specifically, compounds were placed into columns 3–22 of the plates, leaving columns 1–2 and 23–24 vacant to allow for untreated control wells.

Two different *Drosophila* RNAi libraries were used in this screen: UCSF DmRNAi library version 1 and UCSF DmRNAi library version 2. These libraries have been used previously in [175, 329]. Both libraries are available in 96-well format from Open Biosystems, now a part of GE Healthcare. Three out of four wells from each 384-well screening plate (Griener Bio-one) were set aside for experimental use. The fourth quadrant of wells was used for controls to define baselines for (1) untreated wells with standard levels of infected cells and (2) wells carrying significant reductions in infection, as induced by pararosaniline pamoate, administered to 100 mM final concentration [1].

Cells were plated in 384-well, clear bottom plates (Griener Bio- one) pre-coated with 0.5 mg/mL Concanavalin A. JW18 cells were added to 22 columns, and JW18TET cells were added to the remaining 2 columns at a concentration of 6,500 cells per well. For the drug screen, after the cells adhered to the plates for 4–6 hours, compounds were transferred into 20 columns of JW18 cells in the center of the plate using a Janus MDT pin tool. The final concentration of compound was 100 μM per well. All treatments were distributed into 3 plate replicates. For the RNAi screen, after the cells adhered to the plates for 50 min, double-stranded RNA (dsRNA) was transferred into the plate of JW18 cells using a Janus MDT pin tool and media containing 40% fetal bovine serum (FBS) was added for a final concentration

of 10% FBS. The average concentration of dsRNA was 0.223 mg/well. All treatments were distributed into two plate replicates.

After a 5-day incubation with the compounds at 25°C, the cells were prepared for imaging. Cells were fixed for 20 minutes in 4% formaldehyde and rinsed with PBS using an automated BioTek liquid handler. All staining solutions were administered using a Multidrop robot, with extensive rinsing between treatments. Mouse anti-histone (MAB052, Millipore) and goat anti-mouse Alexa 594 (Invitrogen) was diluted to 1:1250 in PBS/0.1% Triton. A stock solution saturated with DAPI was used at a final concentration of 1:40. After staining, PBS+sodium azide was added to all wells of the plates.

Screen data analysis

Stained plates were imaged using an ImageXpress Micro system (Molecular Devices, Sunnyvale, CA). 10 images were acquired per well at 40x magnification. These images were analyzed using customized analysis software provided by Molecular Devices. The software routine masks any areas where clumps of cells are detected, based upon intensity of the Jupiter-GFP. The boundaries of the remaining cells and their nuclei are recognized based upon the Jupiter-GFP and anti-histone stains. A mask was applied to the nuclei to obscure fluorescent signal from those areas. A threshold for DAPI fluorescence detection is set to detect as much *Wolbachia* as possible in JW18 control cells while minimizing detection of background DAPI signal in JW18TET control and pararosaniline pamoate-treated control cells, then applied to analysis of the entire plate. Cytoplasmic DAPI attributable to *Wolbachia* nucleoids was scored in each cell to classify it as *Wolbachia*-infected or uninfected. A spreadsheet from the data analysis software indicated the quantity of *Wolbachia*-infected cells versus total cells measured in each well. Average and standard deviation values were calculated for the frequency of *Wolbachia* infection in JW18, JW18TET control cells, and pararosaniline pamoate-treated JW18 control cells, using the descriptive statistics function in Statistical Package for the Social Sciences (SPSS by IBM). These values were used to

calculate a Z' factor for each plate. The Z' factor represents 1 – (three multiplied by the absolute value of the sum of the SD for each control divided by the absolute value of the difference between mean values for each control) [330]. Z' factors regarded as acceptable in this field range from 0 to 1. Our Z' factors ranged from 0.2 to 0.65 per plate for the drug screen and 0.25 to 0.85 per plate for the RNAi screen, confirming that the controls were clearly distinguishable by the assay. To identify preliminary "hit" compounds that substantially reduced intracellular *Wolbachia* titer, an initial hit range was calculated to lie between the JW18 average infection frequency - 3 SD, and the average JW18TET infection or pararosaniline pamoate-treated JW18 infection frequency + 3 SD. To enable comparison of hits identified on different treatment plates, the scaling of this initial hit range was next reset to span from 0 to 1, thus applying a uniform, normalized hit range to all plates. To further increase the stringency for identifying hits, we also calculated an average infection frequency for all JW18 cells on the plate (treated or not), as most treatment wells are expected to be indistinguishable from untreated controls. Wells that lay within 3 SD of the mean were excluded from the hit list. For the RNAi screen, hit wells identified in only one of two replicates were also removed. For the drug screen, hit wells identified in only 1 of 3 replicates were also removed from the hit list. From the remaining hit candidates, we further identified compounds designated as hazardous by the National Cancer Institute, which includes alkylating agents, corrosives, carcinogens, explosives, flammables, oxidizers, poisons and known toxins. Any hits falling into these hazard classes were removed from further consideration. The hit compounds not excluded by these stringent criteria were designated as finalized hits.

The cytotoxicity of each hit from the Spectrum and NCI library screens was determined using a stepwise classification process. The Pubchem Bioassay Database was mined to assess the impact of our hits in prior mammalian tumor cell cytotoxicity screens conducted by the NCI. The majority of our hit compounds have already been tested for cytotoxicity in 45–115 screens conducted by the NCI. For those hits, if over 50% of the NCI screens indicated the

drug to be cytotoxic, we designated that hit as ‘‘toxic’’ in our listing. If 10%–50% of the NCI screens indicated cytotoxic properties for that compound, we classified it as ‘‘moderately toxic.’’ If less than 10% of NCI screens indicated toxicity, we classified it ‘‘non-toxic.’’ A subset of our hit compounds have been run in 2 or fewer prior NCI screens. For those, hits, a preliminary cytotoxicity designation was assigned based upon the cell density reported by our screen. The average cell density per well was first calculated for each set of treatments, and treatments that failed to shift the cell density of a single well more than +/- 33% from the plate average were designated as ‘‘non-toxic.’’ Treatments that increased the average cell density to more that 33% over the average density were classified as ‘‘toxicity unclear’’, while treatments that reduced average cell density to 33%–66% below the average cell density were classified as ‘‘moderately toxic.’’

Live imaging of tissue culture cells

Tissue culture chamber slides were coated with 0.5 mg/mL Concanavalin A, followed by addition of JW18 cells. After a 24-hour incubation at 25°C, cells were exposed to Syto-11 (Molecular Probes) for one minute at a dilution of 1:50,000. Cells were imaged on a Leica SP2 confocal microscope at 100x magnification and 2.75x optical zoom using FITC filters. Images were acquired at 5-second intervals for up to 10 minutes.

Primary neuroblast cell culture and infections

Drosophila stocks homozygous for neuroblast-specific GAL4 expression (OK371, as identified in [331]) and CD-ChRFP [7] under an upstream activation sequence (UAS) promoter (Bloomington stock 27391) were crossed. Third-instar larvae were collected for brain dissection and primary culture [332], modified to exclude antibiotics from all reagents except for the Shields and Sang medium used to wash the cells, which contained 1:1,000 penicillin- streptomycin. The brain homogenate was plated on concanavalin A-coated glass

coverslips as described above and incubated at 25°C overnight. Neuroblasts were tested for cell-to-cell transfer as described above.

Passive uptake of fluorescently labeled dextran

S2 cells and neuroblasts were incubated with 20 mg/ml 1:1,000 fluorescently labeled dextran (molecular weight, 40,000) overnight at 25°C. Culture medium with beads was aspirated, and cells were processed for detection of *Wolbachia* bacteria by using FISH (see next section).

FISH detection of *Wolbachia*

For FISH assays, cells were seeded on glass coverslips in untreated 6-well polystyrene plates (Costar). In transwell assays, uninfected cells were seeded in the same manner, while infected cells were seeded on polyester transwell membrane inserts with a pore size of 3.0 μm (Costar). For assays of dynamin inhibition, uninfected cells on coverslips in the bottom transwell were treated with 80 μM dynasore [149] or an equal volume of DMSO (control) for 1 h, and the medium was then changed prior to seeding infected cells on the top well or prior to adding crude *Wolbachia* preparations directly to the culture medium for an additional 24 h. For assays of clathrin inhibition, uninfected cells on coverslips in the bottom transwell were treated with 10 μM chlorpromazine [150] for 1 h, and the medium was changed prior to seeding infected cells on the top well. Crude *Wolbachia* extracts were prepared by running infected cells in culture medium through 5.0-μm filter spin columns (Millipore) for lysis to release *Wolbachia* bacteria and remove large cellular debris.

Wolbachia detection by FISH was performed 1, 2, or 3 days after coculture of uninfected and infected cells and 24 h after the addition of crude *Wolbachia* preparations to cured cells. Cells on glass coverslips were fixed with 8% paraformaldehyde for 20 min at room temperature, washed 3 times with phosphate-buffered saline (PBS), and treated with prehybridization buffer for 90 min at room temperature. The prehybridization buffer consisted

of 50% deionized formamide by volume, 4X saline sodium citrate (SSC), 0.5X Denhardt's solution, 0.1 M dithiothreitol (DTT), and 0.1% Tween 20 in deionized water. After prehybridization, cells were hybridized overnight at 37°C in hybridization buffer (prehybridization buffer minus detergent) containing 500 nM *Wolbachia* W2 fluorescent DNA probe (5-CTTCTGTGAGTACCGTCATTATC-3) (Bioresearch Technologies) [333]. After hybridization, cells were washed 3 times with 1X SSC plus 0.1% Tween 20, 3 times with 0.5X SSC, and 3 times with PBS to remove any free *Wolbachia* bacteria on the slide. The last step of each wash series was performed at 42°C to eliminate nonspecific binding of the FISH probe. Slides were then mounted and stained using Vectashield fluorescent mounting medium with DAPI (4,6-diamidino-2-phenylindole) (Vector Laboratories).

Microscopy and image analysis

All fluorescence and differential interference contrast (DIC) imaging was performed on a Leica DMI 6000 inverted wide-field microscope under equal exposure times and conditions. For quantitation of *Wolbachia* infection during coculture over time, 3 to 7 fields (technical replicates) for each group from 3 independent experiments (biological replicates) were scored for the proportion of cells displaying red puncta in the ImageJ cell counter tool (http://imagej.nih.gov/ij/). Only cells with *Wolbachia* puncta in close association with the nucleus were scored as infected to reduce the number of false-positive infections from *Wolbachia* on the slides outside the cell, despite them being negligible. Counts from each field were plotted as the proportion infected per field of view ± standard error of the mean (SEM) and were pooled for analysis by one-way ANOVA followed by Newman-Keuls multiple-comparison test or by *t* test to determine differences in infection over time and between the treated and untreated groups. For electron microscopy, samples were fixed with 2% glutaraldehyde and 0.5% paraformaldehyde in 0.075 M cacodylate buffer and postfixed with 2% osmium tetroxide. Samples were dehydrated through a graded series of ethanol and embedded in epoxy resin. Ultrathin (70-nm) sections (Ultracut UC6, Leica) were collected on

Formvar/carbon-coated copper grids. Sections were then poststained with aqueous 4% uranyl acetate and lead citrate. All samples were observed in a Tecnai 12 (FEI, The Netherlands) transmission electron microscope at 80 kV equipped with a 1K-by-1K-resolution Keen View camera.

Drug treatments in *Drosophila* and *Brugia*

ALB (Sigma), ALB-SO and ALB-SO2 (Santa Cruz Biotechnology) were dissolved into DMSO to create 10 mM stock solutions. The flies used for this study, w; Sp/Cyo; Sb/TM6B, were reared on fly food consisting of 0.5% agar, 7% molasses, 6% cornmeal, and 0.8% killed yeast. Newly eclosed flies were collected, reared for 3 days, starved one day, and then fed compounds of interest for one day. For titer assessment experiments, compounds were diluted to a final concentration of 100 μM in yeast paste. Equivalent amounts of carrier DMSO diluted into these nutrient sources were used as a control.

For ERAD testing, newly eclosed flies of the genotype w; Sp/Cyo; Sb/TM6B were collected, reared for 2 days, and then exposed to food containing lactacystin diluted to a final concentration of 100 mM for 3 days. Equivalent amounts of carrier DMSO diluted into these nutrient sources were used as a control. For the TORC1 testing, 50μL of either control DMSO or 30mM rapamycin/DMSO stock was mixed into 5mL standard food. For tests of IPC function, 50μL of either control DMSO or a 10mM mifepristone-DMSO stock was mixed into 5mL standard food.

Brugia microfilariae were provided by TRS (Athens, Georgia). These were resuspended in 2 mL tissue culture media containing 50 μM of each compound of interest, except for colchicine, which was administered at 20 μM. Control worms were provided an equivalent dilution of carrier DMSO alone. Microfilariae were incubated with the compounds for 1 day at 37°C with 7.5% CO_2. Adult *Brugia* were incubated for 3 days.

Tissue staining and analysis

A combination of fixation and staining methods was used. Samples were prepared from a minimum of 10–15 flies per condition in each replicate. Ovary dissection, fixation, and propidium iodide staining were done as previously described in order to label germ line *Wolbachia* nucleoids [84]. Ovarian tissues for all samples in each replicate were mounted on slides in parallel to ensure maximal consistency in sample compression between slide and coverslip. All samples were then imaged on a Leica SP2 confocal microscope at 63X magnification with 1.5X zoom. Experimental samples verified to exhibit the same degree of compression as the control sample were pursued further, while any experimental samples deviating from that were discarded. Z-series images were acquired from each egg chamber of interest at 1.5 μm intervals. Uniform intensity settings were applied to all egg chambers imaged within each replicate. A minimum of 7–10 oocytes were ultimately imaged from each condition, with all experimental oocytes matched for morphological consistency against control oocytes of the same replicate. Using this rigorous method, significant fold-differences in *Wolbachia* titer were consistently identified between control and experimental conditions, regardless of the baseline quantity of *Wolbachia* detected in each replicate.

To quantify *Wolbachia* titer in the confocal images, we used established methods to identify the deepest possible focal plane where *Wolbachia* are clearly visible in all samples tested for each replicate [95]. The images were processed in Photoshop to remove everything from the images except oocyte *Wolbachia*, which were then quantified using the Analyze Particles feature in Image J. This analysis ultimately quantifies the *Wolbachia* nucleoids carried per oocyte, or per nurse cell, within a single, representative focal plane of each egg chamber. Although the graphical data displayed in the figures present all experimental averages as normalized against the control averages, all statistical calculations were run by comparing each condition only against controls that were run in parallel. Significant differences were indicated by ANOVA. A minimum of 2–3 replicates were performed for most germ line staining experiments described in this study. The only exception was the experiment in

which *Wolbachia* titer responses were analyzed in both brain and ovary tissues. In that case, single replicates were done for each type of tissue stained, with all conditions run in parallel.

To analyze *Wolbachia* titer by real-time quantitative PCR, single flies were homogenized with a pestle in 250 µl of Tris HCl 0.1M, EDTA 0.1M and SDS 1% (pH 9) and incubated for 30 minutes at 70 ºC. After 35 µl of KAc were added the sample was incubated 30 minutes on ice, centrifuged for 15 minutes at 13.000 rpm at 4ºC and the supernatant stored. Samples were diluted 100x for qPCR. qPCr was performed as described previously [316], using the CFX384 Real-Time PCR Detection System and iQ SYBR Green Supermix (both BioRad). The relative amount of *Wolbachia* was calculated with the Pfaffl method [334], using the primers for the gene wsp to determine *Wolbachia* DNA levels and primers for host Rpl32 and Actin5C genes to normalize male and female samples, respectively [316]. Data from males were analyzed using a linear model on the log of the relative wsp levels (lm in R) [335]. Data from females were analyzed using a mixed linear model on the logs of relative wsp levels (lmer in R).

To analyze *Wolbachia* in the *Drosophila* central nervous system, brains were dissected and fixed as previously described [296]. Brains were incubated in anti-rabbit wsp antibody + PBST (0.1% Triton X-100) for 4 hours at room temperature or at least 12 hours at 4 degrees. For secondary antibody staining, goat anti-rabbit Alexa Fluor 546 (Invitrogen) was used at room temperature or at least 12 hours at four degrees. Actin labeling was done with phalloidin conjugated to Alexa 488, diluted 1:100 in PBST, for one hour at room temperature. Brain tissues were imaged on a Leica SP2 confocal microscope at 63X magnification. Brains were quantified with Leica LAF AS software. One representative focal plane per brain was scored. Cells containing one or more *Wolbachia* were scored as infected. *Wolbachia* aggregates larger than 10 microns^2 were scored as a “cluster” [296].

To assess *Wolbachia* nucleoid shape, we acquired Z-series images of stage 10A oocytes at 63X magnification with 5X zoom. Then we created a projection of 4 images from each Z-series, located just beneath the follicle cell layer, and measured the length of individual

nucleoids using the “line” tool located within the Profile function of Quantification Tools in the Leica SP2 software. Elongation index was calculated as a function of length divided by width. It is assumed that the bacteria are random in orientation, and thus detecting a range of nucleoid morphologies ranging from spherical to rod-shaped is possible. Chi square tests were used to compare *Wolbachia* length and elongation index exhibited by bacterial populations from each treatment condition.

Brugia staining was performed as previously described [313]. Briefly, worms were sectioned and fixed in PFA 3.2% for 10 minutes, rinsed in PBS+0.1% Triton-X100, and incubated overnight in RNAseA (10 mg/mL) in PBST, prior a 30 second incubation in a propidium iodide solution (1 mg/mL diluted100X in PBST). Worm fragments were washed for 1 minute in PBST and mounted in DAPI Vectashield mounting medium (Vector Labs). For FtsZ staining, worm fragments were incubated with rabbit anti-FtsZ [275] in PBST after a 1:500 dilution, after RNAse treatment, washed three times for 10 minutes, before adding a CY5-conjugated anti-rabbit secondary antibody, followed by 3 washes of 10 minutes in PBST and mounting in DAPI Vectashield mounting medium. Microtubules were stained using the monoclonal antibody DM1a (Sigma) at 1:250 and an Alexa488-conjugated goat anti-mouse secondary antibody (Molecular Probes) was used at 1:250. Mouse anti-histone H1 (Millipore MAB052) was used at 1:500, and rabbit anti-phospho-histone H3 (Millipore) was used at 1:1000. All tissues were imaged using Leica SP2 and Leica SP5 confocal microscopes. *Wolbachia* were quantified in single focal planes of stage 10A *Drosophila* oocytes using established methods [264]. To measure *Wolbachia* length in the *Brugia* ovaries, 11 images representing a 2 micrometer-thick Z-stack were merged to make a single image, followed by assessment of bacterial length using the Leica SP2 line quantification function. Average *Wolbachia* titer values associated with drug treatments were normalized against their respective DMSO controls as previously to ensure comparability between experiments [264].

Statistical analysis was conducted using established methods. The ANOVA function in SPSS was used to evaluate *Wolbachia* titer differences in *Drosophila* oogenesis and differences in

Wolbachia length in *B. malayi*. Chi-square tests were used to compare the frequency of *Wolbachia* posterior localization in *Drosophila* oogenesis and to evaluate ratios of *Wolbachia* per host nucleus in the *Brugia* ovary.

Ubiquitin foci staining and quantification

For analysis of ubiquitin foci in tissue culture cells, chamber slides were coated with 0.5 mg/ml Concanavalin A, followed by addition of JW18 cells. After a 24-hr incubation at 25°C, cells were fixed for 20 min in 4% formaldehyde, blocked using 1% BSA, and stained with anti-ubiquitin [Enzo Mono- and Poly- ubiquitinylated Conjugates (FK2) BML-PW8805] for 1 hr at 1:100 dilution. Goat anti-mouse Alexa 594 (Invitrogen) was used at a 1:1250 dilution in PBS/0.1% Triton. Cells were imaged on a Leica DMI6000B wide-field inverted microscope equipped with a Hamamatsu EM CCD camera (ORCA C9100-02) at 3100 magnification. Areas to image were selected randomly without bias. Foci were quantified by eye from cells with all boundaries visible in the image. Chi-squared analysis in SPSS was used to determine significance, and post hoc tests performed as previously described [336] .

For analysis of ubiquitin foci in *D. melanogaster* oogenesis, flies of the genotype w; Sp/Cyo; Sb/TM6B were reared on fly food consisting of 0.5% agar, 7% molasses, 6% cornmeal, and 0.8% killed yeast. Newly eclosed flies were collected and reared for 5 days. Ovaries were dissected in EBR (Ringer's solution) and fixed for 5 min in 600 ml heptane and 100 ml devitellinizing solution (100 ml Buffer B, 112.5 ml 32% paraformaldehyde, and 387.5 ml of diH2O) [337]. Ovaries were then rinsed, treated with RNAse overnight, blocked with 1% BSA, and incubated with anti-ubiquitin [Enzo Mono- and Poly- ubiquitinylated Conjugates (FK2) BML-PW8805] overnight at a 1:50 dilution. Last, the ovaries were incubated with goat anti-mouse:Alexa 488 at a 1:500 dilution and resuspended overnight in mounting media containing propidium iodide (PI). All samples were then imaged on a Leica SP2 confocal microscope at x63 magnification with x1.5 zoom. Experimental samples verified to exhibit the same degree of compression as the control sample were pursued further, while any

experimental samples deviating from that were discarded. Z-series images were acquired from oocytes at 1.5-mm intervals. Uniform intensity settings were applied to all egg chambers imaged within each replicate. A minimum of 7–10 oocytes were ultimately imaged from each condition per replicate with all experimental oocytes matched for morphological consistency against control oocytes of the same replicate. Significance was determined by ANOVA.

Fly strains

*w*Mel *Wolbachia* were crossed from w; Sp/Cyo; Sb/TM6B into a germ line triple driver stock [338] to ultimately generate infected flies of the genotype w; P(GAL4-Nos.NGT)40; P(GAL4::VP16-Nos.UTR)MVD1 [4]. Females from this infected driver stock were then crossed to males from responder stocks that carried the following upstream activation sequence (UAS) dsRNA transgenes: the Ubc6 Valium20 TRiP line: y,v; P(TRiP.HMS02466)attP40; the psGEF Valium20 TRiP line: y, sc,v; P(TRiP.HMS00320)attP2; the mtt Valium20 TRiP line: y,sc,v; P(TRiP.HMS00367) attP2; the ND-B17.2 Valium20 line: y,sc,v; P(TRiP. HMS01584)attP2; and the CG18324 Valium20 line: y,sc,v; P(TRiP.HMS01199)attP2/TM3, Sb. *Wolbachia*-infected driver females were also outcrossed to OreR uninfected males in parallel for analysis as a control.

Natural *D. melanogaster* and *D. simulans* flies were harvested daily from collection buckets distributed in the Santa Cruz, CA area. As the female flies of these species are morphologically indistinguishable, but both species were well-represented in the area, this wild-caught population was presumed to represent both species. The laboratory strain of *D. simulans* used was a w- stock that carried the endogenous *w*Ri *Wolbachia* strain. The *D. melanogaster* strain used for the initial nutrient feeds and for crossing *w*Mel *Wolbachia* into the other fly strains was w; Sp/ Cyo; Sb/TM6B. Other *D. melanogaster* fly strains used were the gigas VALIUM20 TRiP line: y, sc, v; P(TRiP.HMS01217)attP2/TM3, Sb; the chico VALIUM20 TRiP line: y, sc, v; P(TRiP. HMS01553)attP2/TM3, Sb; the somatic daughterless

driver: w; P(w+, GMR12B08-GAL4)attP2; the germ line triple driver: P(otu-GAL4::VP16.1); P(GAL4-Nos.NGT)40; P(GAL4::VP16-Nos. UTR)MVD1; and the stocks used for IPC ablation: w; P(w+, dilp2::GS-GAL4)/Cyo, and w; P(w+, UAS::Reaper). During this work, *w*Mel was introduced into the somatic daughterless driver, the germ line triple driver, and the dilp2::GS-GAL4 driver, and the infected versions of these stocks were crossed to the TRiP or UAS:Reaper responders. DrosDel isogenic flies carrying *w*Mel were used for real-time quantitative PCR analyses [316].

Food preparation and administration

The standard food recipe used was based upon that of the Bloomington *Drosophila* Stock Center [339]. The food was prepared in large batches that consisted of 20L water, 337g yeast, 190g soy flour, 1325g yellow corn meal, 96g agar, 1.5L Karo light corn syrup and 94mL propionic acid. To create yeast paste for this study, live bakers yeast was mixed together with water to create a smooth, thick paste. To create the "control food" used in this study, we mixed together 1.5mL ddH2O and 3.5mL of melted standard food in a narrow-mouthed vial, then let cool in an ice bucket to solidify the food suspension. The same procedure applied to creation of all other nutrient-altered foods used in this study. For "corn-syrup-enriched" food condition, 1.5mL Karo light corn syrup was used. For "yeast-enriched" food condition, 1.5mL of heat- killed yeast paste was used. The "BSA-enriched" food carried 0.4g BSA, 1.5mL water, and 3.5mL standard food. For the "sucrose-enriched", "glucose-enriched" and "fructose-enriched" foods, fresh sugar solutions were prepared at a final concentration of 1g/mL, then 1.5mL of this concentrate was combined with 3.5mL standard food for each vial. The "glucose + fructose enriched" condition carried 0.75mL of 1g/mL glucose, 0.75mL 1g/mL fructose, and 3.5mL standard food. Alternate methods were used to prepare food for the other treatments. For the branched chain amino acid condition, the control condition contained 400µL water and 50µL DMSO mixed with 4.5mL standard food,

whereas the experimental condition carried 200µL of 1mg/mL Arginine, 200uL of 1mg/mL Isoleucine and 50µL DMSO mixed with 4.5mL standard food.

Laboratory *Drosophila* stocks were maintained on standard food at 23–24°C. Identical population density was used in all vials, and control and experimental conditions run in parallel. Flies of the genotype w; Sp/Cyo; Sb/TM6B were used in all imaging experiments that assessed nutrition as the only variable. In the cases where crosses were needed to drive expression from TRIP line stocks or the dilp2:GAL4 stocks were used, we performed all crosses using identical population density and female age distribution in all vials, with control crosses always run in parallel. Virgin female flies were collected during the first 3 days of eclosion only, then subjected to nutrient conditions. The procedure was to collect a range of 0–24 hour old adults, age these young flies for 2 days on standard food, and expose to treatment conditions for 3 more days. The mixture of *D. melanogaster* and *D. simulans* flies collected from nature likely varied in age. These flies were also exposed to standard food for 2 days, and transferred to experimental food for 3 days. In the case of IPC ablation, the collected flies were allowed to mature 2 days, then transferred to mifepristone-containing food or DMSO control food. The flies were maintained on this food for 14 days, transferring the population to a fresh vial every 3 days of the treatment period. After this was completed, the flies were exposed to nutrient-altered food for 3 days.

Quantification of Wolbachia nucleoids in oogenesis

PI staining of *Drosophila* ovarian tissue was done using established methods [1]. Data collection was conducted as previously. All tissues were imaged using a Leica SP2 confocal microscope. *Wolbachia* were quantified in single focal planes of stage 10 oocytes using established methods [4]. Average *Wolbachia* titer values associated with drug treatments were normalized against their respective DMSO controls as previously to ensure comparability between experiments in displays of the data [4]. Statistical analysis was conducted on raw data only using ANOVA, as described previously [1]. A minimum of 2–3

experimental replicates were performed for the germ line staining experiments described in this study.

Transmission electron microscopy

LDW1 cells and the cured equivalent LDW1DOX were fixed with 2% glutaraldehyde and 0.5% paraformaldehyde in Cacodylate buffer 0.075M and postfixed with 2% osmium tetroxide. Samples were dehydrated through a graded series of ethanol and embedded in epoxy resin. Ultrathin (70 nm) sections (Ultracut UC6, Leica) were collected on formvar/carbon-coated copper grids. Sections were then poststained by aqueous 4% uranyl acetate and lead citrate. All samples were observed in a Tecnai12 (FEI, The Netherlands) transmission electron microscope at 80 kV equipped with a 1Kx1K Keen View camera. Chi-square analysis was used to determine significance, with post hoc tests performed as previously [336].

Supplementary files

Supplementary files for Chapter 2 can be found at:

https://doi.org/10.1371/journal.ppat.1002922.

Supplementary files for Chapter 3 can be found at: https://doi.org/10.1128/ AEM.03425-16.

Supplementary files for Chapter 4 can be found at: www.genetics.org/lookup/suppl/doi:10.

1534/genetics.116.198903/-/DC1.

Supplementary files for Chapter 5 can be found at:

https://doi.org/10.1371/journal.ppat.1004777

References

1. Serbus, L.R., et al., *A cell-based screen reveals that the albendazole metabolite, albendazole sulfone, targets Wolbachia.* PLoS Pathog, 2012. **8**(9): p. e1002922.
2. White, P.M., et al., *Mechanisms of Horizontal Cell-to-Cell Transfer of Wolbachia spp. in Drosophila melanogaster.* Appl Environ Microbiol, 2017. **83**(7).
3. White, P.M., et al., *Reliance of Wolbachia on High Rates of Host Proteolysis Revealed by a Genome-Wide RNAi Screen of Drosophila Cells.* Genetics, 2017. **205**(4): p. 1473-1488.
4. Serbus, L.R., et al., *The impact of host diet on Wolbachia titer in Drosophila.* PLoS Pathog, 2015. **11**(3): p. e1004777.
5. Hilgenboecker, K., et al., *How many species are infected with Wolbachia?--A statistical analysis of current data.* FEMS Microbiol Lett, 2008. **281**(2): p. 215-20.
6. Serbus, L.R., et al., *The genetics and cell biology of Wolbachia-host interactions.* Annu Rev Genet, 2008. **42**: p. 683-707.
7. Werren, J.H., L. Baldo, and M.E. Clark, *Wolbachia: master manipulators of invertebrate biology.* Nat Rev Microbiol, 2008. **6**(10): p. 741-51.
8. Harris, H.L. and H.R. Braig, *Sperm chromatin remodelling and Wolbachia-induced cytoplasmic incompatibility in Drosophila.* Biochem Cell Biol, 2003. **81**(3): p. 229-40.
9. Hoerauf, A., et al., *Filariasis in Africa--treatment challenges and prospects.* Clin Microbiol Infect, 2011. **17**(7): p. 977-85.
10. Taylor, M.J., A. Hoerauf, and M. Bockarie, *Lymphatic filariasis and onchocerciasis.* Lancet, 2010. **376**(9747): p. 1175-85.
11. WHO, *World Health Organization Global Programme to Eliminate Lymphatic Filariasis, Progress Report 2000–2009 and Strategic Plan 2010–2020*. 2010: Geneva: World Health Organization. p. 78.
12. Debrah, A.Y., et al., *Reduction in levels of plasma vascular endothelial growth factor-A and improvement in hydrocele patients by targeting endosymbiotic Wolbachia sp.*

in Wuchereria bancrofti with doxycycline. Am J Trop Med Hyg, 2009. **80**(6): p. 956-63.

13. Debrah, A.Y., et al., *Doxycycline reduces plasma VEGF-C/sVEGFR-3 and improves pathology in lymphatic filariasis.* PLoS Pathog, 2006. **2**(9): p. e92.
14. Turner, J.D., et al., *Wolbachia lipoprotein stimulates innate and adaptive immunity through Toll-like receptors 2 and 6 to induce disease manifestations of filariasis.* J Biol Chem, 2009. **284**(33): p. 22364-78.
15. Brattig, N.W., et al., *The major surface protein of Wolbachia endosymbionts in filarial nematodes elicits immune responses through TLR2 and TLR4.* J Immunol, 2004. **173**(1): p. 437-45.
16. Brattig, N.W., D.W. Büttner, and A. Hoerauf, *Neutrophil accumulation around Onchocerca worms and chemotaxis of neutrophils are dependent on Wolbachia endobacteria.* Microbes Infect, 2001. **3**(6): p. 439-46.
17. Saint André, A., et al., *The role of endosymbiotic Wolbachia bacteria in the pathogenesis of river blindness.* Science, 2002. **295**(5561): p. 1892-5.
18. Taylor, M.J., H.F. Cross, and K. Bilo, *Inflammatory responses induced by the filarial nematode Brugia malayi are mediated by lipopolysaccharide-like activity from endosymbiotic Wolbachia bacteria.* J Exp Med, 2000. **191**(8): p. 1429-36.
19. Hise, A.G., et al., *Innate immune responses to endosymbiotic Wolbachia bacteria in Brugia malayi and Onchocerca volvulus are dependent on TLR2, TLR6, MyD88, and Mal, but not TLR4, TRIF, or TRAM.* J Immunol, 2007. **178**(2): p. 1068-76.
20. Turner, J.D., et al., *Wolbachia endosymbiotic bacteria of Brugia malayi mediate macrophage tolerance to TLR- and CD40-specific stimuli in a MyD88/TLR2-dependent manner.* J Immunol, 2006. **177**(2): p. 1240-9.
21. Pfarr, K.M., et al., *Filariasis and lymphoedema.* Parasite Immunol, 2009. **31**(11): p. 664-72.

22. Korten, S., et al., *Natural death of adult Onchocerca volvulus and filaricidal effects of doxycycline induce local FOXP3+/CD4+ regulatory T cells and granzyme expression.* Microbes Infect, 2008. **10**(3): p. 313-24.

23. Bosshardt, S.C., et al., *Prophylactic activity of tetracycline against Brugia pahangi infection in jirds (Meriones unguiculatus).* J Parasitol, 1993. **79**(5): p. 775-7.

24. Hoerauf, A., et al., *Endosymbiotic bacteria in worms as targets for a novel chemotherapy in filariasis.* Lancet, 2000. **355**(9211): p. 1242-3.

25. Hoerauf, A., *Targeting of wolbachia endobacteria in litomosoides sigmodontis: comparison of tetracyclines with chloramphenicol, macrolides and ciprofloxacin.* Trop Med Int Health, 2000. **5**(4): p. 275-9.

26. Bandi, C., et al., *Effects of tetracycline on the filarial worms Brugia pahangi and Dirofilaria immitis and their bacterial endosymbionts Wolbachia.* Int J Parasitol, 1999. **29**(2): p. 357-64.

27. Landmann, F., et al., *Anti-filarial activity of antibiotic therapy is due to extensive apoptosis after Wolbachia depletion from filarial nematodes.* PLoS Pathog, 2011. **7**(11): p. e1002351.

28. Fenn, K. and M. Blaxter, *Are filarial nematode Wolbachia obligate mutualist symbionts?* Trends Ecol Evol, 2004. **19**(4): p. 163-6.

29. Ghedin, E., et al., *Draft genome of the filarial nematode parasite Brugia malayi.* Science, 2007. **317**(5845): p. 1756-60.

30. Foster, J., et al., *The Wolbachia genome of Brugia malayi: endosymbiont evolution within a human pathogenic nematode.* PLoS Biol, 2005. **3**(4): p. e121.

31. Sironi, M., et al., *Molecular evidence for a close relative of the arthropod endosymbiont Wolbachia in a filarial worm.* Mol Biochem Parasitol, 1995. **74**(2): p. 223-7.

32. Hoerauf, A., et al., *Doxycycline in the treatment of human onchocerciasis: Kinetics of Wolbachia endobacteria reduction and of inhibition of embryogenesis in female Onchocerca worms.* Microbes Infect, 2003. **5**(4): p. 261-73.

33. Hoerauf, A., et al., *Depletion of wolbachia endobacteria in Onchocerca volvulus by doxycycline and microfilaridermia after ivermectin treatment.* Lancet, 2001. **357**(9266): p. 1415-6.

34. Hoerauf, A., et al., *Wolbachia endobacteria depletion by doxycycline as antifilarial therapy has macrofilaricidal activity in onchocerciasis: a randomized placebo-controlled study.* Med Microbiol Immunol, 2008. **197**(3): p. 295-311.

35. Hoerauf, A., et al., *Efficacy of 5-week doxycycline treatment on adult Onchocerca volvulus.* Parasitol Res, 2009. **104**(2): p. 437-47.

36. Taylor, M.J., et al., *Macrofilaricidal activity after doxycycline treatment of Wuchereria bancrofti: a double-blind, randomised placebo-controlled trial.* Lancet, 2005. **365**(9477): p. 2116-21.

37. Debrah, A.Y., et al., *Macrofilaricidal effect of 4 weeks of treatment with doxycycline on Wuchereria bancrofti.* Trop Med Int Health, 2007. **12**(12): p. 1433-41.

38. Debec, A., T.L. Megraw, and A. Guichet, *Methods to Establish Drosophila Cell Lines.* Methods Mol Biol, 2016. **1478**: p. 333-351.

39. Kose, H. and T.L. Karr, *Organization of Wolbachia pipientis in the Drosophila fertilized egg and embryo revealed by an anti-Wolbachia monoclonal antibody.* Mech Dev, 1995. **51**(2-3): p. 275-88.

40. Albertson, R., et al., *Symmetric and asymmetric mitotic segregation patterns influence Wolbachia distribution in host somatic tissue.* J Cell Sci, 2009. **122**(Pt 24): p. 4570-83.

41. Karpova, N., et al., *Jupiter, a new Drosophila protein associated with microtubules.* Cell Motil Cytoskeleton, 2006. **63**(5): p. 301-12.

42. Dyson, E.A., M.K. Kamath, and G.D. Hurst, *Wolbachia infection associated with all-female broods in Hypolimnas bolina (Lepidoptera: Nymphalidae): evidence for horizontal transmission of a butterfly male killer.* Heredity (Edinb), 2002. **88**(3): p. 166-71.

43. Morrow, J.L., et al., *Tropical tephritid fruit fly community with high incidence of shared Wolbachia strains as platform for horizontal transmission of endosymbionts.* Environ Microbiol, 2014. **16**(12): p. 3622-37.

44. Haine, E.R., N.J. Pickup, and J.M. Cook, *Horizontal transmission of Wolbachia in a Drosophila community*. 2005: **Ecological Entomology**. p. 464-472.

45. Rigaud, T. and P. Juchault, *Success and failure of horizontal transfers of feminizing Wolbachia endosymbionts in woodlice*. 1995: Journal of Evolutionary Biology. p. 249-255.

46. Hughes, G.L., et al., *Invasion of Wolbachia into Anopheles and other insect germlines in an ex vivo organ culture system.* PLoS One, 2012. **7**(4): p. e36277.

47. Rasgon, J.L., C.E. Gamston, and X. Ren, *Survival of Wolbachia pipientis in cell-free medium.* Appl Environ Microbiol, 2006. **72**(11): p. 6934-7.

48. Frydman, H.M., et al., *Somatic stem cell niche tropism in Wolbachia.* Nature, 2006. **441**(7092): p. 509-12.

49. Van Meer, M.M. and R. Stouthamer, *Cross-order transfer of Wolbachia from Muscidifurax uniraptor (Hymenoptera: Pteromalidae) to Drosophila simulans (Diptera: Drosophilidae).* Heredity (Edinb), 1999. **82 (Pt 2)**: p. 163-9.

50. Huigens, M.E., et al., *Natural interspecific and intraspecific horizontal transfer of parthenogenesis-inducing Wolbachia in Trichogramma wasps.* Proc Biol Sci, 2004. **271**(1538): p. 509-15.

51. Doherty, G.J. and H.T. McMahon, *Mechanisms of endocytosis.* Annu Rev Biochem, 2009. **78**: p. 857-902.

52. Francis, C.L., et al., *Ruffles induced by Salmonella and other stimuli direct macropinocytosis of bacteria.* Nature, 1993. **364**(6438): p. 639-42.

53. Clerc, P. and P.J. Sansonetti, *Entry of Shigella flexneri into HeLa cells: evidence for directed phagocytosis involving actin polymerization and myosin accumulation.* Infect Immun, 1987. **55**(11): p. 2681-8.

54. Veiga, E., et al., *Invasive and adherent bacterial pathogens co-Opt host clathrin for infection.* Cell Host Microbe, 2007. **2**(5): p. 340-51.

55. Tu, X., et al., *EspH, a new cytoskeleton-modulating effector of enterohaemorrhagic and enteropathogenic Escherichia coli.* Mol Microbiol, 2003. **47**(3): p. 595-606.

56. Zhou, D., et al., *A Salmonella inositol polyphosphatase acts in conjunction with other bacterial effectors to promote host cell actin cytoskeleton rearrangements and bacterial internalization.* Mol Microbiol, 2001. **39**(2): p. 248-59.

57. Cossart, P., J. Pizarro-Cerdá, and M. Lecuit, *Invasion of mammalian cells by Listeria monocytogenes: functional mimicry to subvert cellular functions.* Trends Cell Biol, 2003. **13**(1): p. 23-31.

58. Navarro, L., N.M. Alto, and J.E. Dixon, *Functions of the Yersinia effector proteins in inhibiting host immune responses.* Curr Opin Microbiol, 2005. **8**(1): p. 21-7.

59. Más, V. and J.A. Melero, *Entry of enveloped viruses into host cells: membrane fusion.* Subcell Biochem, 2013. **68**: p. 467-87.

60. Mohr, S.E., et al., *RNAi screening comes of age: improved techniques and complementary approaches.* Nat Rev Mol Cell Biol, 2014. **15**(9): p. 591-600.

61. Agaisse, H., et al., *Genome-wide RNAi screen for host factors required for intracellular bacterial infection.* Science, 2005. **309**(5738): p. 1248-51.

62. Derré, I., et al., *RNAi screen in Drosophila cells reveals the involvement of the Tom complex in Chlamydia infection.* PLoS Pathog, 2007. **3**(10): p. 1446-58.

63. Philips, J.A., E.J. Rubin, and N. Perrimon, *Drosophila RNAi screen reveals CD36 family member required for mycobacterial infection.* Science, 2005. **309**(5738): p. 1251-3.

64. Akimana, C., S. Al-Khodor, and Y. Abu Kwaik, *Host factors required for modulation of phagosome biogenesis and proliferation of Francisella tularensis within the cytosol.* PLoS One, 2010. **5**(6): p. e11025.

65. Fernando, S.D., C. Rodrigo, and S. Rajapakse, *Current evidence on the use of antifilarial agents in the management of bancroftian filariasis.* J Trop Med, 2011. **2011**: p. 175941.

66. McGarry, H.F., L.D. Plant, and M.J. Taylor, *Diethylcarbamazine activity against Brugia malayi microfilariae is dependent on inducible nitric-oxide synthase and the cyclooxygenase pathway.* Filaria J, 2005. **4**: p. 4.

67. Omura, S. and A. Crump, *The life and times of ivermectin - a success story.* Nat Rev Microbiol, 2004. **2**(12): p. 984-9.

68. Moreno, Y., et al., *Ivermectin disrupts the function of the excretory-secretory apparatus in microfilariae of Brugia malayi.* Proc Natl Acad Sci U S A, 2010. **107**(46): p. 20120-5.

69. Horton, J., *The development of albendazole for lymphatic filariasis.* Ann Trop Med Parasitol, 2009. **103 Suppl 1**: p. S33-40.

70. Marriner, S.E., et al., *Pharmacokinetics of albendazole in man.* Eur J Clin Pharmacol, 1986. **30**(6): p. 705-8.

71. Mirfazaelian, A., S. Dadashzadeh, and M.R. Rouini, *Effect of gender in the disposition of albendazole metabolites in humans.* Eur J Clin Pharmacol, 2002. **58**(6): p. 403-8.

72. Gottschall, D.W., V.J. Theodorides, and R. Wang, *The metabolism of benzimidazole anthelmintics.* Parasitol Today, 1990. **6**(4): p. 115-24.

73. Gaur, R.L., et al., *Anti-filarial activity of novel formulations of albendazole against experimental brugian filariasis.* Parasitology, 2007. **134**(Pt 4): p. 537-44.

74. Bockarie, M.J., et al., *Efficacy of single-dose diethylcarbamazine compared with diethylcarbamazine combined with albendazole against Wuchereria bancrofti infection in Papua New Guinea.* Am J Trop Med Hyg, 2007. **76**(1): p. 62-6.

75. El Setouhy, M., et al., *A randomized clinical trial comparing single- and multi-dose combination therapy with diethylcarbamazine and albendazole for treatment of bancroftian filariasis.* Am J Trop Med Hyg, 2004. **70**(2): p. 191-6.

76. Hussein, O., et al., *Duplex Doppler sonographic assessment of the effects of diethylcarbamazine and albendazole therapy on adult filarial worms and adjacent host tissues in Bancroftian filariasis.* Am J Trop Med Hyg, 2004. **71**(4): p. 471-7.

77. Ismail, M.M., et al., *Efficacy of single dose combinations of albendazole, ivermectin and diethylcarbamazine for the treatment of bancroftian filariasis.* Trans R Soc Trop Med Hyg, 1998. **92**(1): p. 94-7.

78. Ismail, M.M., et al., *Long-term efficacy of single-dose combinations of albendazole, ivermectin and diethylcarbamazine for the treatment of bancroftian filariasis.* Trans R Soc Trop Med Hyg, 2001. **95**(3): p. 332-5.

79. Boussinesq, M., et al., *Clinical picture, epidemiology and outcome of Loa-associated serious adverse events related to mass ivermectin treatment of onchocerciasis in Cameroon.* Filaria J, 2003. **2 Suppl 1**: p. S4.

80. Turner, J.D., et al., *Macrofilaricidal activity after doxycycline only treatment of Onchocerca volvulus in an area of Loa loa co-endemicity: a randomized controlled trial.* PLoS Negl Trop Dis, 2010. **4**(4): p. e660.

81. Turner, J.D., et al., *A randomized, double-blind clinical trial of a 3-week course of doxycycline plus albendazole and ivermectin for the treatment of Wuchereria bancrofti infection.* Clin Infect Dis, 2006. **42**(8): p. 1081-9.

82. Szollosi, A. and A. Debec, *Presence of Rickettsias in Haploid Drosophila melanogaster Cell Lines*. 1980: Extrait Biologie Cellulaire. p. 129-134.

83. Ferree, P.M., et al., *Wolbachia utilizes host microtubules and Dynein for anterior localization in the Drosophila oocyte.* PLoS Pathog, 2005. **1**(2): p. e14.

84. Serbus, L.R. and W. Sullivan, *A cellular basis for Wolbachia recruitment to the host germline.* PLoS Pathog, 2007. **3**(12): p. e190.

85. Mayer, T.U., et al., *Small molecule inhibitor of mitotic spindle bipolarity identified in a phenotype-based screen.* Science, 1999. **286**(5441): p. 971-4.

86. Perrimon, N., et al., *Drug-target identification in Drosophila cells: combining high-throughout RNAi and small-molecule screens.* Drug Discov Today, 2007. **12**(1-2): p. 28-33.

87. Jaiswal, R., et al., *Totarol inhibits bacterial cytokinesis by perturbing the assembly dynamics of FtsZ.* Biochemistry, 2007. **46**(14): p. 4211-20.

88. Kapitzky, L., et al., *Cross-species chemogenomic profiling reveals evolutionarily conserved drug mode of action.* Mol Syst Biol, 2010. **6**: p. 451.

89. Tischer, M., et al., *Quaternary ammonium salts and their antimicrobial potential: targets or nonspecific interactions?* ChemMedChem, 2012. **7**(1): p. 22-31.

90. Muggia, F.M. and M.D. Green, *New anthracycline antitumor antibiotics.* Crit Rev Oncol Hematol, 1991. **11**(1): p. 43-64.

91. Skladanowski, A. and J. Konopa, *Interstrand DNA crosslinking induced by anthracyclines in tumour cells.* Biochem Pharmacol, 1994. **47**(12): p. 2269-78.

92. Pommier, Y., et al., *DNA topoisomerases and their poisoning by anticancer and antibacterial drugs.* Chem Biol, 2010. **17**(5): p. 421-33.

93. Tomasz, M. and Y. Palom, *The mitomycin bioreductive antitumor agents: cross-linking and alkylation of DNA as the molecular basis of their activity.* Pharmacol Ther, 1997. **76**(1-3): p. 73-87.

94. Bell, A.J., S.M. McBride, and T.C. Dockendorff, *Flies as the ointment: Drosophila modeling to enhance drug discovery.* Fly (Austin), 2009. **3**(1): p. 39-49.

95. Serbus, L.R., et al., *A feedback loop between Wolbachia and the Drosophila gurken mRNP complex influences Wolbachia titer.* J Cell Sci, 2011. **124**(Pt 24): p. 4299-308.

96. King, R., *Ovarian development in Drosophila melanogaster*. 1970: New York: Academic Press.

97. Kimble, J. and S.L. Crittenden, *Germline proliferation and its control.* WormBook, 2005: p. 1-14.

98. Lacey, E., *The role of the cytoskeletal protein, tubulin, in the mode of action and mechanism of drug resistance to benzimidazoles.* Int J Parasitol, 1988. **18**(7): p. 885-936.

99. Borgers, M. and S. De Nollin, *Ultrastructural changes in Ascaris suum intestine after mebendazole treatment in vivo.* J Parasitol, 1975. **61**(1): p. 110-22.

100. Lubega, G.W. and R.K. Prichard, *Interaction of benzimidazole anthelmintics with Haemonchus contortus tubulin: binding affinity and anthelmintic efficacy.* Exp Parasitol, 1991. **73**(2): p. 203-13.

101. Schaffner-Barbero, C., et al., *Targeting the assembly of bacterial cell division protein FtsZ with small molecules.* ACS Chem Biol, 2012. **7**(2): p. 269-77.

102. Robinson, M.W., et al., *A possible model of benzimidazole binding to beta-tubulin disclosed by invoking an inter-domain movement.* J Mol Graph Model, 2004. **23**(3): p. 275-84.

103. Veneti, Z., et al., *Heads or tails: host-parasite interactions in the Drosophila-Wolbachia system.* Appl Environ Microbiol, 2004. **70**(9): p. 5366-72.

104. Serbus, L.R., et al., *Dynein and the actin cytoskeleton control kinesin-driven cytoplasmic streaming in Drosophila oocytes.* Development, 2005. **132**(16): p. 3743-52.

105. Theurkauf, W.E., et al., *Reorganization of the cytoskeleton during Drosophila oogenesis: implications for axis specification and intercellular transport.* Development, 1992. **115**(4): p. 923-36.

106. Landmann, F., et al., *Both asymmetric mitotic segregation and cell-to-cell invasion are required for stable germline transmission of Wolbachia in filarial nematodes.* Biol Open, 2012. **1**(6): p. 536-47.

107. Fenollar, F., et al., *Culture and phenotypic characterization of a Wolbachia pipientis isolate.* J Clin Microbiol, 2003. **41**(12): p. 5434-41.

108. Dobson, S.L., et al., *Characterization of Wolbachia host cell range via the in vitro establishment of infections.* Appl Environ Microbiol, 2002. **68**(2): p. 656-60.

109. Frentiu, F.D., et al., *Wolbachia-mediated resistance to dengue virus infection and death at the cellular level.* PLoS One, 2010. **5**(10): p. e13398.

110. Voronin, D.A., et al., *[Influence of Drosophila melanogaster genotype on biological effects of endocymbiont Wolbachia (stamm wMelPop)].* Tsitologiia, 2009. **51**(4): p. 335-45.

111. Venard, C.M., P.R. Crain, and S.L. Dobson, *SYTO11 staining vs FISH staining: a comparison of two methods to stain Wolbachia pipientis in cell cultures.* Lett Appl Microbiol, 2011. **52**(2): p. 168-76.

112. O'Neill, S.L., et al., *In vitro cultivation of Wolbachia pipientis in an Aedes albopictus cell line.* Insect Mol Biol, 1997. **6**(1): p. 33-9.

113. Casper-Lindley, C., et al., *Rapid fluorescence-based screening for Wolbachia endosymbionts in Drosophila germ line and somatic tissues.* Appl Environ Microbiol, 2011. **77**(14): p. 4788-94.

114. Li, Z., et al., *Targeting the Wolbachia cell division protein FtsZ as a new approach for antifilarial therapy.* PLoS Negl Trop Dis, 2011. **5**(11): p. e1411.

115. Katz, M., *Anthelmintics.* Drugs, 1977. **13**(2): p. 124-36.

116. Cline, B.L., *Current drug regimens for the treatment of intestinal helminth infections.* Med Clin North Am, 1982. **66**(3): p. 721-42.

117. Bordenstein, S.R., D.H. Fitch, and J.H. Werren, *Absence of wolbachia in nonfilariid nematodes.* J Nematol, 2003. **35**(3): p. 266-70.

118. Lin, M., et al., *Analysis of complete genome sequence of Neorickettsia risticii: causative agent of Potomac horse fever.* Nucleic Acids Res, 2009. **37**(18): p. 6076-91.

119. WHO, *Lymphatic Filariasis, Fact Sheet No. 102*. 2000: World Health Organization.

120. Barrowman, M.M., S.E. Marriner, and J.A. Bogan, *The binding and subsequent inhibition of tubulin polymerization in Ascaris suum (in vitro) by benzimidazole anthelmintics.* Biochem Pharmacol, 1984. **33**(19): p. 3037-40.

121. Ridoux, O. and M. Drancourt, *In vitro susceptibilities of the microsporidia Encephalitozoon cuniculi, Encephalitozoon hellem, and Encephalitozoon intestinalis to albendazole and its sulfoxide and sulfone metabolites.* Antimicrob Agents Chemother, 1998. **42**(12): p. 3301-3.

122. Ramsden, A.E., D.W. Holden, and L.J. Mota, *Membrane dynamics and spatial distribution of Salmonella-containing vacuoles.* Trends Microbiol, 2007. **15**(11): p. 516-24.

123. Steele-Mortimer, O., *The Salmonella-containing vacuole: moving with the times.* Curr Opin Microbiol, 2008. **11**(1): p. 38-45.

124. Rajashekar, R. and M. Hensel, *Dynamic modification of microtubule-dependent transport by effector proteins of intracellular Salmonella enterica.* Eur J Cell Biol, 2011. **90**(11): p. 897-902.

125. Hackstadt, T., et al., *Chlamydia trachomatis interrupts an exocytic pathway to acquire endogenously synthesized sphingomyelin in transit from the Golgi apparatus to the plasma membrane.* EMBO J, 1996. **15**(5): p. 964-77.

126. Clausen, J.D., et al., *Chlamydia trachomatis utilizes the host cell microtubule network during early events of infection.* Mol Microbiol, 1997. **25**(3): p. 441-9.

127. Hackstadt, T., et al., *The Chlamydia trachomatis IncA protein is required for homotypic vesicle fusion.* Cell Microbiol, 1999. **1**(2): p. 119-30.

128. Grieshaber, S.S., N.A. Grieshaber, and T. Hackstadt, *Chlamydia trachomatis uses host cell dynein to traffic to the microtubule-organizing center in a p50 dynamitin-independent process.* J Cell Sci, 2003. **116**(Pt 18): p. 3793-802.

129. Capmany, A. and M.T. Damiani, *Chlamydia trachomatis intercepts Golgi-derived sphingolipids through a Rab14-mediated transport required for bacterial development and replication.* PLoS One, 2010. **5**(11): p. e14084.

130. Erickson, H.P., *FtsZ, a tubulin homologue in prokaryote cell division.* Trends Cell Biol, 1997. **7**(9): p. 362-7.

131. Margolin, W., *FtsZ and the division of prokaryotic cells and organelles.* Nat Rev Mol Cell Biol, 2005. **6**(11): p. 862-71.

132. Slayden, R.A., D.L. Knudson, and J.T. Belisle, *Identification of cell cycle regulators in Mycobacterium tuberculosis by inhibition of septum formation and global transcriptional analysis.* Microbiology, 2006. **152**(Pt 6): p. 1789-97.

133. White, E.L., et al., *2-Alkoxycarbonylaminopyridines: inhibitors of Mycobacterium tuberculosis FtsZ.* J Antimicrob Chemother, 2002. **50**(1): p. 111-4.

134. Reynolds, R.C., et al., *A new 2-carbamoyl pteridine that inhibits mycobacterial FtsZ.* Bioorg Med Chem Lett, 2004. **14**(12): p. 3161-4.

135. Margalit, D.N., et al., *Targeting cell division: small-molecule inhibitors of FtsZ GTPase perturb cytokinetic ring assembly and induce bacterial lethality.* Proc Natl Acad Sci U S A, 2004. **101**(32): p. 11821-6.

136. Sarcina, M. and C.W. Mullineaux, *Effects of tubulin assembly inhibitors on cell division in prokaryotes in vivo.* FEMS Microbiol Lett, 2000. **191**(1): p. 25-9.

137. Haydon, D.J., et al., *An inhibitor of FtsZ with potent and selective anti-staphylococcal activity.* Science, 2008. **321**(5896): p. 1673-5.

138. Nova, E., et al., *4',6-Diamidino-2-phenylindole (DAPI) induces bundling of Escherichia coli FtsZ polymers inhibiting the GTPase activity.* Arch Biochem Biophys, 2007. **465**(2): p. 315-9.

139. Adams, D.W., et al., *Multiple effects of benzamide antibiotics on FtsZ function.* Mol Microbiol, 2011. **80**(1): p. 68-84.

140. Andreu, J.M., et al., *The antibacterial cell division inhibitor PC190723 is an FtsZ polymer-stabilizing agent that induces filament assembly and condensation.* J Biol Chem, 2010. **285**(19): p. 14239-46.

141. Kumar, K., et al., *Novel trisubstituted benzimidazoles, targeting Mtb FtsZ, as a new class of antitubercular agents.* J Med Chem, 2011. **54**(1): p. 374-81.

142. Czaplewski, L.G., et al., *Antibacterial alkoxybenzamide inhibitors of the essential bacterial cell division protein FtsZ.* Bioorg Med Chem Lett, 2009. **19**(2): p. 524-7.

143. Susanto, C., *Design and Synthesis of Novel Benzimidazole Library for the Discovery and Development of the Next Generation Antibacterial Agents*. 2010: Stony Brook: Stony Brook University.

144. Bi, E. and J. Lutkenhaus, *Cell division inhibitors SulA and MinCD prevent formation of the FtsZ ring.* J Bacteriol, 1993. **175**(4): p. 1118-25.

145. Cordell, S.C., E.J. Robinson, and J. Lowe, *Crystal structure of the SOS cell division inhibitor SulA and in complex with FtsZ.* Proc Natl Acad Sci U S A, 2003. **100**(13): p. 7889-94.

146. Pietri, J.E., H. DeBruhl, and W. Sullivan, *The rich somatic life of Wolbachia.* Microbiologyopen, 2016. **5**(6): p. 923-936.

147. Cho, K.O., G.W. Kim, and O.K. Lee, *Wolbachia bacteria reside in host Golgi-related vesicles whose position is regulated by polarity proteins.* PLoS One, 2011. **6**(7): p. e22703.

148. Fischer, K., et al., *High pressure freezing/freeze substitution fixation improves the ultrastructural assessment of Wolbachia endosymbiont-filarial nematode host interaction.* PLoS One, 2014. **9**(1): p. e86383.

149. Pietilä, T.E., et al., *Inhibition of dynamin-dependent endocytosis interferes with type III IFN expression in bacteria-infected human monocyte-derived DCs.* J Leukoc Biol, 2010. **88**(4): p. 665-74.

150. Ivanov, A.I., *Pharmacological inhibitors of exocytosis and endocytosis: novel bullets for old targets.* Methods Mol Biol, 2014. **1174**: p. 3-18.

151. Rejman, J., A. Bragonzi, and M. Conese, *Role of clathrin- and caveolae-mediated endocytosis in gene transfer mediated by lipo- and polyplexes.* Mol Ther, 2005. **12**(3): p. 468-74.

152. Stuart, L.M. and R.A. Ezekowitz, *Phagocytosis and comparative innate immunity: learning on the fly.* Nat Rev Immunol, 2008. **8**(2): p. 131-41.

153. Rocha, J.J., et al., *A phagocytic route for uptake of double-stranded RNA in RNAi.* PLoS One, 2011. **6**(4): p. e19087.

154. Jha, A., S.C. Watkins, and L.M. Traub, *The apoptotic engulfment protein Ced-6 participates in clathrin-mediated yolk uptake in Drosophila egg chambers.* Mol Biol Cell, 2012. **23**(9): p. 1742-64.

155. Byrne, G.I. and J.W. Moulder, *Parasite-specified phagocytosis of Chlamydia psittaci and Chlamydia trachomatis by L and HeLa cells.* Infect Immun, 1978. **19**(2): p. 598-606.

156. Wyrick, P.B., et al., *Entry of genital Chlamydia trachomatis into polarized human epithelial cells.* Infect Immun, 1989. **57**(8): p. 2378-89.

157. Rengarajan, M., A. Hayer, and J.A. Theriot, *Endothelial Cells Use a Formin-Dependent Phagocytosis-Like Process to Internalize the Bacterium Listeria monocytogenes.* PLoS Pathog, 2016. **12**(5): p. e1005603.

158. Veiga, E. and P. Cossart, *Listeria hijacks the clathrin-dependent endocytic machinery to invade mammalian cells.* Nat Cell Biol, 2005. **7**(9): p. 894-900.

159. Harvey, H.A., et al., *Receptor-mediated endocytosis of Neisseria gonorrhoeae into primary human urethral epithelial cells: the role of the asialoglycoprotein receptor.* Mol Microbiol, 2001. **42**(3): p. 659-72.

160. Shen, Y., et al., *InlB-dependent internalization of Listeria is mediated by the Met receptor tyrosine kinase.* Cell, 2000. **103**(3): p. 501-10.

161. Galán, J.E., J. Pace, and M.J. Hayman, *Involvement of the epidermal growth factor receptor in the invasion of cultured mammalian cells by Salmonella typhimurium.* Nature, 1992. **357**(6379): p. 588-9.

162. Zhu, W., et al., *EGFR and HER2 receptor kinase signaling mediate epithelial cell invasion by Candida albicans during oropharyngeal infection.* Proc Natl Acad Sci U S A, 2012. **109**(35): p. 14194-9.

163. Moreno-Ruiz, E., et al., *Candida albicans internalization by host cells is mediated by a clathrin-dependent mechanism.* Cell Microbiol, 2009. **11**(8): p. 1179-89.

164. Mooren, O.L., B.J. Galletta, and J.A. Cooper, *Roles for actin assembly in endocytosis.* Annu Rev Biochem, 2012. **81**: p. 661-86.

165. Newton, I.L., O. Savytskyy, and K.B. Sheehan, *Wolbachia utilize host actin for efficient maternal transmission in Drosophila melanogaster.* PLoS Pathog, 2015. **11**(4): p. e1004798.

166. Sheehan, K.B., et al., *Identification and Characterization of a Candidate Wolbachia pipientis Type IV Effector That Interacts with the Actin Cytoskeleton.* MBio, 2016. **7**(4).

167. Toomey, M.E., et al., *Evolutionarily conserved Wolbachia-encoded factors control pattern of stem-cell niche tropism in Drosophila ovaries and favor infection.* Proc Natl Acad Sci U S A, 2013. **110**(26): p. 10788-93.

168. Unckless, R.L., et al., *Wolbachia as populations within individual insects: causes and consequences of density variation in natural populations.* Proc Biol Sci, 2009. **276**(1668): p. 2805-11.

169. Müller, M.J., et al., *Reevaluating the infection status by the Wolbachia endosymbiont in Drosophila Neotropical species from the willistoni subgroup.* Infect Genet Evol, 2013. **19**: p. 232-9.

170. Poinsot, D., et al., *Wolbachia transfer from Drosophila melanogaster into D. simulans: Host effect and cytoplasmic incompatibility relationships.* Genetics, 1998. **150**(1): p. 227-37.

171. Min, K.T. and S. Benzer, *Wolbachia, normally a symbiont of Drosophila, can be virulent, causing degeneration and early death.* Proc Natl Acad Sci U S A, 1997. **94**(20): p. 10792-6.

172. Mouton, L., et al., *Effect of temperature on Wolbachia density and impact on cytoplasmic incompatibility.* Parasitology, 2006. **132**(Pt 1): p. 49-56.

173. Van Voorhis, W.C., et al., *Open Source Drug Discovery with the Malaria Box Compound Collection for Neglected Diseases and Beyond.* PLoS Pathog, 2016. **12**(7): p. e1005763.

174. Moser, T.S., L.R. Sabin, and S. Cherry, *RNAi screening for host factors involved in Vaccinia virus infection using Drosophila cells.* J Vis Exp, 2010(42).

175. Goshima, G., et al., *Genes required for mitotic spindle assembly in Drosophila S2 cells.* Science, 2007. **316**(5823): p. 417-21.

176. Zhou, Y. and Y. Zhu, *Diversity of bacterial manipulation of the host ubiquitin pathways.* Cell Microbiol, 2015. **17**(1): p. 26-34.

177. Wu, M., et al., *Phylogenomics of the reproductive parasite Wolbachia pipientis wMel: a streamlined genome overrun by mobile genetic elements.* PLoS Biol, 2004. **2**(3): p. E69.

178. Fujimuro, M., H. Sawada, and H. Yokosawa, *Production and characterization of monoclonal antibodies specific to multi-ubiquitin chains of polyubiquitinated proteins.* FEBS Lett, 1994. **349**(2): p. 173-80.

179. Everett, R.D., *ICP0 induces the accumulation of colocalizing conjugated ubiquitin.* J Virol, 2000. **74**(21): p. 9994-10005.

180. Yang, H., et al., *Natural compounds with proteasome inhibitory activity for cancer prevention and treatment.* Curr Protein Pept Sci, 2008. **9**(3): p. 227-39.

181. Hudson, A.M. and L. Cooley, *Methods for studying oogenesis.* Methods, 2014. **68**(1): p. 207-17.

182. Lemus, L. and V. Goder, *Regulation of Endoplasmic Reticulum-Associated Protein Degradation (ERAD) by Ubiquitin.* Cells, 2014. **3**(3): p. 824-47.

183. Metzger, M.B., et al., *Degradation of a cytosolic protein requires endoplasmic reticulum-associated degradation machinery.* J Biol Chem, 2008. **283**(47): p. 32302-16.

184. Ashton-Beaucage, D., et al., *The Deubiquitinase USP47 Stabilizes MAPK by Counteracting the Function of the N-end Rule ligase POE/UBR4 in Drosophila.* PLoS Biol, 2016. **14**(8): p. e1002539.

185. Voronin, D.A., N.V. Dudkina, and E.V. Kiseleva, *A new form of symbiotic bacteria Wolbachia found in the endoplasmic reticulum of early embryos of Drosophila melanogaster.* Dokl Biol Sci, 2004. **396**: p. 227-9.

186. Chagas-Moutinho, V.A., et al., *Identification and ultrastructural characterization of the Wolbachia symbiont in Litomosoides chagasfilhoi.* Parasit Vectors, 2015. **8**: p. 74.

187. Brownlie, J.C. and S.L. O'Neill, *Wolbachia genomes: insights into an intracellular lifestyle.* Curr Biol, 2005. **15**(13): p. R507-9.

188. Baldridge, G.D., et al., *Proteomic profiling of a robust Wolbachia infection in an Aedes albopictus mosquito cell line.* Mol Microbiol, 2014. **94**(3): p. 537-56.

189. Caragata, E.P., et al., *Competition for amino acids between Wolbachia and the mosquito host, Aedes aegypti.* Microb Ecol, 2014. **67**(1): p. 205-18.

190. Fallon, A.M. and B.A. Witthuhn, *Proteasome activity in a naïve mosquito cell line infected with Wolbachia pipientis wAlbB.* In Vitro Cell Dev Biol Anim, 2009. **45**(8): p. 460-6.

191. Strunov, A. and E. Kiseleva, *Drosophila melanogaster brain invasion: pathogenic Wolbachia in central nervous system of the fly.* Insect Sci, 2016. **23**(2): p. 253-64.

192. Vaishnava, S. and B. Striepen, *The cell biology of secondary endosymbiosis--how parasites build, divide and segregate the apicoplast.* Mol Microbiol, 2006. **61**(6): p. 1380-7.

193. Agrawal, S., et al., *An apicoplast localized ubiquitylation system is required for the import of nuclear-encoded plastid proteins.* PLoS Pathog, 2013. **9**(6): p. e1003426.

194. Perlman, S.J., et al., *Maternal transmission, sex ratio distortion, and mitochondria.* Proc Natl Acad Sci U S A, 2015. **112**(33): p. 10162-8.

195. Molloy, J.C., et al., *Wolbachia Modulates Lipid Metabolism in Aedes albopictus Mosquito Cells.* Appl Environ Microbiol, 2016. **82**(10): p. 3109-20.

196. Herren, J.K., et al., *Insect endosymbiont proliferation is limited by lipid availability.* Elife, 2014. **3**: p. e02964.

197. Ehrt, S. and D. Schnappinger, *Mycobacterium tuberculosis virulence: lipids inside and out.* Nat Med, 2007. **13**(3): p. 284-5.

198. Robertson, D.K., et al., *Inclusion biogenesis and reactivation of persistent Chlamydia trachomatis requires host cell sphingolipid biosynthesis.* PLoS Pathog, 2009. **5**(11): p. e1000664.

199. Johnson, K.N., *The Impact of Wolbachia on Virus Infection in Mosquitoes.* Viruses, 2015. **7**(11): p. 5705-17.

200. Le Clec'h, W., et al., *High virulence of Wolbachia after host switching: when autophagy hurts.* PLoS Pathog, 2012. **8**(8): p. e1002844.

201. Pan, X., et al., *Wolbachia induces reactive oxygen species (ROS)-dependent activation of the Toll pathway to control dengue virus in the mosquito Aedes aegypti.* Proc Natl Acad Sci U S A, 2012. **109**(1): p. E23-31.

202. Caragata, E.P., et al., *Dietary cholesterol modulates pathogen blocking by Wolbachia.* PLoS Pathog, 2013. **9**(6): p. e1003459.

203. Wong, Z.S., J.C. Brownlie, and K.N. Johnson, *Oxidative stress correlates with Wolbachia-mediated antiviral protection in Wolbachia-Drosophila associations.* Appl Environ Microbiol, 2015. **81**(9): p. 3001-5.

204. Romero-Brey, I. and R. Bartenschlager, *Endoplasmic Reticulum: The Favorite Intracellular Niche for Viral Replication and Assembly.* Viruses, 2016. **8**(6).

205. Noack, J., R. Bernasconi, and M. Molinari, *How viruses hijack the ERAD tuning machinery.* J Virol, 2014. **88**(18): p. 10272-5.

206. Marceau, C.D., et al., *Genetic dissection of Flaviviridae host factors through genome-scale CRISPR screens.* Nature, 2016. **535**(7610): p. 159-63.

207. den Boon, J.A., A. Diaz, and P. Ahlquist, *Cytoplasmic viral replication complexes.* Cell Host Microbe, 2010. **8**(1): p. 77-85.

208. Roy, C.R., S.P. Salcedo, and J.P. Gorvel, *Pathogen-endoplasmic-reticulum interactions: in through the out door.* Nat Rev Immunol, 2006. **6**(2): p. 136-47.

209. Davy, S.K., D. Allemand, and V.M. Weis, *Cell biology of cnidarian-dinoflagellate symbiosis.* Microbiol Mol Biol Rev, 2012. **76**(2): p. 229-61.

210. Feldhaar, H., et al., *Nutritional upgrading for omnivorous carpenter ants by the endosymbiont Blochmannia.* BMC Biol, 2007. **5**: p. 48.

211. Gibson, K.E., H. Kobayashi, and G.C. Walker, *Molecular determinants of a symbiotic chronic infection.* Annu Rev Genet, 2008. **42**: p. 413-41.

212. Hosokawa, T., et al., *Wolbachia as a bacteriocyte-associated nutritional mutualist.* Proc Natl Acad Sci U S A, 2010. **107**(2): p. 769-74.

213. Johnson, M.D., *The acquisition of phototrophy: adaptive strategies of hosting endosymbionts and organelles.* Photosynth Res, 2011. **107**(1): p. 117-32.

214. Nakabachi, A. and H. Ishikawa, *Provision of riboflavin to the host aphid, Acyrthosiphon pisum, by endosymbiotic bacteria, Buchnera.* J Insect Physiol, 1999. **45**(1): p. 1-6.

215. Oldroyd, G.E., *Speak, friend, and enter: signalling systems that promote beneficial symbiotic associations in plants.* Nat Rev Microbiol, 2013. **11**(4): p. 252-63.

216. Parniske, M., *Arbuscular mycorrhiza: the mother of plant root endosymbioses.* Nat Rev Microbiol, 2008. **6**(10): p. 763-75.

217. PUCHTA, O., *[Experimental studies on the significance of symbiosis in the clothes louse Pediculus vestimenti Burm].* Z Parasitenkd, 1955. **17**(1): p. 1-40.

218. Sabree, Z.L., S. Kambhampati, and N.A. Moran, *Nitrogen recycling and nutritional provisioning by Blattabacterium, the cockroach endosymbiont.* Proc Natl Acad Sci U S A, 2009. **106**(46): p. 19521-6.

219. Sabree, Z.L., et al., *The nutrient supplying capabilities of Uzinura, an endosymbiont of armoured scale insects.* Environ Microbiol, 2013. **15**(7): p. 1988-99.

220. Shigenobu, S., et al., *Genome sequence of the endocellular bacterial symbiont of aphids Buchnera sp. APS.* Nature, 2000. **407**(6800): p. 81-6.

221. Snyder, A.K., et al., *Nutrient provisioning facilitates homeostasis between tsetse fly (Diptera: Glossinidae) symbionts.* Proc Biol Sci, 2010. **277**(1692): p. 2389-97.

222. Snyder, A.K., C. McLain, and R.V. Rio, *The tsetse fly obligate mutualist Wigglesworthia morsitans alters gene expression and population density via exogenous nutrient provisioning.* Appl Environ Microbiol, 2012. **78**(21): p. 7792-7.

223. Nogge, G., *Significance of Symbionts for the Maintenance of an Optimal Nutritional State for Successful Reproduction in Hematophagous Arthropods*. 1981, Parasitology. p. 101-104.

224. Stambler, N., *Zooxanthellae: The yellow symbionts inside animals*. 2011, Coral reefs: an ecosystem in transition. p. 87-106.

225. Zug, R. and P. Hammerstein, *Still a host of hosts for Wolbachia: analysis of recent data suggests that 40% of terrestrial arthropod species are infected.* PLoS One, 2012. **7**(6): p. e38544.

226. Ashburner, M., *Drosophila, a Laboratory Handbook*. 1989, New York: Cold Spring Harbor Laboratory Press. p. 1331.

227. Snook, R.R., et al., *Offsetting effects of Wolbachia infection and heat shock on sperm production in Drosophila simulans: analyses of fecundity, fertility and accessory gland proteins.* Genetics, 2000. **155**(1): p. 167-78.

228. Bressac, C. and F. Rousset, *The reproductive incompatibility system in Drosophila simulans: DAPI-staining analysis of the Wolbachia symbionts in sperm cysts.* J Invertebr Pathol, 1993. **61**(3): p. 226-30.

229. Clark, M.E., et al., *The distribution and proliferation of the intracellular bacteria Wolbachia during spermatogenesis in Drosophila.* Mech Dev, 2002. **111**(1-2): p. 3-15.

230. Turelli, M. and A.A. Hoffmann, *Cytoplasmic incompatibility in Drosophila simulans: dynamics and parameter estimates from natural populations.* Genetics, 1995. **140**(4): p. 1319-38.

231. Hoffmann, A.A., M. Hercus, and H. Dagher, *Population dynamics of the Wolbachia infection causing cytoplasmic incompatibility in Drosophila melanogaster.* Genetics, 1998. **148**(1): p. 221-31.

232. Kugler, J.M. and P. Lasko, *Localization, anchoring and translational control of oskar, gurken, bicoid and nanos mRNA during Drosophila oogenesis.* Fly (Austin), 2009. **3**(1): p. 15-28.

233. Ashburner, M., *Developmental Biology. Drosophila, a Laboratory Handbook*. 1989, Cold Spring Harbor: Cold Spring Harbor Laboratory Press. p. 139-204.

234. Spradling, A.C., *Developmental Genetic of Oogenesis*. 1993, New York: Cold Spring Harbor Laboratory Press. p. 1-70.

235. Fast, E.M., et al., *Wolbachia enhance Drosophila stem cell proliferation and target the germline stem cell niche.* Science, 2011. **334**(6058): p. 990-2.

236. Hadfield, S.J. and J.M. Axton, *Germ cells colonized by endosymbiotic bacteria.* Nature, 1999. **402**(6761): p. 482.

237. Coluccio, A.E., et al., *The yeast spore wall enables spores to survive passage through the digestive tract of Drosophila.* PLoS One, 2008. **3**(8): p. e2873.

238. Anagnostou, C., M. Dorsch, and M. Rohlfs, *Influence of dietary yeasts on Drosophila melanogaster life-history traits*. 2010, Entomologia Experimentalis et Applicata. p. 1-11.

239. Begon, M., *Yeasts and Drosophila. The Genetics and Biology of Drosophila*. 1982, San Francisco: Academic Press. p. 345-384.

240. Shorrocks, B., *The Breeding Sites of Temperate Woodland Drosophila. The Genetics and Biology of Drosophila*. 1982, San Francisco: Academic Press. p. 385-428.

241. Brncic, D., *Ecology of Flower-Breeding Drosophila. The Genetics and Biology of Drosophila*. 1983, San Francisco: Academic Press. p. 333-382.

242. Kukor, J.J. and M.M. Martin, *Nutritional Ecology of Fungus-feeding Arthropods. Nutritional Ecology of Insects, Mites, Spiders, and Related Invertebrates*. 1987, New York: John Wiley and Sons. p. 791-836.

243. Teleman, A.A., *Molecular mechanisms of metabolic regulation by insulin in Drosophila.* Biochem J, 2009. **425**(1): p. 13-26.

244. Bradley, G.L. and S.J. Leevers, *Amino acids and the humoral regulation of growth: fat bodies use slimfast.* Cell, 2003. **114**(6): p. 656-8.

245. Colombani, J., et al., *A nutrient sensor mechanism controls Drosophila growth.* Cell, 2003. **114**(6): p. 739-49.

246. Chen, J., et al., *Identification of an 11-kDa FKBP12-rapamycin-binding domain within the 289-kDa FKBP12-rapamycin-associated protein and characterization of a critical serine residue.* Proc Natl Acad Sci U S A, 1995. **92**(11): p. 4947-51.

247. Choi, J., et al., *Structure of the FKBP12-rapamycin complex interacting with the binding domain of human FRAP.* Science, 1996. **273**(5272): p. 239-42.

248. Guertin, D.A. and D.M. Sabatini, *The pharmacology of mTOR inhibition.* Sci Signal, 2009. **2**(67): p. pe24.

249. Yip, C.K., et al., *Structure of the human mTOR complex I and its implications for rapamycin inhibition.* Mol Cell, 2010. **38**(5): p. 768-74.

250. González, I.M., et al., *Leucine and arginine regulate trophoblast motility through mTOR-dependent and independent pathways in the preimplantation mouse embryo.* Dev Biol, 2012. **361**(2): p. 286-300.

251. Wang, Y., et al., *Dietary L-arginine supplementation improves the intestinal development through increasing mucosal Akt and mammalian target of rapamycin signals in intra-uterine growth retarded piglets.* Br J Nutr, 2012. **108**(8): p. 1371-81.

252. Yao, K., et al., *Dietary arginine supplementation increases mTOR signaling activity in skeletal muscle of neonatal pigs.* J Nutr, 2008. **138**(5): p. 867-72.

253. Xi, P., et al., *Regulation of protein turnover by L-glutamine in porcine intestinal epithelial cells.* J Nutr Biochem, 2012. **23**(8): p. 1012-7.

254. Atherton, P.J., et al., *Distinct anabolic signalling responses to amino acids in C2C12 skeletal muscle cells.* Amino Acids, 2010. **38**(5): p. 1533-9.

255. Norton, L.E., et al., *The leucine content of a complete meal directs peak activation but not duration of skeletal muscle protein synthesis and mammalian target of rapamycin signaling in rats.* J Nutr, 2009. **139**(6): p. 1103-9.

256. Dibble, C.C., et al., *TBC1D7 is a third subunit of the TSC1-TSC2 complex upstream of mTORC1.* Mol Cell, 2012. **47**(4): p. 535-46.

257. Stocker, H., et al., *Rheb is an essential regulator of S6K in controlling cell growth in Drosophila.* Nat Cell Biol, 2003. **5**(6): p. 559-65.

258. Saucedo, L.J., et al., *Rheb promotes cell growth as a component of the insulin/TOR signalling network.* Nat Cell Biol, 2003. **5**(6): p. 566-71.

259. Inoki, K., et al., *TSC2 is phosphorylated and inhibited by Akt and suppresses mTOR signalling.* Nat Cell Biol, 2002. **4**(9): p. 648-57.

260. Cai, S.L., et al., *Activity of TSC2 is inhibited by AKT-mediated phosphorylation and membrane partitioning.* J Cell Biol, 2006. **173**(2): p. 279-89.

261. Ito, N. and G.M. Rubin, *gigas, a Drosophila homolog of tuberous sclerosis gene product-2, regulates the cell cycle.* Cell, 1999. **96**(4): p. 529-39.

262. Huang, J. and B.D. Manning, *A complex interplay between Akt, TSC2 and the two mTOR complexes.* Biochem Soc Trans, 2009. **37**(Pt 1): p. 217-22.

263. Inoki, K. and K.L. Guan, *Tuberous sclerosis complex, implication from a rare genetic disease to common cancer treatment.* Hum Mol Genet, 2009. **18**(R1): p. R94-100.

264. Tapon, N., et al., *The Drosophila tuberous sclerosis complex gene homologs restrict cell growth and cell proliferation.* Cell, 2001. **105**(3): p. 345-55.

265. Gao, X. and D. Pan, *TSC1 and TSC2 tumor suppressors antagonize insulin signaling in cell growth.* Genes Dev, 2001. **15**(11): p. 1383-92.

266. Ni, J.Q., et al., *A genome-scale shRNA resource for transgenic RNAi in Drosophila.* Nat Methods, 2011. **8**(5): p. 405-7.

267. Ni, J.Q., et al., *Vector and parameters for targeted transgenic RNA interference in Drosophila melanogaster.* Nat Methods, 2008. **5**(1): p. 49-51.

268. Wodarz, A., et al., *Expression of crumbs confers apical character on plasma membrane domains of ectodermal epithelia of Drosophila.* Cell, 1995. **82**(1): p. 67-76.

269. Petrella, L.N., T. Smith-Leiker, and L. Cooley, *The Ovhts polyprotein is cleaved to produce fusome and ring canal proteins required for Drosophila oogenesis.* Development, 2007. **134**(4): p. 703-12.

270. Broughton, S.J., et al., *Longer lifespan, altered metabolism, and stress resistance in Drosophila from ablation of cells making insulin-like ligands.* Proc Natl Acad Sci U S A, 2005. **102**(8): p. 3105-10.

271. Haselton, A., et al., *Partial ablation of adult Drosophila insulin-producing neurons modulates glucose homeostasis and extends life span without insulin resistance.* Cell Cycle, 2010. **9**(15): p. 3063-71.

272. Pasco, M.Y. and P. Léopold, *High sugar-induced insulin resistance in Drosophila relies on the lipocalin Neural Lazarillo.* PLoS One, 2012. **7**(5): p. e36583.

273. Morris, S.N., et al., *Development of diet-induced insulin resistance in adult Drosophila melanogaster.* Biochim Biophys Acta, 2012. **1822**(8): p. 1230-7.

274. Yang, Q., et al., *Serum retinol binding protein 4 contributes to insulin resistance in obesity and type 2 diabetes.* Nature, 2005. **436**(7049): p. 356-62.

275. Graham, T.E., et al., *Retinol-binding protein 4 and insulin resistance in lean, obese, and diabetic subjects.* N Engl J Med, 2006. **354**(24): p. 2552-63.

276. Norseen, J., et al., *Retinol-binding protein 4 inhibits insulin signaling in adipocytes by inducing proinflammatory cytokines in macrophages through a c-Jun N-terminal kinase- and toll-like receptor 4-dependent and retinol-independent mechanism.* Mol Cell Biol, 2012. **32**(10): p. 2010-9.

277. Böhni, R., et al., *Autonomous control of cell and organ size by CHICO, a Drosophila homolog of vertebrate IRS1-4.* Cell, 1999. **97**(7): p. 865-75.

278. Ogawa, W., T. Matozaki, and M. Kasuga, *Role of binding proteins to IRS-1 in insulin signalling.* Mol Cell Biochem, 1998. **182**(1-2): p. 13-22.

279. Werz, C., et al., *The Drosophila SH2B family adaptor Lnk acts in parallel to chico in the insulin signaling pathway.* PLoS Genet, 2009. **5**(8): p. e1000596.

280. Drummond-Barbosa, D. and A.C. Spradling, *Stem cells and their progeny respond to nutritional changes during Drosophila oogenesis.* Dev Biol, 2001. **231**(1): p. 265-78.

281. Tatar, M., et al., *A mutant Drosophila insulin receptor homolog that extends life-span and impairs neuroendocrine function.* Science, 2001. **292**(5514): p. 107-10.

282. Richard, D.S., et al., *Insulin signaling is necessary for vitellogenesis in Drosophila melanogaster independent of the roles of juvenile hormone and ecdysteroids: female sterility of the chico1 insulin signaling mutation is autonomous to the ovary.* J Insect Physiol, 2005. **51**(4): p. 455-64.

283. LaFever, L. and D. Drummond-Barbosa, *Direct control of germline stem cell division and cyst growth by neural insulin in Drosophila.* Science, 2005. **309**(5737): p. 1071-3.

284. LaFever, L., et al., *Specific roles of Target of rapamycin in the control of stem cells and their progeny in the Drosophila ovary.* Development, 2010. **137**(13): p. 2117-26.

285. Ikeya, T., et al., *The endosymbiont Wolbachia increases insulin/IGF-like signalling in Drosophila.* Proc Biol Sci, 2009. **276**(1674): p. 3799-807.

286. Grönke, S., et al., *Molecular evolution and functional characterization of Drosophila insulin-like peptides.* PLoS Genet, 2010. **6**(2): p. e1000857.

287. Hsu, H.J. and D. Drummond-Barbosa, *Insulin levels control female germline stem cell maintenance via the niche in Drosophila.* Proc Natl Acad Sci U S A, 2009. **106**(4): p. 1117-21.

288. Hsu, H.J., L. LaFever, and D. Drummond-Barbosa, *Diet controls normal and tumorous germline stem cells via insulin-dependent and -independent mechanisms in Drosophila.* Dev Biol, 2008. **313**(2): p. 700-12.

289. Heifetz, Y., U. Tram, and M.F. Wolfner, *Male contributions to egg production: the role of accessory gland products and sperm in Drosophila melanogaster.* Proc Biol Sci, 2001. **268**(1463): p. 175-80.

290. Soller, M., M. Bownes, and E. Kubli, *Mating and sex peptide stimulate the accumulation of yolk in oocytes of Drosophila melanogaster.* Eur J Biochem, 1997. **243**(3): p. 732-8.

291. Soller, M., M. Bownes, and E. Kubli, *Control of oocyte maturation in sexually mature Drosophila females.* Dev Biol, 1999. **208**(2): p. 337-51.

292. KING, R.C. and J.H. SANG, *Oögenesis in adult Drosophila melanogaster. VIII. The role of folic acid in oögenesis.* Growth, 1959. **23**(1): p. 37-53.

293. Carvalho, G.B., et al., *Allocrine modulation of feeding behavior by the Sex Peptide of Drosophila.* Curr Biol, 2006. **16**(7): p. 692-6.

294. Pierce, A., D. Gillette, and P.G. Jones, *Escherichia coli cold shock protein CsdA effects an increase in septation and the resultant formation of coccobacilli at low temperature.* Arch Microbiol, 2011. **193**(5): p. 373-84.

295. Frenkiel-Krispin, D. and A. Minsky, *Nucleoid organization and the maintenance of DNA integrity in E. coli, B. subtilis and D. radiodurans.* J Struct Biol, 2006. **156**(2): p. 311-9.

296. Albertson, R., et al., *Mapping Wolbachia distributions in the adult Drosophila brain.* Cell Microbiol, 2013. **15**(9): p. 1527-44.

297. Markov, A.V. and I.A. Zakharov, *The parasitic bacterium Wolbachia and the origin of the eukaryotic cell*. 2006, Paleontological Journal. p. 115-124.

298. Ponton, F., et al., *Macronutrients mediate the functional relationship between Drosophila and Wolbachia.* Proc Biol Sci, 2015. **282**(1800): p. 20142029.

299. Matilainen, O., et al., *Insulin/IGF-1 signaling regulates proteasome activity through the deubiquitinating enzyme UBH-4.* Cell Rep, 2013. **3**(6): p. 1980-95.

300. Blakesley, V.A., et al., *Replacement of tyrosine 1251 in the carboxyl terminus of the insulin-like growth factor-I receptor disrupts the actin cytoskeleton and inhibits proliferation and anchorage-independent growth.* J Biol Chem, 1998. **273**(29): p. 18411-22.

301. Coletta, D.K. and L.J. Mandarino, *Mitochondrial dysfunction and insulin resistance from the outside in: extracellular matrix, the cytoskeleton, and mitochondria.* Am J Physiol Endocrinol Metab, 2011. **301**(5): p. E749-55.

302. Hwang, H., et al., *Proteomics analysis of human skeletal muscle reveals novel abnormalities in obesity and type 2 diabetes.* Diabetes, 2010. **59**(1): p. 33-42.

303. Abe, Y., et al., *p90 ribosomal S6 kinase and p70 ribosomal S6 kinase link phosphorylation of the eukaryotic chaperonin containing TCP-1 to growth factor, insulin, and nutrient signaling.* J Biol Chem, 2009. **284**(22): p. 14939-48.

304. Huang, J. and J.H. Brumell, *Bacteria-autophagy interplay: a battle for survival.* Nat Rev Microbiol, 2014. **12**(2): p. 101-14.

305. Steele, S., et al., *Francisella tularensis harvests nutrients derived via ATG5-independent autophagy to support intracellular growth.* PLoS Pathog, 2013. **9**(8): p. e1003562.

306. Yu, H.B., et al., *Autophagy facilitates Salmonella replication in HeLa cells.* MBio, 2014. **5**(2): p. e00865-14.

307. Voronin, D., et al., *Autophagy regulates Wolbachia populations across diverse symbiotic associations.* Proc Natl Acad Sci U S A, 2012. **109**(25): p. E1638-46.

308. Hedges, L.M., et al., *Wolbachia and virus protection in insects.* Science, 2008. **322**(5902): p. 702.

309. Teixeira, L., A. Ferreira, and M. Ashburner, *The bacterial symbiont Wolbachia induces resistance to RNA viral infections in Drosophila melanogaster.* PLoS Biol, 2008. **6**(12): p. e2.

310. Rainey, S.M., et al., *Understanding the Wolbachia-mediated inhibition of arboviruses in mosquitoes: progress and challenges.* J Gen Virol, 2014. **95**(Pt 3): p. 517-30.

311. Kriesner, P., et al., *Rapid sequential spread of two Wolbachia variants in Drosophila simulans.* PLoS Pathog, 2013. **9**(9): p. e1003607.

312. Hoffmann, A.A., et al., *Successful establishment of Wolbachia in Aedes populations to suppress dengue transmission.* Nature, 2011. **476**(7361): p. 454-7.

313. Walker, T., et al., *The wMel Wolbachia strain blocks dengue and invades caged Aedes aegypti populations.* Nature, 2011. **476**(7361): p. 450-3.

314. Osborne, S.E., et al., *Variation in antiviral protection mediated by different Wolbachia strains in Drosophila simulans.* PLoS Pathog, 2009. **5**(11): p. e1000656.

315. Osborne, S.E., et al., *Antiviral protection and the importance of Wolbachia density and tissue tropism in Drosophila simulans.* Appl Environ Microbiol, 2012. **78**(19): p. 6922-9.

316. Chrostek, E., et al., *Wolbachia variants induce differential protection to viruses in Drosophila melanogaster: a phenotypic and phylogenomic analysis.* PLoS Genet, 2013. **9**(12): p. e1003896.

317. Chrostek, E., et al., *High anti-viral protection without immune upregulation after interspecies Wolbachia transfer.* PLoS One, 2014. **9**(6): p. e99025.

318. Lu, P., et al., *Wolbachia induces density-dependent inhibition to dengue virus in mosquito cells.* PLoS Negl Trop Dis, 2012. **6**(7): p. e1754.

319. Klarmann-Schulz, U., et al., *Comparison of Doxycycline, Minocycline, Doxycycline plus Albendazole and Albendazole Alone in Their Efficacy against Onchocerciasis in a Randomized, Open-Label, Pilot Trial.* PLoS Negl Trop Dis, 2017. **11**(1): p. e0005156.

320. Gayen, P., et al., *A double-blind controlled field trial of doxycycline and albendazole in combination for the treatment of bancroftian filariasis in India.* Acta Trop, 2013. **125**(2): p. 150-6.

321. De Britto, R.L., et al., *Enhanced efficacy of sequential administration of Albendazole for the clearance of Wuchereria bancrofti infection: Double blind RCT.* Trop Biomed, 2015. **32**(2): p. 198-209.

322. Sharma, R., et al., *Filamentation temperature-sensitive protein Z (FtsZ) of Wolbachia, endosymbiont of Wuchereria bancrofti: a potential target for anti-filarial chemotherapy.* Acta Trop, 2013. **125**(3): p. 330-8.

323. McGraw, E.A., et al., *Wolbachia density and virulence attenuation after transfer into a novel host.* Proc Natl Acad Sci U S A, 2002. **99**(5): p. 2918-23.

324. Camacho, M., M. Oliva, and L.R. Serbus, *Dietary saccharides and sweet tastants have differential effects on colonization of Drosophila oocytes by Wolbachia endosymbionts.* Biol Open, 2017. **6**(7): p. 1074-1083.

325. Moullan, N., et al., *Tetracyclines Disturb Mitochondrial Function across Eukaryotic Models: A Call for Caution in Biomedical Research.* Cell Rep, 2015.

326. Genchi, C., et al., *Preliminary results on the effect of tetracycline on the embryogenesis and symbiotic bacteria (Wolbachia) of Dirofilaria immitis. An update and discussion.* Parassitologia, 1998. **40**(3): p. 247-9.

327. Hoerauf, A., et al., *Tetracycline therapy targets intracellular bacteria in the filarial nematode Litomosoides sigmodontis and results in filarial infertility.* J Clin Invest, 1999. **103**(1): p. 11-8.

328. Clare, R.H., et al., *Development and validation of a high-throughput anti-Wolbachia whole-cell screen: a route to macrofilaricidal drugs against onchocerciasis and lymphatic filariasis.* J Biomol Screen, 2015. **20**(1): p. 64-9.

329. Echard, A., et al., *Terminal cytokinesis events uncovered after an RNAi screen.* Curr Biol, 2004. **14**(18): p. 1685-93.

330. Zhang, J.H., T.D. Chung, and K.R. Oldenburg, *A Simple Statistical Parameter for Use in Evaluation and Validation of High Throughput Screening Assays.* J Biomol Screen, 1999. **4**(2): p. 67-73.

331. Mahr, A. and H. Aberle, *The expression pattern of the Drosophila vesicular glutamate transporter: a marker protein for motoneurons and glutamatergic centers in the brain.* Gene Expr Patterns, 2006. **6**(3): p. 299-309.

332. Egger, B., et al., *In vitro imaging of primary neural cell culture from Drosophila.* Nat Protoc, 2013. **8**(5): p. 958-65.

333. Heddi, A., et al., *Four intracellular genomes direct weevil biology: nuclear, mitochondrial, principal endosymbiont, and Wolbachia.* Proc Natl Acad Sci U S A, 1999. **96**(12): p. 6814-9.

334. Pfaffl, M.W., *A new mathematical model for relative quantification in real-time RT-PCR.* Nucleic Acids Res, 2001. **29**(9): p. e45.

335. Team", q.R.D.C., *A language and Environment for Statistical Computing*. 2011, Vienna, Austria: The R Foundation for Statistical Computing.

336. Beasley, M.T. and R.E. Schumacker, *Multiple regression approach to analyzing contingency tables: post hoc and planned comparison procedures*. 1995, The Journal of Experimental Education. p. 79-93.

337. Verheyen, E. and L. Cooley, *Looking at oogenesis.* Methods Cell Biol, 1994. **44**: p. 545-61.

338. Mazzalupo, S. and L. Cooley, *Illuminating the role of caspases during Drosophila oogenesis.* Cell Death Differ, 2006. **13**(11): p. 1950-9.

339. http://flystocks.bio.indiana.edu/Fly_Work/media-recipes/bloomfood.htm.